Robust High-Dimensional Mean Estimation With Low Data Size, an Empirical Study

Cullen Anderson   *cyanderson@umass.edu*
University of Massachusetts Amherst

Jeff M. Phillips   *jeffp@cs.utah.edu*
University of Utah

Abstract

Robust statistics aims to compute quantities to represent data where a fraction of it may be arbitrarily corrupted. The most essential statistic is the mean, and in recent years, there has been a flurry of theoretical advancement for efficiently estimating the mean in high dimensions on corrupted data. While several algorithms have been proposed that achieve near-optimal error, they all rely on large data size requirements as a function of dimension. In this paper, we perform an extensive experimentation over various mean estimation techniques where data size might not meet this requirement due to the high-dimensional setting.

For data with inliers generated from a Gaussian with known covariance, we find experimentally that several robust mean estimation techniques can practically improve upon the sample mean, with the *quantum entropy scaling* approach from Dong *et.al.* (NeurIPS 2019) performing consistently the best. However, this consistent improvement is conditioned on a couple of simple modifications to how the steps to prune outliers work in the high-dimension low-data setting, and when the inliers deviate significantly from Gaussianity. In fact, with these modifications, they are typically able to achieve roughly the same error as taking the sample mean of the uncorrupted inlier data, even with very low data size. In addition to controlled experiments on synthetic data, we also explore these methods on large language models, deep pretrained image models, and non-contextual word embedding models that do not necessarily have an inherent Gaussian distribution. Yet, in these settings, a mean point of a set of embedded objects is a desirable quantity to learn, and the data exhibits the high-dimension low-data setting studied in this paper. We show both the challenges of achieving this goal, and that our updated robust mean estimation methods can provide significant improvement over using just the sample mean. We additionally publish a library of Python implementations of robust mean estimation algorithms, allowing practitioners and researchers to apply these techniques and to perform further experimentation.

1 Introduction

Given samples from an unknown distribution, mean estimation is perhaps the most-fundamental and oldest problems in data analysis. And it is even more relevant in modern analysis for learning and AI tasks where data is very high dimensional, and there is little else one can reliably compute – at least not without first grappling with the mean.

In the past several years, there has been a flurry of theoretical advancement on this topic, including improved asymptotic bounds (Lee & Valiant, 2022; Gupta et al., 2023; Catoni, 2011; Gupta et al., 2024; Lugosi & Mendelson, 2017), and the development of more robust methods for dealing with adversarially corrupted

data distributions (Lai et al., 2016; Diakonikolas et al., 2017a; 2019a; Cheng et al., 2019a; Dong et al., 2019; Deshmukh et al., 2022). This paper supports this development in two key ways:

1. We provide a large experimental study of many new methods, which had not been thoroughly compared. In the non-corrupted case, with moderate data size we do not see substantial improvement over the classic sample mean approach. However, in the corrupted setting, we find that some methods can significantly improve upon the sample mean. In some cases consistent improvement on the sample mean requires adjustments that we develop. As a summary, the quantum entropy scaling approach of Dong et al. (2019) (using an adjustment we describe) consistently performs the best as long as inliers are reasonable similar to Gaussian, and often basically matches the mean of the (unknown) inlier data.

2. We bring to the fore the $d > n$ setting, where there are more dimensions d than data points n, or at least we do not have n as substantially larger than d. This setting is becoming more common as dimensionality grows, but has not typically been considered because the theoretical advancements did not provide exciting new bounds here. In this setting, we revisit some algorithmic derivations and empirically explore what is possible. In particular, we revise a common and critical outlier pruning step, and the key adjustment is ultimately simple: a $\sqrt{d/n}$ term, which vanishes when $n \gg d$, needs to be included in a key threshold. This is detailed in Section 3.1.

Our experimental study considers mean estimation in a variety of settings, focusing on when $n < d$ or n is not much larger than d. While other experimental studies have been done, many like in Diakonikolas et al. (2017a) provided a comparison in the $n \gg d$ case. And while Deshmukh et al. (2022) has some experiments with n not much larger than d, these are not nearly as comprehensive as our study. First, we consider standard Gaussian data with known covariance, and no corruption. Then we extend this to the setting with various types of adversarial corruption. We also consider some limited cases with unknown covariance. However, because straight-forward adaptations of mean-estimation approaches towards estimating covariance (mapping to a $\binom{d}{2}$-dimensional problem) further stresses the need for data size n as a function of d, we defer a thorough exploration of this challenge to future work. Finally, we consider real world data scenarios where data is generated via embeddings resulting from large language models, deep pretrained image models, and word embedding models; here we do not have direct enforcement of Gaussianity of the data, but desire a high-dimensional mean nonetheless. In all cases, we consider a wide variety of efficient mean estimation approaches, including both classical ones and modern ones with stronger guarantees in the large n setting. We provide an anonymous link to our code for easy reproducability here: `https://github.com/cullena20/RobustMeanEstimation`.

2 Background

We consider as input a set $X \subset \mathbb{R}^d$ of n samples from an unknown distribution, and the goal is to estimate the mean of that distribution. Consider first the case where the distribution is the Gaussian $\mathcal{N}_d(0, I)$ where I is the identity matrix representing an isotropic covariance. For $x \sim \mathcal{N}_d(0, I)$ we have $\mathbb{E}[\|x\|^2] = d$. For the sample mean $\bar{x} \in \mathbb{R}^d$ from n points drawn iid from $\mathcal{N}_d(0, I)$ we have $\mathbb{E}[\|\bar{x}\|^2] = d/n$ and more importantly it strongly concentrates as $\Pr[|\|\bar{x}\|^2 - d/n| > t] \le 2\exp(-Ct^2)$ for a constant C (Vershynin, 2011). This implies for $n = \Omega(d/\varepsilon^2)$ we have $\|\bar{x}\| < \varepsilon$ with high probability; but for $d > n$ we do not

key notation	
n	# data samples
d	# dimensions
ε	error bound
η	true corruption
τ	expected corruption

get useful concentration results. The Gaussian is the most studied and used distribution for many reasons including that it has Normal marginals for any dimension, is easy to sample from, models an ℓ_2 loss, and is the limiting distribution of the central limit theorem. As such, it is our main object of study. However, we note that other distributions have distinct behavior for the large d setting. For instance, for n samples from a distribution with mean μ and covariance Σ, the expected squared deviation from the mean in d dimensions can be bounded by $\text{Tr}(\Sigma)/n$ (c.f., (Lee & Valiant, 2022)). This implies for instance if X is drawn uniformly from a unit ball (so $\text{Tr}(\Sigma) = 1$) or other distributions with bounded $\text{Tr}(\Sigma)$, then the behavior for $d > n$ can

still be well-concentrated. On the other hand, other unbounded and heavy-tailed distributions where, like Gaussians, $\text{Tr}(\Sigma) = \Theta(d)$ [1], present similar challenges in the $d > n$ setting.

Corrupted data models. Another setting considers some fraction $\eta \in (0, \frac{1}{2})$ of the data to be adversarially corrupted from X (Huber, 1964; Diakonikolas & Kane, 2023). Under the *Huber model*, we draw data $X \sim (1-\eta)P + \eta Q$ where P is the set of inliers with mean μ (we consider $P = \mathcal{N}_d(\mu, I)$ as identity covariance Gaussian data), and Q is any adversarial outlier distribution. The stronger *total variation* corruption model first draws $X' \sim P$ (with mean μ), and then creates X by adversarially changing any η-fraction of X' to a new location. That is, it can also adversarially subtract data from the inlier data in addition to adding outliers. How accurately can we recover the mean μ under these settings? We mostly focus on the Huber model, and observe that subtractive corruption (a component of the stronger total variation model) can induce a consistent and hard to avoid error, and does not seem to expose significant differences between approaches.

As the mean minimizes the sum of squared deviations, the sample mean is very susceptible to outliers. A single point of corruption can arbitrarily affect the sample mean. On the other hand, such corruption can be easily detected by filtering out the furthest points from the sample mean, and recomputing the sample mean on the remainder of the data. A more challenging setting relocates points to roughly $\sqrt{d}$ from the mean, where the inliers are, but all in a tight cluster; then no individual points can be so easily filtered, but the sample mean can be given a non-trivial bias of as much as $\Omega(\eta\sqrt{d})$. We will empirically consider a variety of challenging η-corruption situations.

For many years, when dealing with high dimensions, practitioners were faced with either potentially large error (e.g., on order of $\eta\sqrt{d}$) in using the sample mean or other generalizations of the median (Small, 1990), or one could spend time exponential in d and return an estimator that is guaranteed to be close to the true mean (Tukey, 1975) (or c.f., (Chen et al., 2015; Zhu et al., 2020a)). Around 2016, two papers broke this barrier (Lai et al., 2016) and (Diakonikolas et al., 2019a). They considered $X \sim \mathcal{N}_d(\mu, I)$, and allowed an η fraction of the data to be corrupted and return an estimate of the mean $\hat{\mu}$ so that $\|\mu - \hat{\mu}\| \leq O(\eta\sqrt{\log 1/\eta})$ or $\leq O(\eta\sqrt{\log d})$. These works however assume $n = \Omega(d/\eta^2)$; otherwise one runs into the roadblock that even the sample mean of the inliers (the uncorrupted points) has more than η error. Since then, much follow-up work has furthered our understanding. Some work (Dong et al., 2019; Cheng et al., 2019a; Depersin & Lecué, 2019) improved the time complexity of robust mean estimation algorithms, and our understanding of the problem's hardness (Diakonikolas et al., 2017c; Hopkins & Li, 2019). Others provide formulations where gradient descent can be used despite non-convexity (Cheng et al., 2020; Zhu et al., 2020b). There has also been effort to improve other robust statistics tasks such as covariance estimation (Chen et al., 2015; 2017; Cheng et al., 2019b), sparse estimation (Balakrishnan et al., 2017; Diakonikolas et al., 2019c; Cheng et al., 2022; Diakonikolas et al., 2022; 2024), list decodable learning (Charikar et al., 2017; Diakonikolas et al., 2017b), robustly learning mixtures of Gaussians (Bakshi et al., 2022), robust optimization (Diakonikolas et al., 2019b; Prasad et al., 2018), robust regression (Diakonikolas et al., 2018; Klivans et al., 2020), or in the context of adversarial machine learning (Tran et al., 2018). Importantly, robust statistics are more amenable to differential privacy, in particular to privacy through noise addition, and privacy mechanisms are naturally robust (Dwork & Lei, 2009; Liu et al., 2021a; Hopkins et al., 2023; Asi et al., 2023). Recent work has also expanded methods for different corruptions models (Liu et al., 2021b; Zhu et al., 2020c). For a more thorough review see the recent textbook by Diakonikolas & Kane (2023).

There has also been significant complementary work in mean estimation under heavy-tailed distributions (Lugosi & Mendelson, 2021; Lugosi, 2022; Gupta et al., 2024; Catoni, 2011; Lugosi & Mendelson, 2017; Devroye et al., 2015; Lee & Valiant, 2022); see the recent survey by Lugosi & Mendelson (2019). Recent work has also developed connections between optimality under heavy-tailed distributions, and optimality in the Huber corruption setting (Prasad et al., 2019).

---

[1] We use standard asymptotic notation so for some constants C_1, C_2, C_3 and functions f, g then $g(x) = O(f(x))$ implies $\forall x > C_3$ then $g(x) \leq C_1 f(x) + C_2$; $g(x) = \Omega(f(x))$ implies $\forall x > C_3$ then $g(x) \geq C_1 f(x) + C_2$, with possibly different constants; and $g(x) = \Theta(f(x))$ implies $g(x) = O(f)$ and $g(x) = \Omega(f(x))$.

3 Mean Estimation Algorithms

Here we will document the mean estimation algorithms considered in this paper. Some are classic, and we also include several ones from the recent literature designed to be potentially practical and algorithmically efficient. Some include asymptotic theoretical bounds which use astronomical constants; we make a best effort to replace them with reasonable values so they remain practical. Some use an expected corruption parameter τ, meant to be an upper bound true corruption, η. The ones we consider are as follows:

sample_mean: The *sample mean* simply returns $\hat{\mu} = \frac{1}{|X|} \sum_{x \in X} x$.

coord_median: The *coordinate-wise median* computes the median of each coordinate individually so $\hat{\mu}_j = \mathsf{median}(\{x_{i,j} \mid x_i \in X\})$.

coord_trimmed_mean: First compute a *trimmed mean estimator* for each coordinate individually, parameterized by a value $\tau \in (0,1)$. That is, in one dimension, it sorts the data, and removes $\tau|X|$ points which have the smallest values, and also removes $\tau|X|$ with largest values. Then it computes the mean of the remaining $(1 - 2\tau)|X|$ points. The *coordinate-wise trimmed mean* applies this estimator separately for each coordinate; which points are removed in coordinate j have no bearing on which points are removed from coordinate j' (Lugosi & Mendelson, 2021).

median_of_means: Split the data into k chunks, find the mean of each chunk, take the coordinate wise median of these k means (Lugosi & Mendelson, 2019; Minsker, 2023b;a). As a default, we set $k = 10$; this hyperparameter is explored in Appendix A.5.

geometric_median: The *geometric median* is the point which minimizes the sum of distances to all sample points. This is iteratively approximated using the Weiszfeld algorithm (Small, 1990; Vardi & Zhang, 2001).

lee_valiant: (Lee & Valiant (2022)) The Lee and Valiant algorithm first estimates the mean μ' on a γ percentage of data points X_γ using a mean estimator. It then centers all points to $X' = \{x' = x - \mu' \mid x \in X\}$. Let X_t be the t points in X so their corresponding x' have the largest norm. Let X'_* be the subset consisting of $x' \in X'$ with their corresponding points *not* in X_γ or in X_t. Then return $\mu' + \frac{1}{|X|} \sum_{x' \in X'_*} x'$. Rather than the extremely large constants in the original paper, we set $\gamma = 0.5$ and $t = \tau|X|$. As default, we use $\mathsf{median\_of\_means}_k$ estimator with $k = 10$ to obtain the initial mean estimator μ'.

LRV: (Lai et al. (2016)) The LRV method recursively reduces the dimension by half, until 1 or 2 dimensions remain. Following the original author's code[2], in the (≤ 2)-dimensional base case, it returns $\mathsf{coord\_median}$. The recursive step has three components. First, it calculates a weight w_i for each point x_i as $w_i = \exp(-\|x_i - a\|^2/(Cs^2))$ where s^2 is a robust sample estimate of the trace of the true covariance matrix, a is a rough estimator of the mean chosen as $\mathsf{coord\_median}$, and C is a hyperparameter. We use $C = 1$; this hyper parameter is explored in Appendix A.5. Second, it computes $\mu_w = \frac{1}{|X|} \sum_{x_i \in X} w_i x_i$, which is the weighted mean of the input, and $\Sigma_w = \frac{1}{|X|} \sum_{x_i \in X} w_i (x_i - \mu_w)(x_i - \mu_w)^T$, which is the weighted covariance of the input. Let V by the span of the top $\lfloor d/2 \rfloor$ singular vectors of Σ_w; let $V_\perp$ be the span of the bottom $\lceil d/2 \rceil$ singular vectors of Σ_w. Third, recurse on data projected onto V, and return an estimate μ_1. We also build an estimator μ_2 of the data projected onto the $\lceil d/2 \rceil$-dimensional remainder space $V_\perp$ using the weighted sample mean projected onto $V_\perp$: that is $\mu_2 = \frac{1}{|X_\perp|} \sum_{x_i^\perp \in X_\perp} w_i x_i^\perp$ where $X_\perp$ is the data projected onto $V_\perp$. Finally return $\mu_1 + \mu_2$.

ev_filtering: (Diakonikolas et al. (2019a;b)) This method observes that when inliers are from a standard Gaussian, then a set of corrupted data which substantially affects the mean estimate must result in a sufficiently large top eigenvalue after centering (i.e., of the sample covariance matrix), and this can be remedied by pruning points which are far along the top eigenvector. In this method, if after centering by the sample mean $\hat{\mu}$, the top eigenvalue exceeds $O(\tau \log 1/\tau)$ (Diakonikolas et al. (2017a)[3] implements this as $1 + 3\tau \log(1/\tau)$), then this data is considered additively corrupted along the direction of the top eigenvector. We call this the corruption detection step. Then they consider all points projected onto the associated top eigenvector and sorted $P = \langle p_1, \ldots, p_n \rangle$; and then a set of points furthest from the median $\mathsf{med}(P)$ are

---

[2] https://github.com/kevinalai/AgnosticMeanAndCovarianceCode
[3] https://github.com/hoonose/robust-filter

pruned. We call this the pruning step. The determination of which points to prune is based on those which exceed a Gaussian concentration inequality. Specifically, it finds the smallest index i so $T_i = p_i - \mathsf{med}(P) - 2\tau$ satisfies $\frac{n-i}{n} > \gamma(\mathsf{erfc}(T_i/\sqrt{2})/2 + \tau/(d\log(d\tau/0.1)))$, where erfc is the complementary error function ($1-$ the cdf of the Normal) and prunes all points i or larger. Intuitively, the centered projected data is expected to be a standard Normal distribution, and this bound compares the true percentage of points that exceed a threshold, T_i, with the probability that points will exceed that threshold, given by erfc with some slack terms added. Then the algorithm is recursively called with all points not-yet pruned until the top eigenvalue threshold is not violated. This algorithm critically assumes identity covariance and $n = \Omega(d/\tau^2) \gg d$.

QUE: (Dong et al. (2019)) Quantum Entropy Scoring, QUE for short, scores outliers based on quantum entropy regularization, and returns a mean using the same structure as ev_filtering, but with a modified pruning procedure. Rather than pruning points based on their projection onto the top eigenvalue, points are given outlier scores relevant to all directions. First, calculate the normalized matrix exponential $U = \exp(\alpha\Sigma)/\mathsf{tr}(\exp(\alpha\Sigma))$ where $\alpha \geq 0$ is a hyperparamater and Σ is the sample covariance. Then, calculate a vector of quantum entropy scores, w, with $w_i = (x_i - \mu')^T U (x_i - \mu')$, where x_i is the ith data point and μ' is the sample mean. This is implemented efficiently using a Chebyshev expansion of the matrix exponential and Johnson-Lindenstrauss approximations. Points with the largest scores are pruned, and the algorithm continues recursively with the remaining points until the top eigenvalue threshold is not violated. Following the original author's code (Dong et al., 2019)[4], we prune $\tau/2$ percentage of points during every iteration. Additionally, while the author's provide a theoretical threshold on the top eigenvalue, the constants are not given. Rather than tuning this threshold, we implement it using the same threshold as ev_filtering; that is $1 + 3\tau\log 1/\tau$. Because of this threshold, the algorithm critically assumes identity covariance and $n = \Omega(d/\tau^2) \gg d$. We set $\alpha = 4$ as in the author code; simple experiments show little variation with α between 0.5 and 200.

PGD: (Cheng et al. (2020)) Projected Gradient Descent, PGD for short, frames robust mean estimation as a non-convex optimization problem, and despite non-convexity, directly solves this using gradient descent. PGD finds a vector, w, of outlier scores, which can then be used to return a mean estimate $\mu' = \frac{1}{|X|}\sum_{x_i \in X} w_i x_i$. w is found to minimize the spectral norm of the standard weighted covariance matrix, Σ_w, subject to the constraint that the weights represent at least a $(1-\tau)$-density fractional subset of the dataset. The vector w is found as an approximate stationary point to this objective by first performing gradient descent on the spectral norm of the weighted covariance matrix, and then projecting onto the simplex of feasible weight vectors. First, define a function $F(u, w) = u^T\Sigma_w u$. Then, repeat the following for γ iterations, where γ, following the conventions of a code implementation by the same author as the original paper (Cheng & Lin, 2021)[5], is a hyperparameter. Calculate the top eigenvector, u_t, of Σ_w, which corresponds to finding the unit vector u_t such that $F(w, u_t) \geq (1-\tau)\mathsf{max}_u F(w, u)$. Then, update w as $w = P(w - \alpha\nabla_w F(w, u_t))$ where P projects onto $\Delta_{n,2\tau} = \{w \in \mathbb{R}^n : \|w\|_1 = 1 \text{ and } 0 \leq w_i \leq \frac{1}{(1-2\tau)n}\}$, and $\nabla_w F(w, u_t)) = X u_t \odot X u_t - 2(w^T X u_t)X u_t$ where $\odot$ indicates element-wise multiplication, and α is the learning rate, initialized as $1/n$ and updated dynamically through learning. We set the number of iterations $\gamma = 15$; this hyperparameter is explored in Appendix A.5.

ℓ_p**_min**: (Deshmukh et al. (2022)) This method frames robust mean estimation as a semi-definite program (SDP). Similar to PGD, a vector, w, of outlier scores is found, and the weighted mean $\mu' = \frac{1}{|X|}\sum_{x_i \in X} w_i x_i$ is returned. The ℓ_p norm for hyperparameter $0 \leq p \leq 1$ is maximized with respect to w, under the constraint that the top eigenvalue of the weighted covariance matrix is less than a constant. The weight vector w is iteratively updated by solving a SDP until the number of iterations is less than a bound determined by τ, in which case $\hat{\mu}$ defined above is returned. Update w by approximately solving an SDP to maximize w in $\|w\|_1$ over $\Delta_{n,\tau}$. Each step of the optimization problem is convex and can be solved as the following packing SDP:

$$\mathsf{max}_w \quad \text{s.t.} \quad w_i \geq 0 \; \forall i, \quad \sum_{i=1}^{n} w_i \begin{bmatrix} e_i e_i^T & \\ & (x_i - \mu_w)(x_i - \mu_w)^T \end{bmatrix} \preceq \begin{bmatrix} I_{n \times n} & \\ & c_\tau n I_{d \times d} \end{bmatrix},$$

where, c_τ is a function of τ. This analysis of this algorithm critically assumes identity covariance and $n = \Omega(d/\tau^2) \gg d$.

---

[4]https://github.com/twistedcubic/que-outlier-detection
[5]https://github.com/chycharlie/robust-bn-faster

3.1 New Algorithms and Variants

We also consider a few new methods, with subtle but important extensions of these existing ones.

The primary insight needed to adapt methods to the $d \geq n$ case is found by revisiting how we identify outliers with respect to a d-dimensional Gaussian distribution. The bounds used in the $n \gg d$ case have enough data in each direction d to concentrate, whereas in the $d \geq n$ case we need to account for this additional variance. The key result leverages a theorem of Vershynin (2011) to understand the concentration of the top eigenvalue of the sample covariance matrix.

Theorem 1. *Let X be a $n \times d$ matrix whose entries are independently drawn from $\mathcal{N}(\mu, I)$. Let $\Sigma = \frac{1}{n}(X - \bar{\mu})^T(X - \bar{\mu})$ be the sample covariance matrix of X, where $\bar{\mu} = \frac{1}{n}\sum_i X_i$ and X_i is the ith row of X. Then for every $t > 0$, with probability of at least $1 - 3\exp(-t^2/2)$, one has*

$$\|\Sigma\|_2 \leq \left(1 + \sqrt{d/n} + t/\sqrt{n} + \frac{\sqrt{d + \sqrt{2d}t + t^2}}{n}\right)^2.$$

The proof is deferred to Appendix A.1. A more convenient form shows that the fourth term is lower-order and can be absorbed into the probability of failure.

Corollary 1.1. *Under the same setting as Theorem 1, if one assumes $d/n \leq 16, n \geq 16, t \geq 5$, then with probability of at least $1 - 3\exp(-t^2/8)$, one has*

$$\|\Sigma\|_2 \leq \left(1 + \sqrt{d/n} + t/\sqrt{n}\right)^2.$$

ev_filtering_low_n: The ev_filtering algorithm assumes the sample size is $n = \Omega(d/\tau^2)$. This assumption is used in several parts of the analysis, and it allows the filtering bound to be simplified to $1 + \tau\log(1/\tau)$; however, when $n = o(d/\tau^2)$, this simplification does not hold, and the filtering bound needs to depend on d. We instead filter points if the top eigenvalue $\lambda_{\max} > (1 + \sqrt{d/n} + t/\sqrt{n})^2$ using Corollary 1.1. We set $t = 10$ to achieve almost 100% (≈ 0.999) success. All other steps of the algorithm remain the same.

QUE_low_n: The QUE_low_n algorithm extends the same filtering bound as ev_filtering. Although their paper mentions a $O(\sqrt{d/n})$ factor in the error, the code seems to assume $n = \Omega(d/\varepsilon^2)$ and is implemented very similar to ev_filtering. As this approach does not work under low data size, in our newly proposed variant, we instead filter points if the top eigenvalue $\lambda_{\max} > (1 + \sqrt{d/n} + t/\sqrt{n})^2$ using Corollary 1.1.

ℓ_p_min_low_n: The ℓ_p_min algorithm uses the condition that the top eigenvalue of the weighted covariance matrix is bounded by $c_\tau n$ where c_τ is a hyperparameter suggested to be set at $1 + \tau\log(1/\tau)$. As previously observed, this threshold does not hold when $n = o(d/\tau^2)$ and to account for this, in our newly proposed variant we set $c_\tau = (1 + \sqrt{d/n} + t/\sqrt{n})^2$, using Corollary 1.1.

lee_valiant_simple: We use a simplified version of the Lee and Valiant algorithm (Lee & Valiant, 2022), which aligns with an informal description in their abstract. It completely removes the τ percentage of points classified as outliers rather than simply downweighting them. That is, it returns $\hat{\mu} = \frac{1}{|X'_*|}\sum_{x' \in X'_*} x$; the average of all points X'_* which were not in the original estimate, nor from the pruned set furthest from μ'.

4 Experiments

We generally evaluate the performance of these mean estimation algorithms as data size n, dimension d, and corruption η are varied. Error is measured as the Euclidean distance $\|\mu - \hat{\mu}\|$ between the true mean μ and the estimate $\hat{\mu}$ returned by a mean estimation algorithm. We set the default values as $n = 500$, $d = 500$, and $\eta = 0.1$. We examine the performance as we fix one of these variables and vary the others under various distributions for both the uncorrupted and corrupted data. We first examine uncorrupted standard normal Gaussian data, demonstrating that nothing really improves upon sample_mean, and observing the robustness of mean estimation techniques when applied to uncorrupted data. We then examine corrupted Gaussian data

over various covariances and noise distributions. The example distributions are chosen among challenging examples in the literature meant to distinguish various models. Experiments were run on a 2022 Macbook Air with Apple M2 Chip, 16GB memory, running MacOS 12.

At one point in our experiment, the values of n, d, and η are used to generate data according to a supplied data generation function and noise scheme (both of which will vary depending on the experiment). A mean estimate is made on this data using each of the mean estimators being tested. For each mean estimator, error is then stored as the Euclidean distance between the true mean of the data and the returned mean estimate. These errors are accumulated over 5 runs and averaged. We additionally plot the error incurred by the sample mean of the original uncorrupted data, which we call the good_sample_mean error. This serves as a valuable baseline for comparison. In practice, we can not expect to achieve error better than the sample mean of the inliers. Therefore, a reasonable goal for a robust estimator is to closely match the performance of good_sample_mean, thereby removing the effects of corrupted data points. Could a robust mean estimator somehow improve upon this? We do not observe this; but we will observe methods that basically match good_sample_mean, even without $n = \Omega(d/\varepsilon^2)$.

Fraction of corrupted data. Some algorithms are designed for data where a η-fraction of the data has been corrupted. And in some cases, this fraction is taken as a parameter τ used within the algorithms (coord_trimmed_mean, lee_valiant_simple, lee_valiant, ev_filtering, ev_filtering_low_n, QUE, QUE_low_n, PGD, ℓ_p_min, ℓ_p_min_low_n).

In theory, these algorithms work best using their parameter τ set to the true fraction of corrupted data η, and may even result in arbitrary error if the parameter τ is not set to at least an upper bound for the true fraction. However, increasing the value of τ in the algorithms also theoretically increases the error incurred by algorithms. Recent work by Jain et al. (2022) showed a meta algorithm that allows robust estimation algorithms to perform asymptotically optimal without knowing true corruption η. We investigate robustness to expected corruption, τ, empirically, in Appendix A.6, as we fix τ and vary true corruption η. We observe that the best algorithms do not show a strong dependence on this relationship, so long as τ is an upper bound on η. Hence, for all other experiments, we simply set the parameter τ according to the true corrupted fraction η or to $\tau = 0.1$ if the data is not corrupted.

Selecting algorithmic variants. There are many algorithms to be considered, and plots can become cluttered. To reduce this, we perform some comparison among variants. We summarize key findings here, with further details deferred to Section 7.

Algorithm	$n = 500$, $d = 500$		$n = 200$, $d = 500$	
	Error	**Time (s)**	**Error**	**Time (s)**
sample_mean	2.47 ± 0.04	0.00019 ± 0.000002	2.74 ± 0.05	0.00019 ± 0.000001
LRV	1.14 ± 0.04	0.81 ± 0.12	1.76 ± 0.10	0.64 ± 0.03
PGD	1.08 ± 0.02	82.4 ± 8.8	1.68 ± 0.05	72.5 ± 3.2
ev_filtering_low_n	1.07 ± 0.02	0.20 ± 0.02	1.69 ± 0.04	0.08 ± 0.03
ev_filtering	13.49 ± 3.56	0.48 ± 0.15	17.06 ± 5.92	0.05 ± 0.02
QUE_low_n	1.04 ± 0.03	0.71 ± 0.05	1.70 ± 0.049	0.35 ± 0.03
QUE	20.81 ± 0.40	2.70 ± 0.08	20.88 ± 0.38	1.99 ± 0.04
ℓ_p_min_low_n	1.17 ± 0.04	1182.6 ± 35.3	1.67 ± 0.03	265.9 ± 15.2
ℓ_p_min	1.62 ± 0.04	1076.8 ± 43.9	5.62 ± 0.40	250.07 ± 17.2

Table 1: Error and Runtime Across Simple Corrupted Identity Covariance Gaussian

First, we do not consider ℓ_p_min and ℓ_p_min_low_n in our plots due their exceptionally large runtimes. We report runtimes and errors (defined as the Euclidean distance from the estimated mean to the true mean) of selected algorithms under $n = 500$ and $d = 500$ and under $n = 200$ and $d = 500$ over a simple corrupted Gaussian distribution in Table 1. We report results as the mean $\pm$ the standard deviation, averaged over 5 runs. With the notable exceptions of ℓ_p_min_low_n, ℓ_p_min, and PGD, most estimators are efficient and took under 3 seconds to run with $n = 500$ and $d = 500$ for a simple corrupted Gaussian distribution. ℓ_p_min

and $\ell_p\_\text{min}\_\text{low}\_\text{n}$ rely on an SDP solver, which we implement with the cvxpy (Diamond & Boyd, 2016; Agrawal et al., 2018) package and the mosek solver. Although this is theoretically efficient, it is slow in practice for the data scale and dimesionality we consider in this paper. For $n = 500$ and $d = 500$, both algorithms took about 1100 seconds, or about 18 minutes, to return a mean estimate over a simple corrupted data scheme. For that reason, and since we run many trials of each input size and error level, we do not consider these algorithms in our plots. However, we note that employing Corollary 1.1 for $\ell_p\_\text{min}\_\text{low}\_\text{n}$ achieves a noticeable performance increase over ℓ_p_min; showing gains from 1.62 error to 1.17 error in the $n = 500, d = 500$ case and from 5.62 to 1.67 error in the $n = 200, d = 500$ case. PGD is also much slower than other robust estimators, taking approximately 80 seconds to run with $n = 500$ and $d = 500$. While this significant slow down is relevant when considering a practical algorithm, it is not as prohibitive as ℓ_p_min. As a result, we include it in all of our plots.

Second, we observe that when the data does not satisfy that $n \gg d$, then both ev_filtering and QUE can have catastrophic failure. Our variants ev_filtering_low_n and QUE_low_n avoid this issue in the $d > n$ and $d \approx n$ settings, while basically matching the effectiveness of their original versions when they do not have catastrophic failure. This result is highlighted in Table 1, where we observe that both QUE and ev_filtering achieve significantly worse error than QUE_low_n and ev_filtering_low_n respectively. As a result, we use ev_filtering_low_n and QUE_low_n in all comparisons.

Thirdly, we find that lee_valiant_simple performs slightly better than the original lee_valiant; however the difference is fairly small. We also do not notice any meaningful advantages from using lee_valiant_simple or lee_valiant with different choices of initial mean estimators. As such, we only use lee_valiant_simple in all comparisons.

4.1 Uncorrupted Gaussian Data with Identity Covariance

We first evaluate the performance of mean estimation algorithms over uncorrupted Gaussian data with identity covariance. In particular, we draw uncorrupted data $X \sim \mathcal{N}_d(\mu, I)$, where μ is an arbitrary mean and I is identity covariance. For these experiments, we set μ to be the all-fives vector, but did not find performance to depend on μ. For algorithms that utilize τ, expected corruption, as input, we use the default value of $\tau = 0.1$.

We provide our first experimental plots in Figure 1; most further experiments will follow this same set-up, consisting of a set of 4 charts, each measuring the Error $\|\mu - \hat{\mu}\|$ on the y-axis. The top two charts vary the data size n along the x-axis, but on different scales. The top left shows a large scale from $n = 20$ to $n = 5020$, focusing on the $n > d = 500$ paradigm. The top right shows $n = 20$ to $n = 520$, focusing on the $n < d$ paradigm. The bottom left plot show the effect of varying the dimension from $d = 20$ to $d = 1020$ while fixing $n = 500$. The bottom right shows varying the algorithm's parameter, τ, for the expected noise from 0 to 0.45 with fixed $n = 500$, $d = 500$. Each algorithm is shown as a curve, with the average error of 5 independent data generations at regular intervals on the x-axis. A shaded area is shown at a radius of 1 standard deviation from that average error value.

The plots are a bit cluttered because most algorithms perform about the same, including sample_mean. No algorithm can be seen to noticeably outperform sample_mean, which, as the MLE for this data, and by the Gauss-Markov theorem, is not surprising. Methods LRV, ev_filtering_low_n, QUE_low_n, PGD, coord_trimmed_mean, geometric_median, and lee_valiant_simple have about the same error in most cases. However, median_of_means, and coord_median perform slightly worse, with the gap becoming more apparent in high dimensions. Moreover, lee_valiant_simple and coord_trimmed_mean do significantly worse with a higher expected corruption parameter τ. This is a result of expected corruption, τ, being a hyperparameter that directly controls the percentage of points to prune. Finally, as predicted by basic theory, with n fixed as the dimension d increases, the measured error increases at a rate roughly $\sqrt{d}$.

4.2 Corrupted Gaussian Data with Identity Covariance

We evaluate corrupting noise added to Gaussian data with identity covariance. In particular, we draw $X \sim (1 - \eta)P + \eta Q$ where $P = \mathcal{N}_d(\mu, I)$ and Q describes the corrupted data distribution. This is equivalent
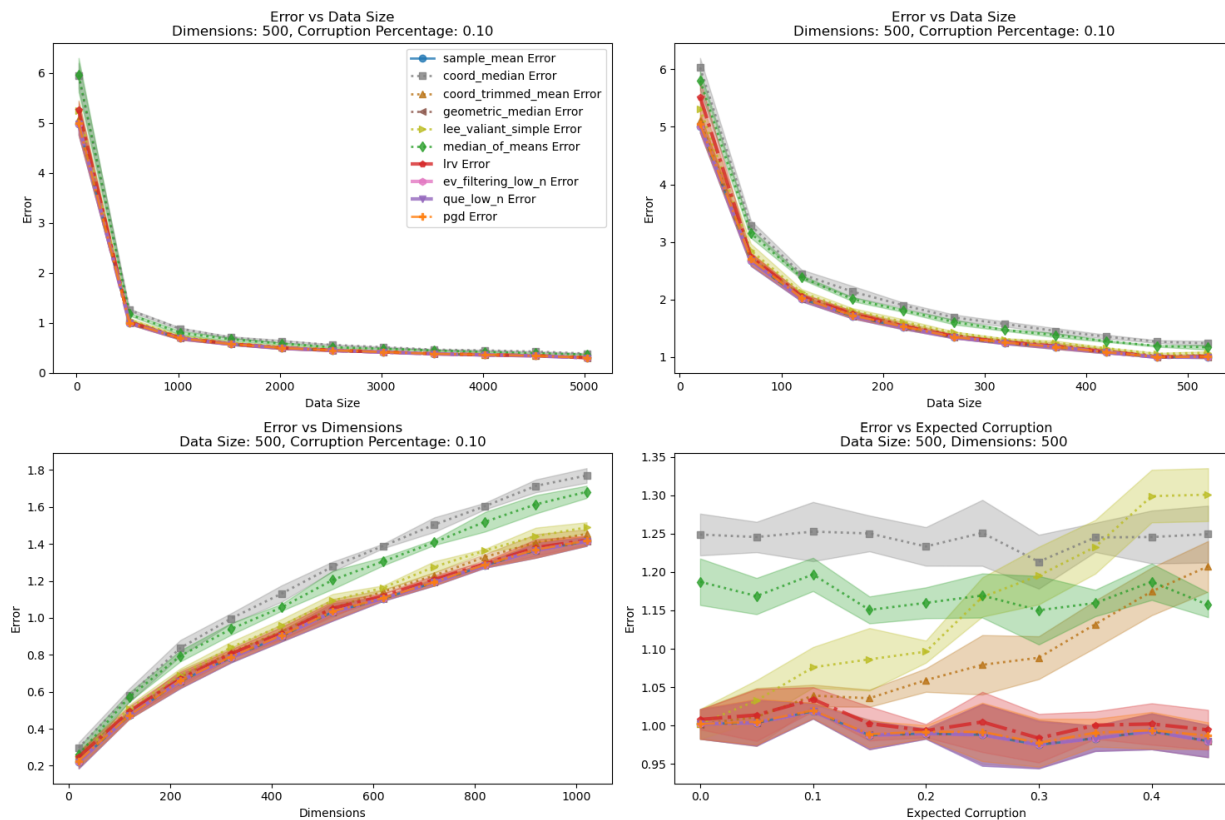
Figure 1: Uncorrupted Gaussian Identity Covariance

to the more general case where any covariance Σ is known, as we could simply scale the data to have identity covariance, apply these methods, and scale the mean estimate back. We provide a wrapper in our implementation to perform this operation.

Gaussian noise shifted to variance shell. We first consider corrupted data distribution $Q = \mathcal{N}_d(\mu', \frac{1}{10}I)$ so $\|\mu - \mu'\| = \sqrt{d}$. Since $\mathbb{E}_{x \sim P}[\|x - \mu\|^2] = d$, corrupted data from Q is not easily identified. The location of this cluster is determined by a random rotation at every generation to ensure that no coordinate-axis specific bias is introduced. This is shown in Figure 2 in the same 4 experiments as with uncorrupted data, except now the bottom right figure varies η, the fraction of corrupted data from Q, along the x-axis. We set the expected corruption hyperparameter equal to true corruption, that is $\tau = \eta$. In Appendix A.6 we explore the relation between expected corruption τ versus actual corruption η; for the most part as long as $\tau > \eta$.

There is now more clear separation between the algorithms designed for adversarial corruption, and those not. Here ev_filtering_low_n, QUE_low_n, and PGD do the best among all settings, with LRV, perhaps doing the best, even appearing better than good_sample_mean for large dimensions, although within 1 standard deviation error margin. Due to the high dimensionality, d, good_sample_mean, the sample mean of points from the uncorrupted part of the distribution P, does not have error approaching 0 until n is very large. ev_filtering_low_n, QUE_low_n, and PGD work so well that they are nearly overlapping this best possible standard. Also, perhaps surprisingly, median_of_means also does nearly as well, especially under larger n, though it degrades much worse with larger η.

In contrast, coord_median, sample_mean, coord_trimmed_mean, geometric_median, and lee_valiant_simple all do considerably worse, even with large data size. With large corruption levels, these all even seem to do worse than just sample_mean, indicating that the algorithms prune the wrong data points or face some other similar issue.
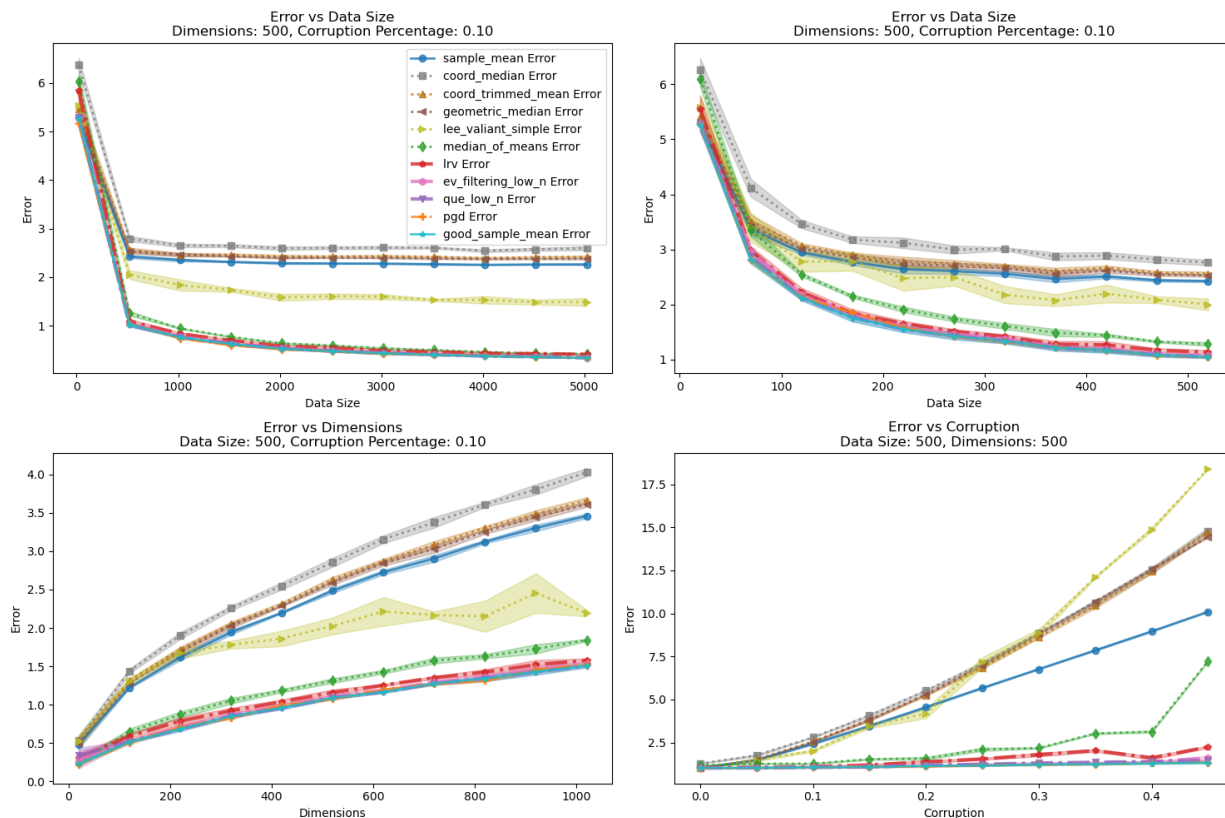
Figure 2: Corrupted Gaussian Identity Covariance: Additive Variance Shell Noise

Large + Subtle outliers: DKK Noise. We now recreate the noise distribution from Diakonikolas et al. (2017a), which utilizes a more sophisticated corruption scheme that includes both easier and harder to detect outliers. Half of the noise is drawn from the product distribution over the hypercube where every coordinate is -1 or 0 away from the true mean at that coordinate with equal probability. The other half is drawn from the product distribution where the first coordinate is either 11 or -1 away from the true mean at that coordinate with equal probability, the second coordinate is -3 or -1 away from the corresponding true mean coordinate with equal probability, and all remaining coordinates are -1 away from the true mean. We call this corruption scheme DKK Noise. This is shown in Figure 3, with similar results. ev_filtering_low_n, QUE_low_n, PGD, and LRV achieve performance nearly matching good_sample_mean, with median_of_means also doing almost as well – at least while the dimension d and rate of corruption τ are on the smaller side. Other than median_of_means, all classic methods perform noticeably worse than good_sample_mean and achieve similar error to sample_mean. The only difference of note here is that lee_valiant_simple exhibits far larger error bars, suggesting that its performance may vary significantly depending on random initializations made within the algorithm. Also, LRV may even outperform good_sample_mean for very large dimensions.

Subtractive noise. We additionally consider subtractive noise in Figure 4. Here, an adversary is able to remove a η percentage of points from the data distribution. We implement this by removing the η-percentage of points which are most extreme in some direction. Unlike in the additive corruption case, there is a strict upper bound on the error under subtractive corruption from a standard Gaussian distribution; the error induced is bounded as $O(\eta)$ even using sample_mean, and clustering the subtracted points as most extreme in some direction ensures their effect is $\Omega(\eta)$ under sample_mean. In general, we wish to consider noise distributions that may add outliers and also remove inliers through such subtractive noise. However, we do not find any surprising capabilities among methods in this scenario. As a result, for the remainder of this paper, we focus on additive corruption.
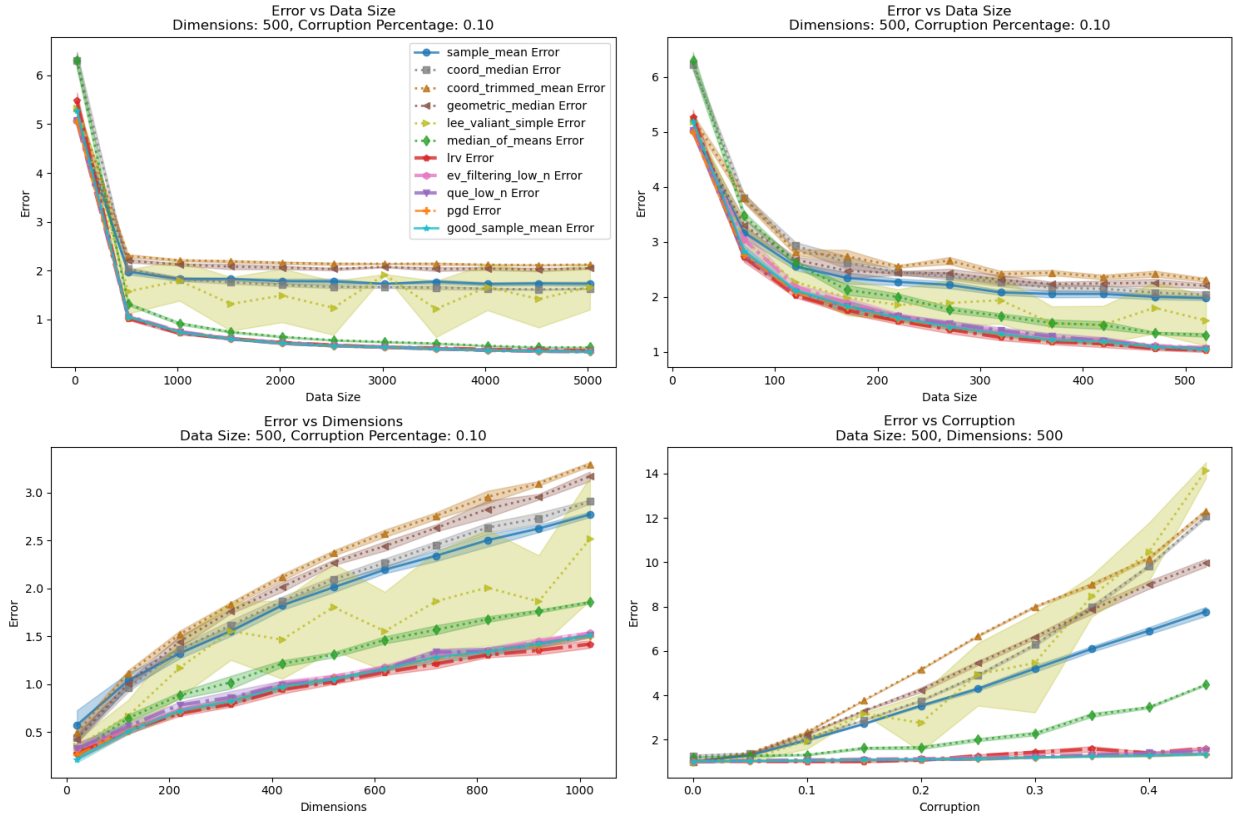
Figure 3: Corrupted Gaussian Identity Covariance: DKK Noise

Under subtractive corruption, nothing outperforms sample_mean; and now nothing can match good_sample_mean in error in most settings. However, ev_filtering_low_n, QUE_low_n, PGD, and LRV all nearly match the performance of sample_mean. Unlike in the previous additive corruption schemes, median_of_means performs significantly worse under subtractive corruption, always achieving error notably worse than sample_mean. Among other estimators, geometric_median nearly matches sample_mean error across all settings, lee_valiant_simple and coord_trimmed_mean perform similarly but degrade much more under larger corruption, while coord_median performs significantly worse.

We find similar results across several other noise distributions. In addition to the hard-to-detect distributions, we also show that ev_filtering_low_n, QUE_low_n, PGD, and LRV are generally robust to arbitrary outliers. These details are deferred to Appendix A.2.

4.3   Corrupted Gaussian Data with Unknown Covariance

We now evaluate corrupted Gaussian data for general unknown covariance. Since ev_filtering_low_n and QUE_low_n rely on the identity covariance assumption, we employ a simple heuristic to adapt these algorithms to the unknown covariance case. We estimate the trace of the covariance as $\text{Tr}(\hat{\Sigma}) = \frac{1}{n-1} \sum_{i=1}^{n} ||x_i - \hat{\mu}||^2$, where $\hat{\mu}$ is the sample mean and $\hat{\Sigma}$ is the sample covariance. We rescale the data to $X' = \{x_i' = x_i/\sqrt{\frac{\text{Tr}(\hat{\Sigma})}{d}} \mid x_i \in X\}$. We then estimate the mean of X', rescale this estimate by $\sqrt{\frac{\text{Tr}(\hat{\Sigma})}{d}}$, and report the results. This heuristic is used for ev_filtering_low_n and QUE_low_n across all unknown covariance experiments, and not used for any other algorithms. The other standard algorithms are either invariant to this linear rescaling, or themselves account for it; this was supported by our own observations.

Another possible method is to utilize a robust covariance estimate instead of a sample trace estimate, as discussed in Diakonikolas & Kane (2023). We do not evaluate such methods, as this would involve a thorough
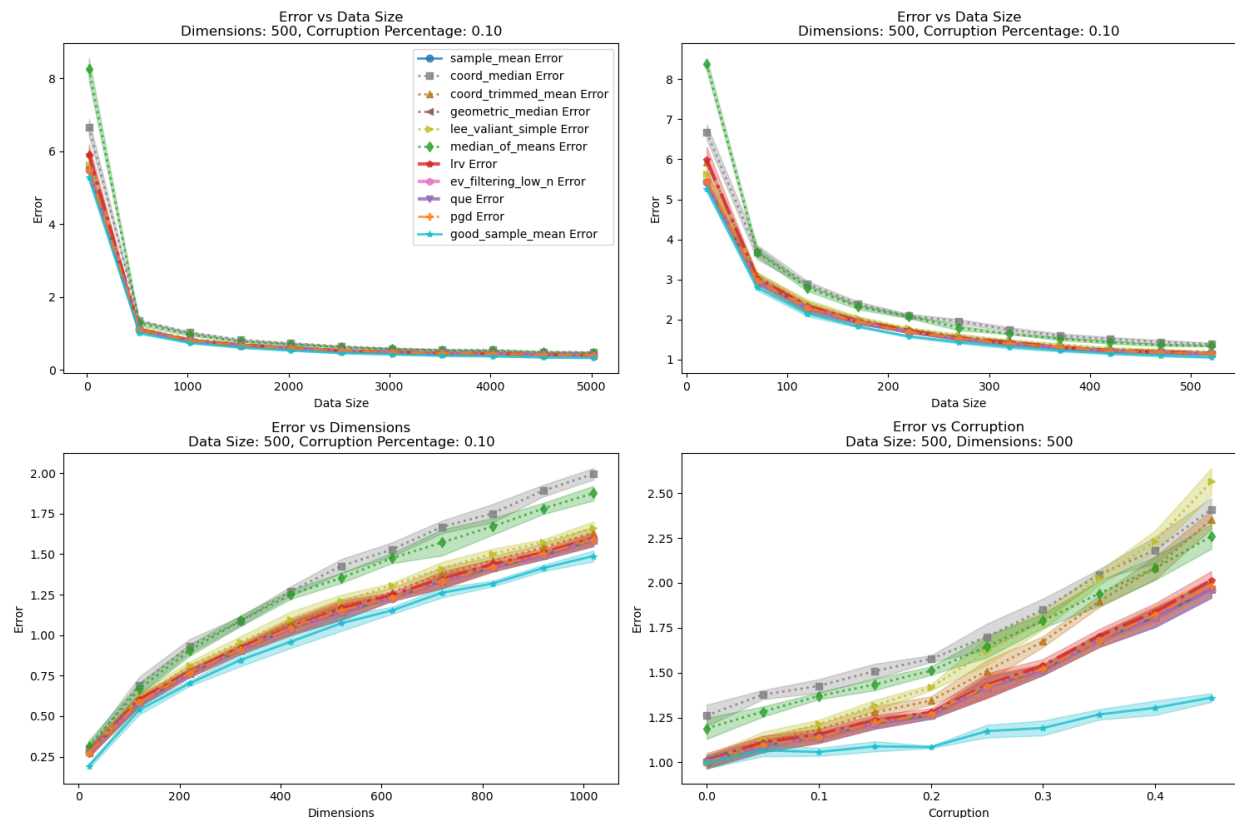
Figure 4: Corrupted Gaussian Identity Covariance: Subtractive Noise

study into robust covariance estimation methods over low data size, which goes beyond the scope of this work. Naively treating robust covariance estimation as robust mean estimation in d^2 dimensions further exasperates issues related to low data size. We also choose to use a simple sample trace estimate rather than the robust approach proposed by Lai et al. (2016). We find that the approach proposed often results in significant underestimates across difficult noise distributions, causing ev_filtering_low_n and QUE_low_n to fail catastrophically. We note that these underestimates are potentially more harmful than overestimates as through them, even the inlier data may not pass the threshold, causing continuous pruning. While a sample trace estimate approach is more prone to overestimates, this can be remedied by naively pruning large outliers. Diakonikolas et al. (2017a) also provides an algorithm for unknown covariance mean estimation similar to ev_filtering, but the corruption detection threshold is not easily adapted to the low data size case.

4.3.1 Unknown Spherical Covariance

We evaluate corrupting noise added to Gaussian data with spherical covariance. We draw $X \sim (1-\eta)P + \eta Q$ where $P = \mathcal{N}_d(\mu, \sigma^2 I)$ and Q describes the additive corrupted data distribution. We consider μ to be the all-fives vector and $\sigma = 5$.

Gaussian noise shifted to scaled variance shell We adapt the identity covariance noise distribution models by appropriately scaling coordinates by σ. We first consider the corrupted data distribution $Q = \mathcal{N}(\mu', \frac{1}{10}I)$ so $\|\mu - \mu'\| = \sigma\sqrt{d}$. With P now having covariance $\sigma^2 I$, $\mathbb{E}_{x \sim P}[\|x - \mu\|^2] = \sigma^2 d$, and corrupted data from Q is not easily identified. Results are show in Figure 5.

While the overall error here is higher, matching the theory that even for uncorrupted data, the sample mean is expected to have error of $O(\sigma\sqrt{d/n})$, the relative performance of algorithms is nearly identical to the identity covariance case. ev_filtering_low_n, QUE_low_n, and PGD nearly match good_sample_mean error
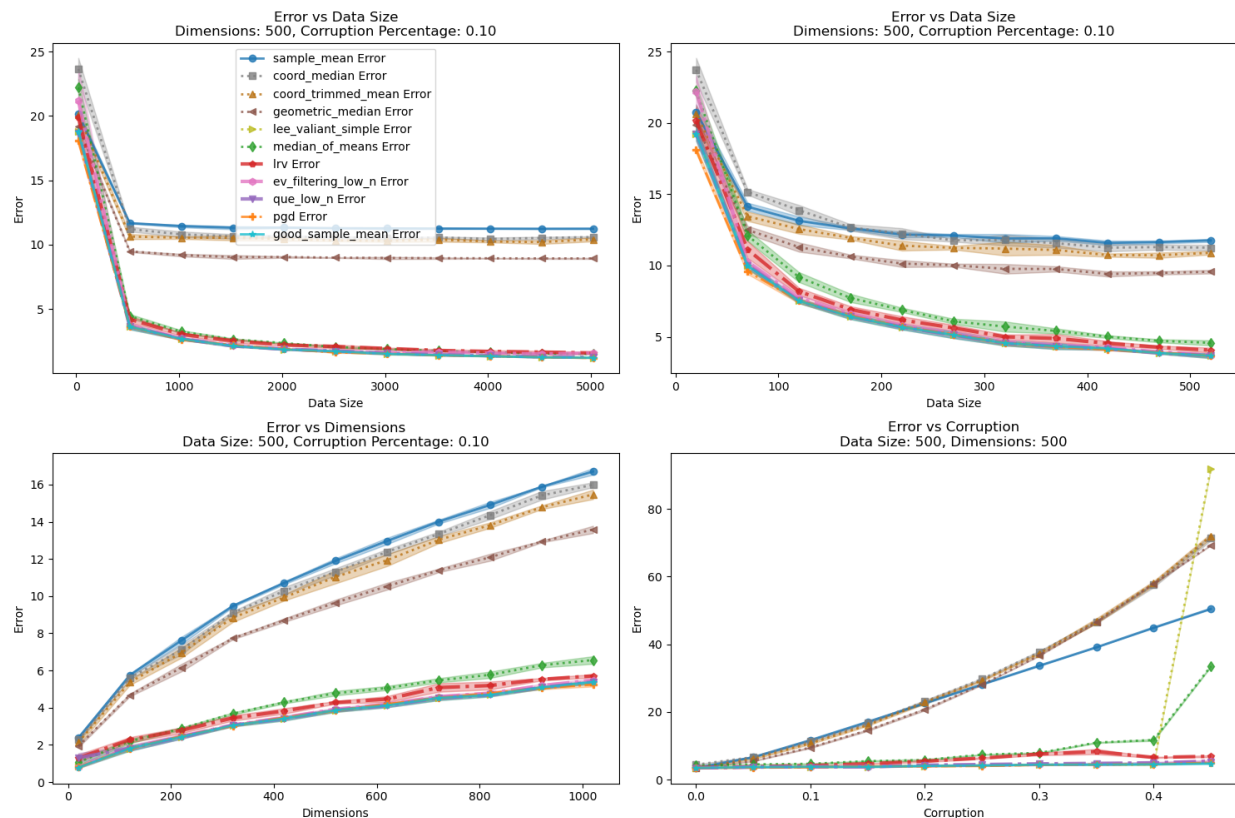
Figure 5: Corrupted Gaussian Large Spherical Covariance: Additive Variance Shell Noise

throughout, with LRV performing only slightly worse. median_of_means lags behind both estimators but still performs noticeably better than sample_mean. However, lee_valiant_simple performs much better in this scenario, nearly exactly matching good_sample_mean except with large enough corruption – where with $\eta = 0.45$, it and median_of_means probably confuse which points are inliers and have much worse error. Other methods perform similarly to sample_mean or worse.

As in the identity covariance case, we find similar results across noise distributions. The only notable exception is for ev_filtering_low_n, which sometimes performs slightly worse and doesn't always converge to good_sample_mean error as n increases, probably due to instabilities in the trace scaling heuristic. We additionally show that relative performance of algorithms is mostly independent of the choice of σ. The exception to this is LRV, which notably outperforms all other methods, including good_sample_mean, with large enough σ across noise distributions. These details are deferred to Appendix A.3.

Unknown Non-Spherical Covariance In Appendix A.4 we also explore the unknown, non-spherical covariance case. This is even more sensitive to the covariance estimate, and so is further outside the primary scope of this study. Nonetheless, we continue to observe that the best robust estimators, including QUE_low_n, continue to perform well.

5 Large Language Model Experiment

To evaluate whether robust mean estimation methods are overly sensitive to distributional assumptions, we evaluate performance over real world data. We first study the problem of estimating the mean of vectors from language models. Such "word embeddings" have had an enormous impact on natural language processing, starting from simple sparse term-frequency vectors (Robertson et al., 2009). Second generation word embeddings (e.g., GloVE (Pennington et al., 2014) and word2vec (Mikolov et al., 2013)) made the

advancement of creating a "low" dimensional vector (about 300 dimensions) for each word, where Euclidean (and cosine) distances could be used as a proxy for the similarity between words based on how they are used. As a serendipitous side-effect, structure emerged where dot-products, means, and linear classifiers made sense in this embedding space (Bolukbasi et al., 2016; Dev & Phillips, 2019). Third generation embeddings created representations for each word in the context of the nearby words; that is, each use of a word had a different embedding. These were a first main use of transformer architectures, and implicitly capture more meaning and context with progressive layers of a neural network. As is most common, we use the last layer of the embedding network as the representation of a word. Our first study, shown next, uses these third generation word embeddings. Further experiments over deep pretrained image model embeddings and second generation word embeddings are deferred to Appendix A.7 and Appendix A.8, respectively.

We first examine performance over third generation embeddings of a homonym word where all instances correspond to the same meaning. We then examine performance where embeddings corresponding to one meaning of a word are corrupted by embeddings corresponding to another meaning of the same word. Effectively calculating this mean may be important to many downstream tasks (e.g., topic modeling (Griffiths & Steyvers, 2004; Blei & Lafferty, 2009), bias estimation and attenuation (Bolukbasi et al., 2016; Dev & Phillips, 2019)). This models a realistic form of corruption that may arise within LLM embedded data.

We build a dataset of 400 sentences that use the word "field" corresponding to the following definition: "an area of open land, especially one planted with crops or pasture, typically bounded by hedges or fences". We build another dataset of 400 sentences that use the word "field" corresponding to the following, alternate definition: "a particular branch of study or sphere of activity or interest". From now on, we refer to these as "fields of land" and "fields of study". We generated these sentences using ChatGPT-4o. For more details on how we generate this dataset, and the exact sentences used, see Appendix A.10. We embed these sentences and extract the in-context embeddings for the word "field" using 4 LLMs of varying embedding dimensions: MiniLM (Wang et al., 2020), T5 (Raffel et al., 2023), BERT (Devlin et al., 2019), and ALBERT (Lan et al., 2020). MiniLM has an embedding dimension of 384, T5 has one of 512, BERT and ALBERT have embedding dimensions of 768. We choose these 4 LLMs to sample a variety of models across different dimensionalities.

5.1 Common Definition Embeddings

We first consider performance over embeddings corresponding to the same definition. This is analogous to the uncorrupted data case. As an error metric, we use Leave One Out Cross Validaton (LOOCV). We only average over the bottom 90% of errors to account for potential bias introduced by words that less clearly belong to a specific category. LOOCV error is defined here as $\frac{1}{n'}\sum_{i=1}^{n'} \|\text{estimator}(X_{-i}) - x_i\|$ where $n' = 0.9n$ is 90% of the number of data points in the dataset X (those with smallest errors), x_i is the ith data point in X, and X_{-i} is X excluding x_i. LOOCV under the sample mean represents a valuable baseline for comparison as it demonstrates the minimum error to be expected across this data set under the 10% expected corruption ($\tau = 0.1$) modeled by the algorithms. We take the dataset of 400 sentences corresponding to the "field of land" definition. We vary data size from $n = 10$ to $n = 400$, and, as in prior experiments, average results over 5 runs and report shaded regions to denote 1 standard deviation of error. For algorithms that utilize τ, expected corruption, as input, we use the default value of $\tau = 0.1$. We employ the sample trace scaling heuristic for ev_filtering_low_n and QUE_low_n. We additionally halt QUE_low_n whenever more than 2τ percentage of the data has been pruned, regardless of whether or not the threshold is passed. We note that the early halting heuristic is necessary for QUE_low_n to perform well under this setting and that it does not meaningfully improve ev_filtering_low_n; this is further explored in Section 5.3. We show results in Figure 6.

Our results do not match our synthetic experiments, suggesting that some robust mean estimation algorithms are sensitive to (Gaussian) distributional assumptions, at least under small data size. Across LLMs, no algorithm significantly beats the error of sample_mean. Moreover, ev_filtering_low_n performs significantly worse than sample_mean over all embeddings. This is unsurprising due to the sensitivity of ev_filtering_low_n to knowledge of the true covariance. Despite having a similar dependency to knowledge of the true covariance, QUE_low_n achieves performance nearly matching sample_mean error throughout. We also find, that LRV performs meaningfully worse than sample_mean across all LLMs except MiniLM, though not quite
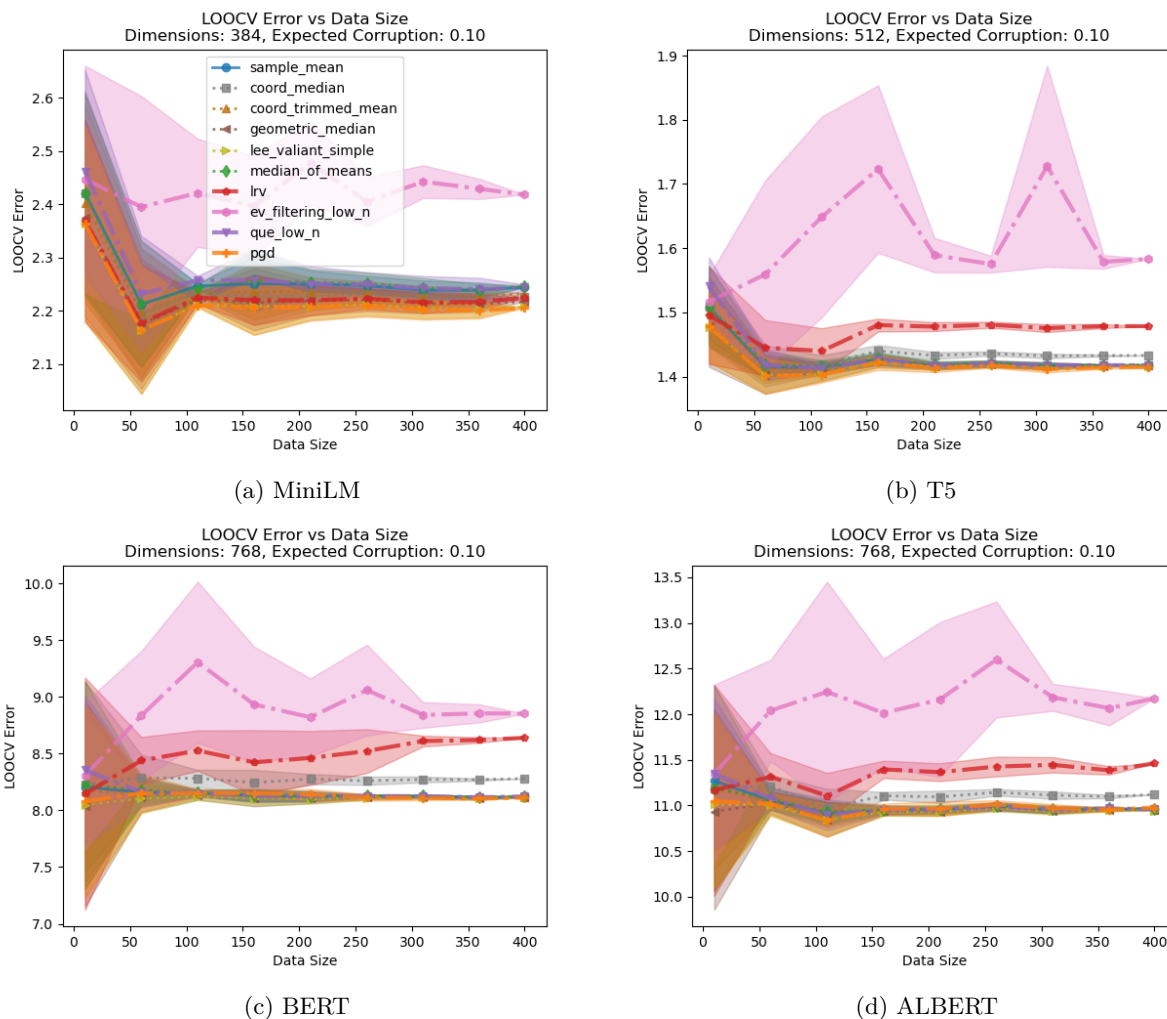
Figure 6: LOOCV Error on "Field of Land" Embeddings

as catostrophically as ev_filtering_low_n. Aside from coord_median, which performs noticeably worse than sample_mean over all LLMs besides MiniLM, all other estimators perform similarly to sample_mean.

5.2 Corrupted Embeddings

We examine performance over corrupted embeddings of the word "field". We draw corrupted data $X \sim (1 - \eta)P + \eta Q$, where the inlier distribution, P, consists of embeddings of the word "field" corresponding to the "field of land" definition, and the outlier distribution, Q, consists of embeddings of the word "field" corresponding to the "field of study" definition. As with previous experiments, we measure the Error $\|\mu - \hat{\mu}\|$ on the y-axis, taking μ as the mean of all 400 "field of land" embeddings, and $\hat{\mu}$ as the estimate returned by a mean estimation algorithm. We measure Error vs η, vary η from 0 to 0.45, and always have $n = 400$. We average results over 5 runs and report shaded regions to represent 1 standard deviation of error. good_sample_mean is plotted to represent the mean of the data before corruption. These results are shown in Figure 7.

We find that mean estimation algorithms can indeed significantly improve performance on this real-world task, but do not observe the same trends as in our synthetic data experiments. QUE_low_n and lee_valiant_simple are the best estimators, with both significantly outperforming sample_mean. In fact, QUE_low_n performs nearly identical to good_sample_mean across all LLMs, and lee_valiant_simple per-
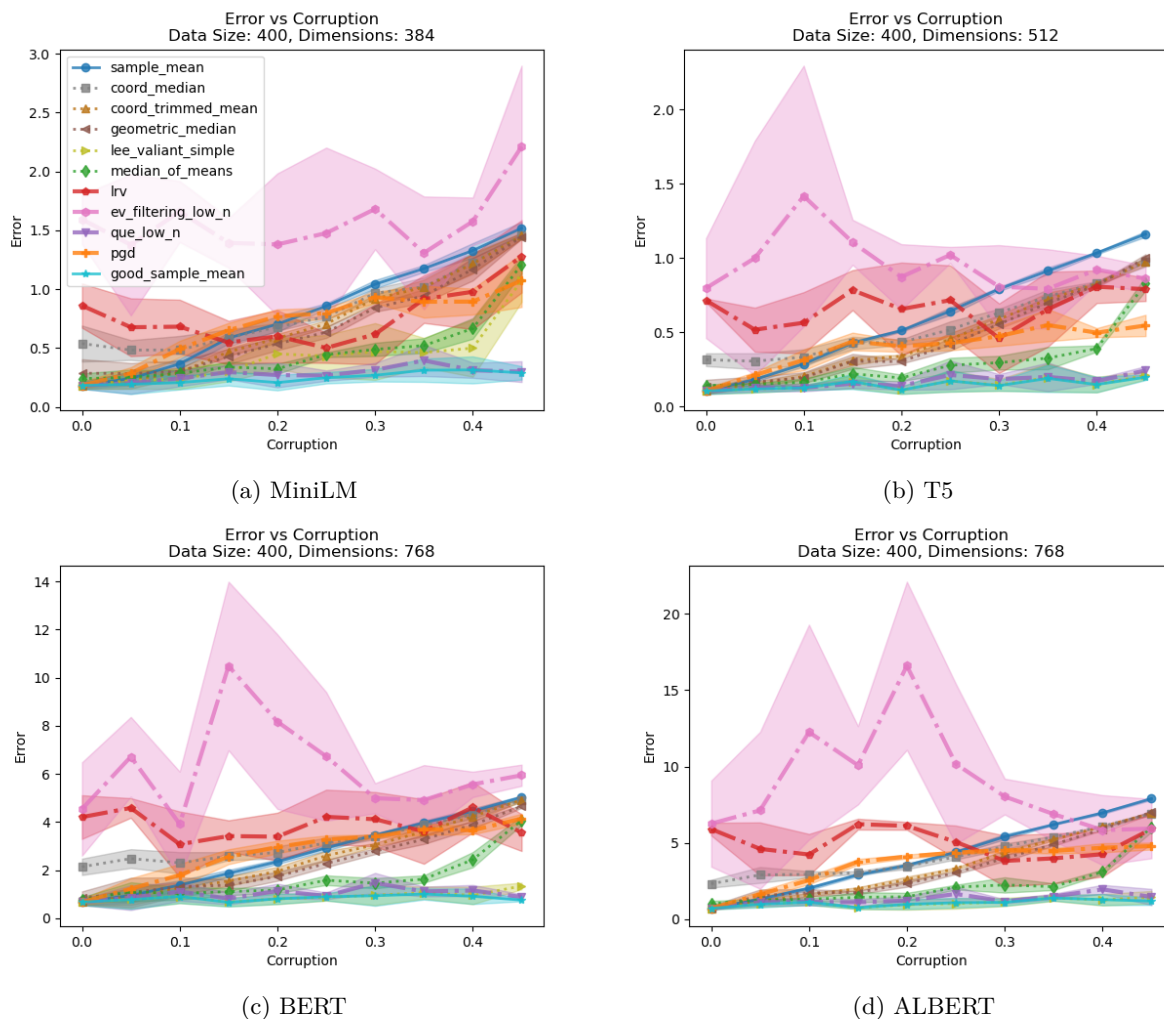
Figure 7: Error on "Field of Land" Embeddings Corrupted with "Field of Study" Embeddings

forms similarly, except on MiniLM, where it degrades worse with larger η but still outperforms sample_mean. The performance of lee_valiant_simple supports the observation that it is a more effective naive pruning method, which happens to work among the best in these experiments. Moreover, median_of_means performs very effectively here, always significantly outperforming sample_mean. However, neither ev_filtering_low_n nor LRV perform effectively. LRV outperforms sample_mean with large enough η, but these results are not consistent across LLMs suggesting sensitivity to distributional assumptions. Additionally, it almost never outperforms median_of_means, lee_valiant_simple, or QUE_low_n and achieves much worse error with lower η. This may suggest that LRV finds irregularities in the uncorrupted data, causing it to return a mean significantly different from good_sample_mean. While this could be beneficial, suggesting that good_sample_mean isn't the best error metric, this is not supported by the "uncorrupted" LOOCV error results, where LRV also generally results in degraded LOOCV error. ev_filtering_low_n fails catastrophically across LLMs. This matches the "uncorrupted" LOOCV error results, supporting the observation that ev_filtering_low_n may fail catostrophically without sufficient knowledge of the true covariance matrix. As in the "uncorrupted" LOOCV error results, there is the somewhat surprising observation that despite seemingly having a similar dependency on knowledge of the true covariance matrix to ev_filtering_low_n, QUE_low_n performs nearly optimally here. This suggests the superiority of the quantum entropy based scoring method over naively ranking outliers based on the top eigenvalue of the sample covariance.

(a) LOOCV - MiniLM

(b) LOOCV - BERT

(c) Corruption - MiniLM

(d) Corruption - BERT
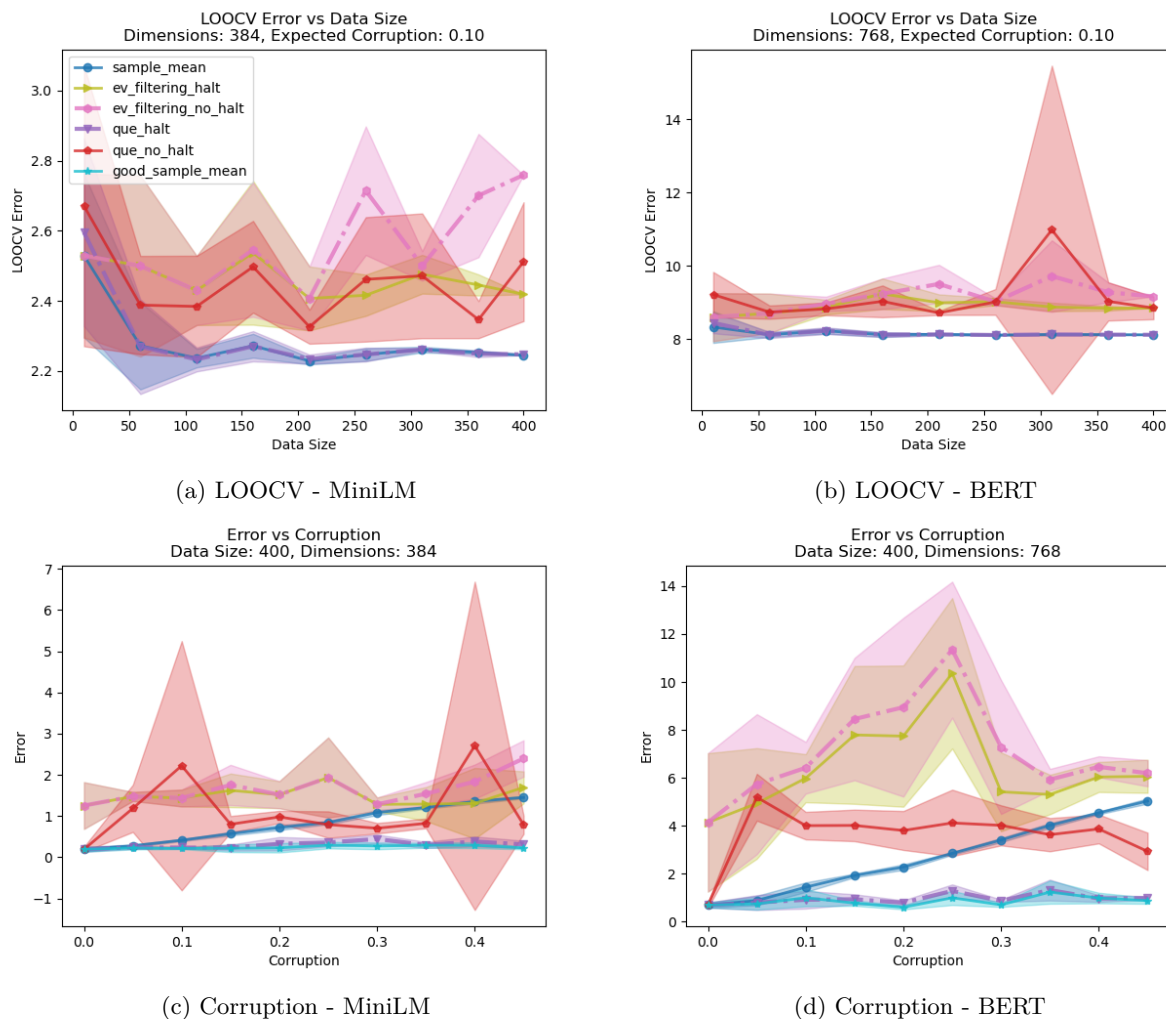
Figure 8: LLM Comparison - With and without *early halting*

5.3 Effect Of Early Halting and Ablation

Early halting is the following strategy with respect to a given threshold τ: If more than 2τ points have been pruned by an algorithm, then this halts the pruning process (independent of other criteria) and returns the sample mean of remaining data.

Here we examine the effect of early halting on QUE_low_n and ev_filtering_low_n in the context of these real world data where inliers are not generated directly from a prescribed Gaussian distribution. In other settings explored in this paper, this strategy is almost never invoked, so has no visible effect. We compare the performance of both of these algorithm with and without enforcing early halting. We examine LOOCV and Corruption Error over MiniLM and BERT embeddings. Results are shown in Figure 8. Across all 4 experiments the performance of QUE_low_n shows significant degradation without early halting, going from nearly matching sample_mean in LOOCV error and nearly matching good_sample_mean in corrupted error, to yielding error significantly worse than sample_mean and good_sample_mean without early halting. Additionally, QUE_low_n without halting yields far larger variance results. Meanwhile, ev_filtering_low_n performs only slightly better with early halting, and still fails catastrophically across experiments.

We perform further ablations on these LLM experiments in Appendix A.9. We explore the effect of different pruning methods on ev_filtering_low_n and different weighting methods on LRV. In both cases, we find that

LOOCV error can be improved using non-Gaussian pruning and weighting methods, whereas corrupted error is not meaningfully improved. The failure of ev_filtering_low_n across pruning methods suggests the fundamental sensitivity of the outlier scoring method used in ev_filtering_low_n to distributional assumptions, which is not seen in QUE_low_n (with early halting). We additionally examine performance over these same experiments with the roles of "field of study" and "field of land" embeddings flipped, finding nearly identical results despite differences in distribution.

(a) ResNet-50 2048 Dimensional Image Embeddings: Cat Images Corrupted With Dog Images

(b) GloVe 300 Dimensional Word Embeddings: Pleasant Words Corrupted With Unpleasant Words
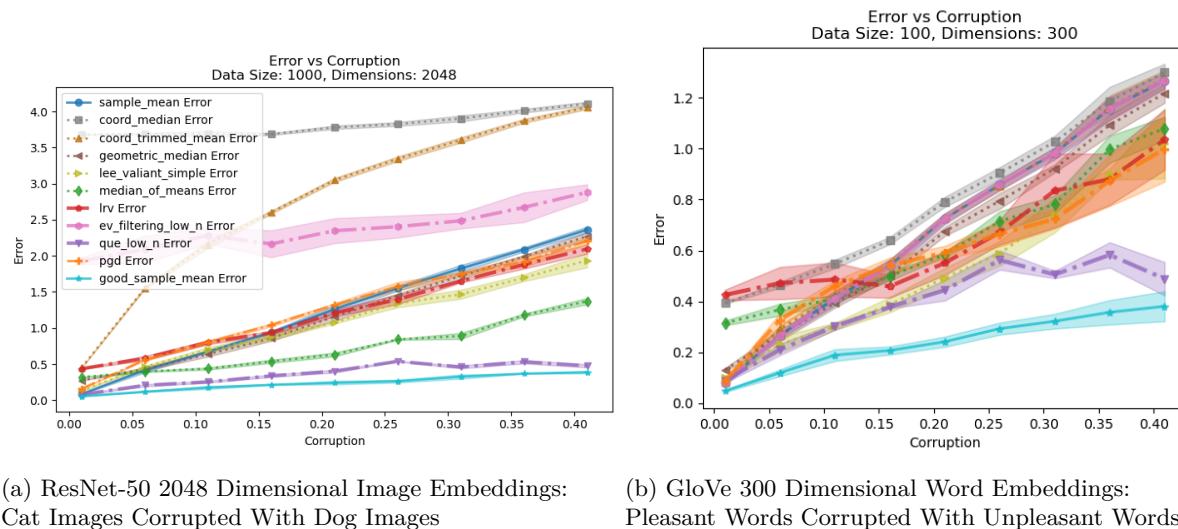
Figure 9: Additional Real World Corrupted Experiments

5.4 Additional Real World Experiments

We additionally examine the performance of robust mean estimation algorithms on corrupted embeddings from deep pretrained image models and non-contextual word embedding models. For the image embedding experiment, we utilize a set of images of cats and dogs from the CIFAR10 dataset (Krizhevsky, 2009) with 2048 dimensional embeddings generated from a pretrained ResNet-50 model (He et al., 2015). For the word embedding experiment, we utilize a dataset of pleasant and unpleasant words from (Aboagye et al., 2023) with 300 dimensional embeddings generated from a pretrained GloVe model (Pennington et al., 2014). Experiments are run analogously to the LLM experiments with identical settings for the mean estimators. For the image embedding experiment, inlier data is defined as embeddings of cat images, outlier data is defined as embeddings of dog images, and data size is fixed at $n = 1000$. For the word embedding experiment, inlier data is defined as embeddings of "pleasant" words, outlier data is defined as embeddings of "unpleasant" words, and data size is fixed at $n = 100$. Results are shown in Figure 9.

We find similar results to the LLM experiments, with QUE_low_n using early halting noticeably outperforming sample_mean across both settings, and nearly matching good_sample_mean over image embeddings. Other robust estimators tend to perform similarly or worse to sample_mean, with ev_filtering_low_n again demonstrating significant degradation without knowledge of distributional assumptions. Additionally, lee_valiant_simple, which performs strongly in the LLM experiments, does not perform as well, demonstrating its sensitivity to distributional assumptions. Similarly, median_of_means, does not perform as well across word embeddings as it does across LLM and image embeddings, no longer noticeably outperforming other estimators.

We find similar results across varying dimensionalities of image embedding and GloVe models. We examine additional image embeddings models of varying dimensionalities under LOOCV and corrupted error in Appendix A.7. We additionally recreate the corrupted data experiment, but vary data size instead of corruption, finding that even with $n \gg d$, only QUE_low_n and median_of_means significantly outperform sample_mean error, with both estimators nearly converging to good_sample_mean error with corruption

$\eta = 0.1$. We also examine GloVe models of varying dimensionalities under LOOCV and corrupted error in Appendix A.8.

6 Non-Gaussian Synthetic Data Experiments

We examine the performance of robust mean estimators across a few non-Gaussian synthetic data experiments. As before, we draw $X \sim (1 - \eta)P + \eta Q$, where P is an inlier data distribution and Q is the corrupted data distribution. Similar to real world experiments, we employ the trace scaling heuristic on ev_filtering_low_n and QUE_low_n and enforce early halting on QUE_low_n if more than a 2τ percentage of the data has been pruned.
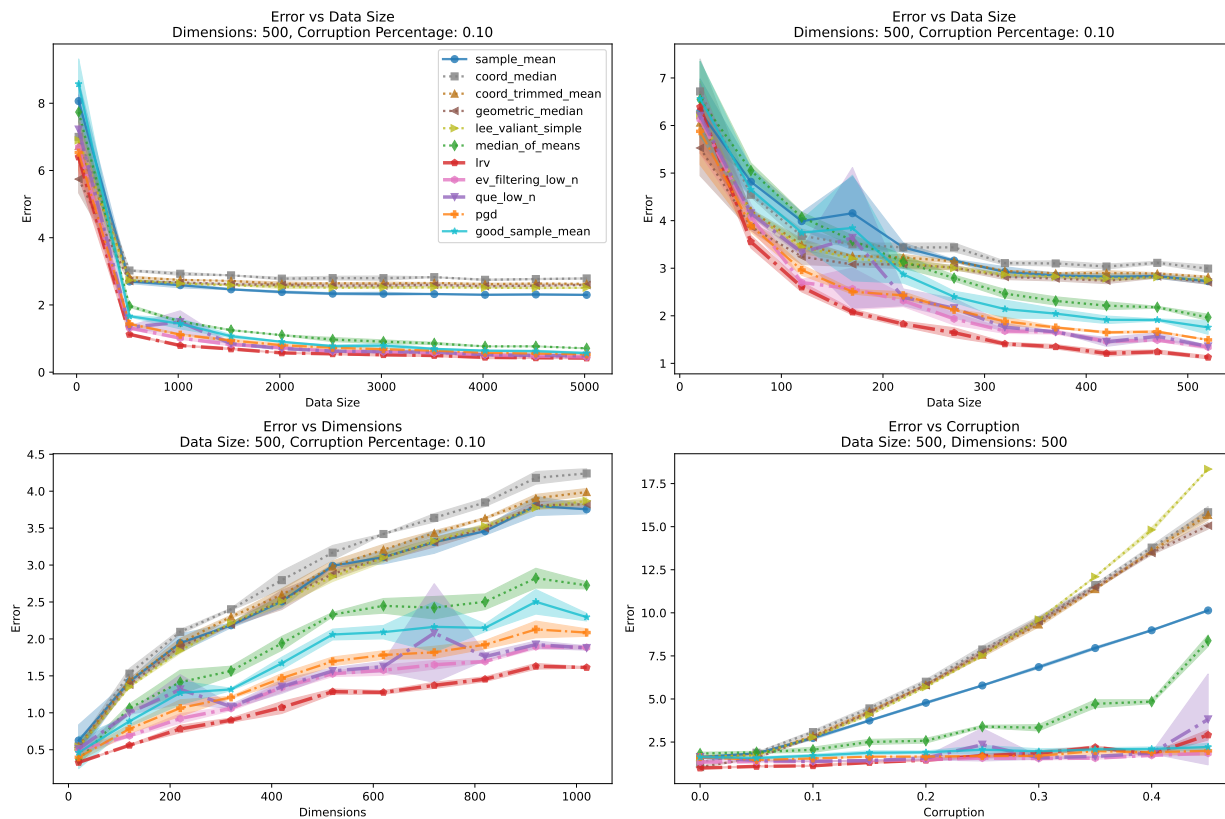
Figure 10: Corrupted Multivariate t-distribution

Multivariate t-distribution Define P as the multivariate t-distribution parametrized by μ as the all-fives vector, Σ as the identity matrix, and degrees of freedom $\nu = 3$. Observe that the covariance is $\frac{\nu}{\nu - 2}\Sigma$, not Σ. This is a heavy-tailed distribution with polynomial tail decay. As in other experiments, consider corrupted data distribution $Q = \mathcal{N}_d(\mu', \frac{1}{10}I)$ where $\|\mu - \mu'\| = \sqrt{d}$. Results are shown in Figure 10. As with the other experiments, QUE_low_n, ev_filtering_low_n, PGD, LRV, and median_of_means all notably outperform sample_mean here. However here, QUE_low_n, ev_filtering_low_n, PGD, and LRV all consistently outperform good_sample_mean. This trend is particularly notable under lower data size and high dimensions. This is explainable given that the sample mean is known to be a sub-optimal estimator for heavy tailed distributions. These results suggest that robust estimators designed for the Huber contamination model have practical application in the heavy-tailed distribution setting. We leave further investigation into this connection to future work, building on Prasad et al. (2019). We also note that there is a more notable separation between the best performing methods in this settings than in the inlier Gaussian data scenario. In

particular, `ev_filtering_low_n` and `LRV` consistently outperform `QUE_low_n`, and also `QUE_low_n` exhibits areas of high variance in error.

Laplace Distribution   Define P as the product distribution of d independent Laplace distributions, each with mean 5 and scale 1. Then, the true mean μ is defined as the all-fives vector. Again, consider corrupted data distribution $Q = \mathcal{N}_d(\mu', \frac{1}{10}I)$ where $\|\mu - \mu'\| = \sqrt{d}$. Results are shown in Figure 11. Results among the best estimators are nearly identical to the Gaussian inlier data scenarios, with `QUE_low_n`, `PGD`, `ev_filtering_low_n` all nearly matching `good_sample_mean` error and with `LRV` performing marginally worse. We note that although the Laplacian distribution has a heavier tail than the Gaussian, we do not observe the same trends as in the multivariate t-distribution. This can be explained by the fact that Laplacian tails still decay exponentially, whereas the tails in the multivariate t-distribution decay polynomially.
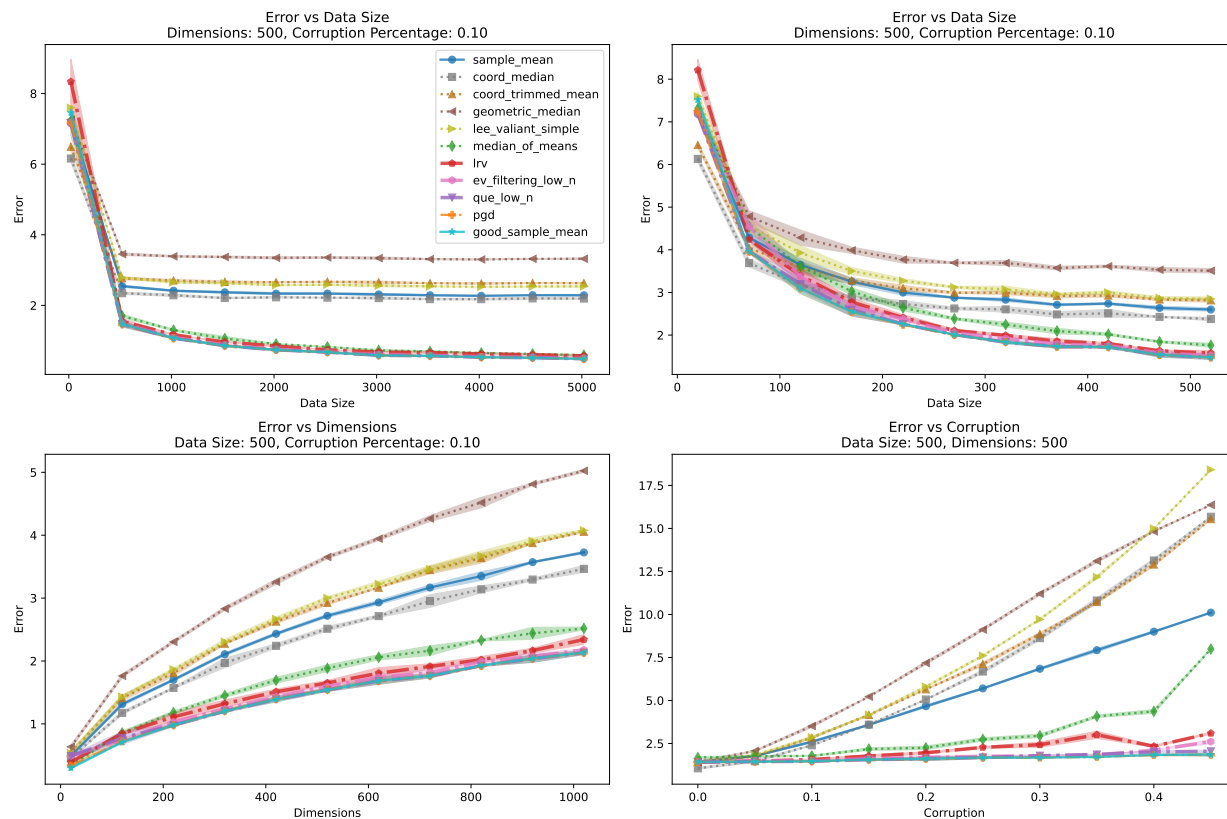
Figure 11: Corrupted Laplace Distribution

Poisson Distribution   Define P as the product distribution of d independent Poisson distributions, each with mean 5. Then, the true mean μ is defined as the all-fives vector. Again consider corrupted data distribution $Q = \mathcal{N}_d(\mu', \frac{1}{10}I)$ where $\|\mu - \mu'\| = \sqrt{d}$. Results are shown in Figure 12. Results among the best estimators are again nearly identical to the Gaussian inlier data scenarios.

Mixture of Gaussians   Define P as a mixture of Gaussians with three components, each equally weighted. The components have means $\mu_1 = \vec{1}$, $\mu_2 = \vec{0}$, and $\mu_3 = -\vec{1}$, where $\vec{1}$ and $\vec{0}$ are the d-dimensional vectors of all ones and all zeros, respectively. Each component has identity covariance. Define Q as $\mathcal{N}(\vec{2}, \frac{1}{10}I)$ where $\vec{2}$ is the all-twos vector. Results are shown in Figure 13. While robust methods tend to outperform `sample_mean`, relative performance here differs from the Gaussian inlier data setting. Firstly, note that `QUE_low_n` does not perform the best and shows irregular areas of high error under lower dimensionality and moderate corruption levels. The observation that `QUE_low_n`, `ev_filtering_low_n`, and `PGD` do not perform as well is likely because they rely significantly on the Gaussianity assumption for the inliers. Methods
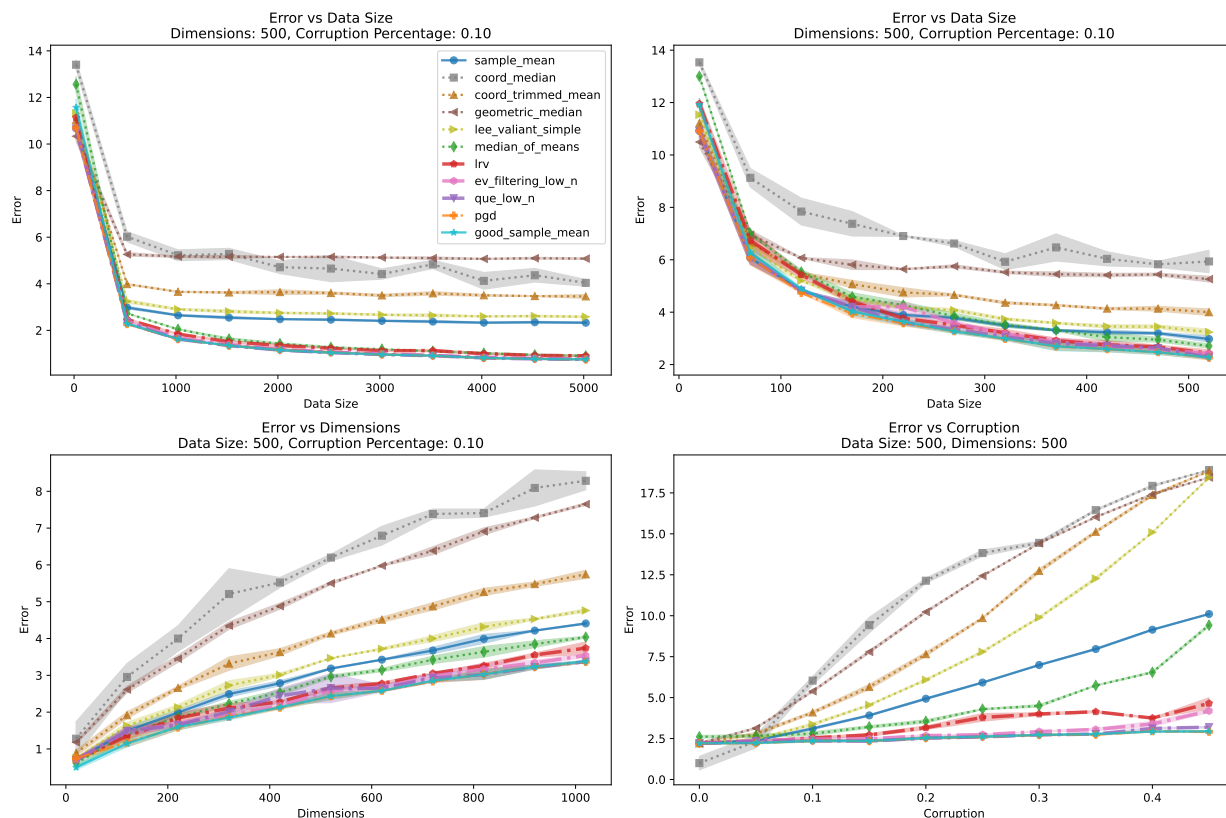
Figure 12: Corrupted Poisson Distribution

such as median_of_means, on the other hand which do not rely as directly on this model are not as effected. Furthermore, ev_filtering_low_n, LRV, and PGD all show significant degradation as corruption levels increase, which is not observed in the Gaussian inlier settings. This may be occurring if they completely filter one of the three "inlier" modes as outliers. Interestingly, LRV notably outperforms all other estimators and even good_sample_mean except with corruption $\tau > 0.2$ and especially for $n < d$. The strong performance of LRV in this setting is interesting, and may be a consequence of the three inlier distributions means lying on a 1-dimensional subspace.

7 Comparing Algorithm Variants and Ablation

In this section, we justify and explore our adaptations to ev_filtering, QUE, and lee_valiant. We use these adaptations for the remainder of our experiments.

Eigenvalue-based Threshold Here we compare ev_filtering and ev_filtering_low_n, along with QUE and QUE_low_n. We observe that when we do not have n very large compared to d, then ev_filtering and QUE can dramatically shift from low error to abysmal error rates.

We recreate the experiment over corrupted Gaussian data with identity covariance and DKK Noise from Section 4.2. This is shown in Figure 14a. We find that ev_filtering and QUE fail catastrophically with insufficient data, performing far worse than sample_mean. However, ev_filtering_low_n and QUE_low_n never perform worse than sample_mean and achieve near optimal performance regardless of data size. With sufficient data, ev_filtering and QUE abruptly begin to work, and achieve near identical performance to their adjusted threshold counterparts.
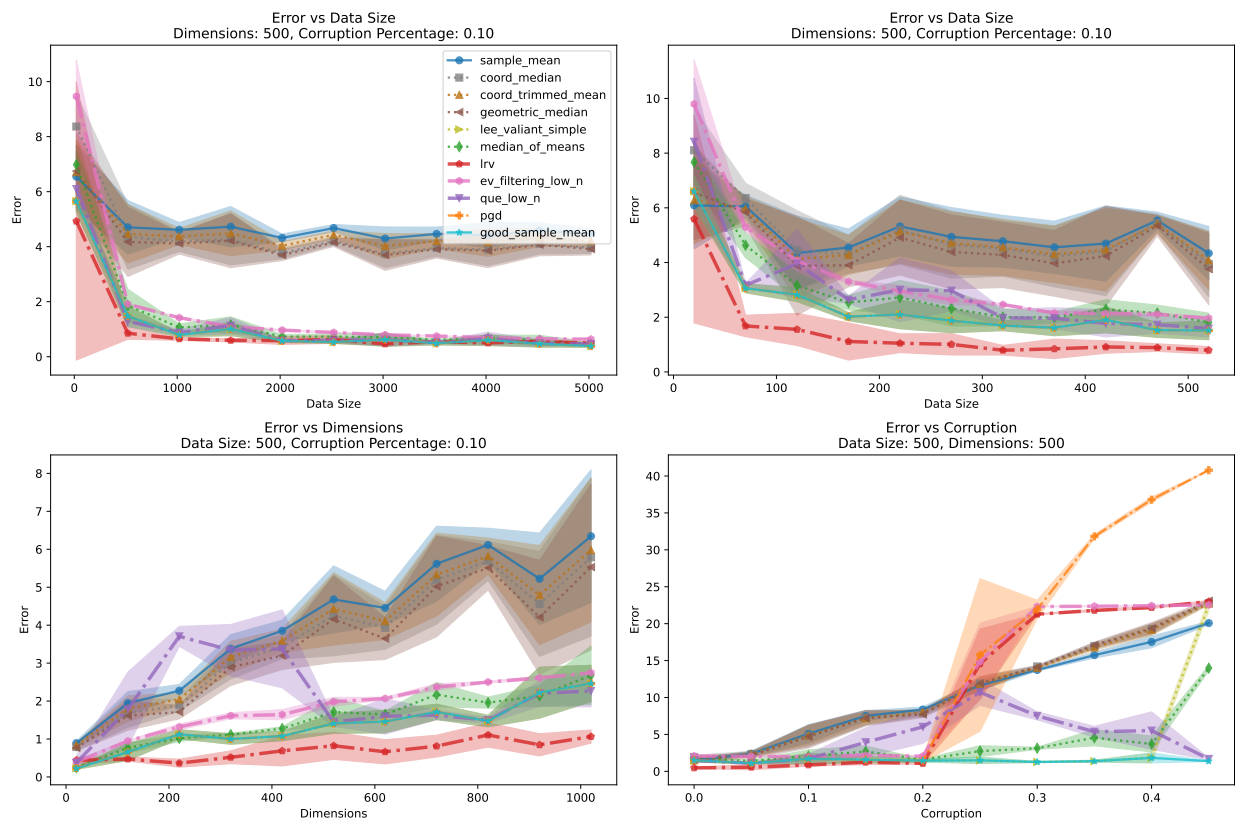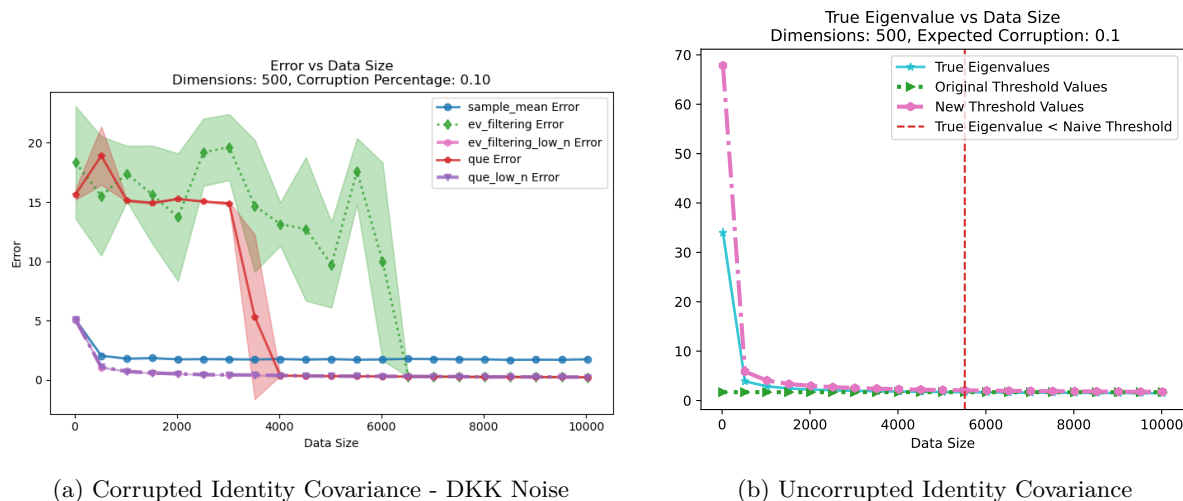
Figure 13: Corrupted Mixture Of Gaussians

(a) Corrupted Identity Covariance - DKK Noise

(b) Uncorrupted Identity Covariance

Figure 14: Eigenvalue Based Filtering Comparison

The failure of ev_filtering and QUE occurs in the corruption detection step. This corruption detection threshold on the top eigenvalue is initialized as $1 + 3\tau \log(1/\tau)$ in ev_filtering and QUE. This constant threshold uses the fact that with large enough data size, the top eigenvalue of an identity covariance matrix approaches 1 and the $3\tau \log(1/\tau)$ term can account for tolerable noise. However, this does not account for corruption due to low data size, in which the top eigenvalue of the uncorrupted data will necessarily

have a larger expectation as data size decreases. Therefore, ev_filtering and QUE can never be expected to work since even without any corruption, the top eigenvalue will exceed the threshold. As a result, we find that ev_filtering and QUE keep on pruning until there are only very few data points left, resulting in the catastrophic error exhibited. ev_filtering_low_n and QUE_low_n remedy this problem by simply incorporating our new result (Corollary 1.1) as a threshold on the top eigenvalue of the covariance matrix in the threshold. This is empirically shown in Figure 14b. The threshold in ev_filtering and QUE does not become a true upper bound on the top eigenvalue of the uncorrupted data until the vertical red line, which roughly corresponds to the point that ev_filtering_low_n begins to perform better. QUE begins to perform better with much less data size than ev_filtering, but this is unsurprising given the rapid convergence of the inlier top eigenvalue to 1. Meanwhile, our new threshold used in ev_filtering_low_n and QUE_low_n is always an upper bound on the top eigenvalue, and is near-optimal in practice.
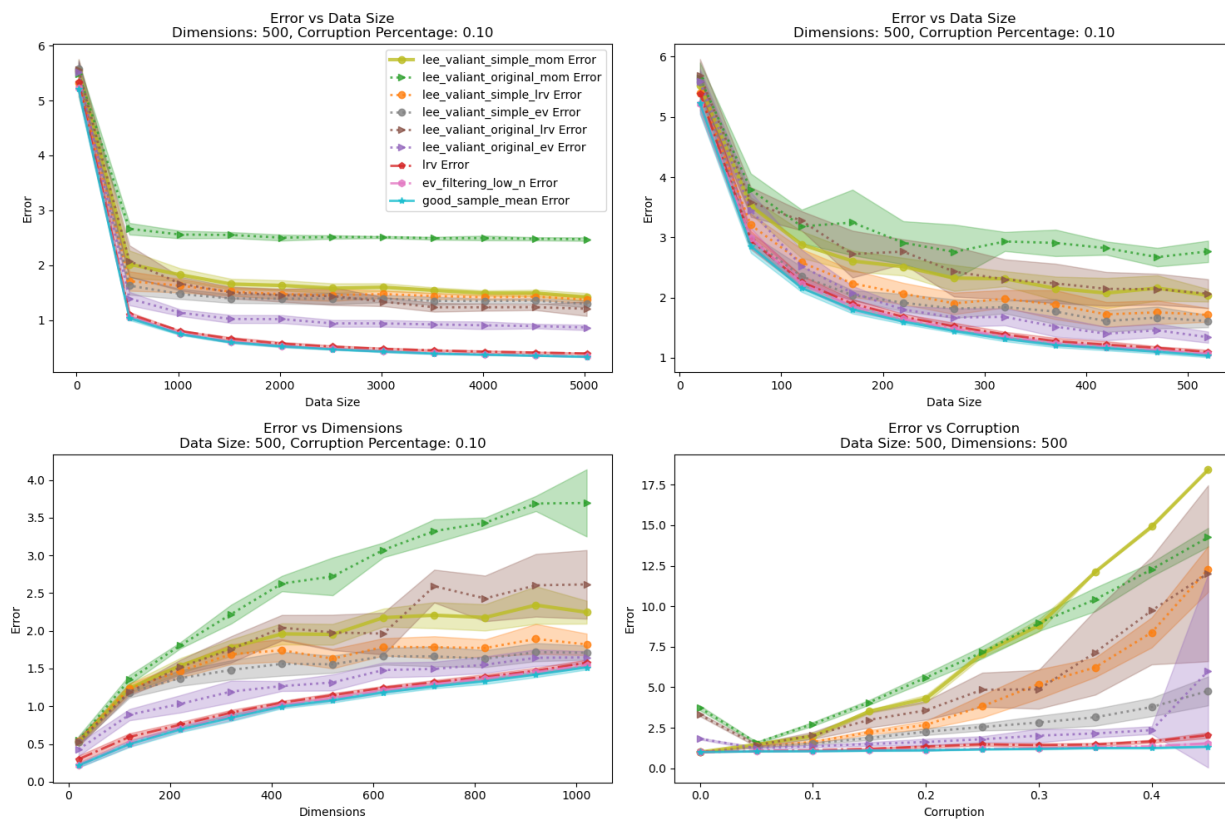

Figure 15: Lee Valiant Variants: Identity Covariance - Additive Variance Shell Noise

Lee and Valiant variants. Here we compare different variants of the Lee and Valiant algorithm. We observe that lee_valiant_simple performs a bit better than lee_valiant, and median_of_means is an illustrative choice for initial estimator. We recreate the experiment over Gaussian data with identity covariance and additive variance shell noise from Section 4.2 across different variants of the Lee and Valiant algorithm. We test lee_valiant_simple and lee_valiant using median_of_means, LRV, and ev_filtering_low_n as initial mean estimators. We additionally plot LRV and ev_filtering_low_n as baselines. This is shown in Figure 15.

lee_valiant_simple differs from lee_valiant in two ways: (1) it removes outliers completely instead of down-weighting them and (2) it does not use initial mean estimate in the final result. We see that lee_valiant_simple performs better than lee_valiant in practice, especially with larger n or d. Both lee_valiant_simple and lee_valiant see benefit in the use of improved initial estimators, with this improvement being more significant in lee_valiant. The difference in the relative improvement in performance between the algorithms is explained by the fact that lee_valiant additively incorporates the initial estimate directly into its final esti-

mate. However, there is no benefit gained from combining lee_valiant or lee_valiant_simple with an improved initial estimator compared to using the initial estimator alone. As a result of these findings, we only evaluate lee_valiant_simple in our experiments.

8 Conclusion

We perform the first wide-scale experimental study of robust mean estimation techniques in high dimensions and relatively-low data size. We showed that under Gaussian data with bounded covariances, robust mean estimation techniques can significantly outperform sample mean, nearly matching the optimal error obtainable, regardless of data size, dimensionality, or corruption level. We provide an updated eigenvalue filtering bound that is useful in this high-dimensional setting, and use it to devise a small but novel and meaningful modification to two existing robust mean estimation algorithms; eigenvalue pruning from Diakonikolas et al. (2019a) and quantum entropy scoring from Dong et al. (2019). This enables these methods to almost exactly match optimal error regardless of data size – that is almost matching the error of the so-called *good sample mean*, which is the mean of the inliers. It seems QUE_low_n works so well because it can identify all ways input distributions deviate from Gaussianity, whereas other methods may require more iterations, which may ultimately prune too many points in the $n \le d$ setting before it is able to filter outliers in each direction that has them.

However, all methods perform significantly worse than the mean of all inliers under *subtractive corruption* where an η-fraction of data points can be removed adversarially. This suggests that in this Gaussian modeled data regime, practical improvements may be possible in considering the effect of subtractive corruption.

We also provide a novel evaluation on realistic settings based on the embeddings generated from large language models, deep pretrained image models, and word embedding models. These are representative of real world settings where the data size n may be smaller or not much larger than the dimension d. In these settings, quantum entropy scoring with early halting tends to perform near optimally, suggesting its potential application to real world data distributions regardless of data size. However, other robust mean estimation algorithms do not work as well as when the inlier data is not Gaussian, as perhaps foreshadowed by theoretical results leveraging this assumption. This suggests that further valuable results may be derived by moving away from the assumption that inliers are precisely Gaussian. Our initial explorations for corrupted data with non-Gaussian inliers shows the same techniques mostly perform well, but which method performs the best can vary based on the inlier distribution. Notably, some methods can even have less error than good_sample_mean when the sample mean is not the MLE.

Overall, our work demonstrates that there is value in applying robust mean estimation techniques to data, even with insufficient data size for the classic theoretical bounds. We hope that our work inspires researchers to further consider, both experimentally and theoretically, the crucial case of high-dimensional robust statistics under low data size.

References

Prince Osei Aboagye, Yan Zheng, Jack Shunn, Chin-Chia Michael Yeh, Junpeng Wang, Zhongfang Zhuang, Huiyuan Chen, Liang Wang, Wei Zhang, and Jeff Phillips. Interpretable debiasing of vectorized language representations with iterative orthogonalization. In *The Eleventh International Conference on Learning Representations*, 2023. URL https://openreview.net/forum?id=TkQ1sxd9P4.

Akshay Agrawal, Robin Verschueren, Steven Diamond, and Stephen Boyd. A rewriting system for convex optimization problems. *Journal of Control and Decision*, 5(1):42–60, 2018.

Hilal Asi, Jonathan Ullman, and Lydia Zakynthinou. From robustness to privacy and back. In *International Conference on Machine Learning*, pp. 1121–1146. PMLR, 2023.

Ainesh Bakshi, Ilias Diakonikolas, He Jia, Daniel M. Kane, Pravesh K. Kothari, and Santosh S. Vempala. Robustly learning mixtures of k arbitrary gaussians. In *Proceedings of the 54th Annual ACM SIGACT Symposium on Theory of Computing*, STOC 2022, pp. 1234–1247, New York, NY, USA, 2022. Association for Computing Machinery. ISBN 9781450392648. doi: 10.1145/3519935.3519953. URL https://doi.org/10.1145/3519935.3519953.

Sivaraman Balakrishnan, Simon S. Du, Jerry Li, and Aarti Singh. Computationally efficient robust sparse estimation in high dimensions. In Satyen Kale and Ohad Shamir (eds.), *Proceedings of the 2017 Conference on Learning Theory*, volume 65 of *Proceedings of Machine Learning Research*, pp. 169–212. PMLR, 07–10 Jul 2017. URL https://proceedings.mlr.press/v65/balakrishnan17a.html.

David M Blei and John D Lafferty. Topic models. In *Text mining*, pp. 101–124. Chapman and Hall/CRC, 2009.

Tolga Bolukbasi, Kai-Wei Chang, James Y Zou, Venkatesh Saligrama, and Adam T Kalai. Man is to computer programmer as woman is to homemaker? debiasing word embeddings. *Advances in neural information processing systems*, 29, 2016.

Olivier Catoni. Challenging the empirical mean and empirical variance: a deviation study, 2011. URL https://arxiv.org/abs/1009.2048.

Moses Charikar, Jacob Steinhardt, and Gregory Valiant. Learning from untrusted data, 2017. URL https://arxiv.org/abs/1611.02315.

Mengjie Chen, Chao Gao, and Zhao Ren. Robust covariance matrix estimation via matrix depth. *arXiv preprint arXiv:1506.00691*, 2015.

Mengjie Chen, Chao Gao, and Zhao Ren. Robust covariance and scatter matrix estimation under huber's contamination model, 2017. URL https://arxiv.org/abs/1506.00691.

Yu Cheng and Honghao Lin. Robust learning of fixed-structure bayesian networks in nearly-linear time, 2021. URL https://arxiv.org/abs/2105.05555.

Yu Cheng, Ilias Diakonikolas, and Rong Ge. High-dimensional robust mean estimation in nearly-linear time. In *Proceedings of the thirtieth annual ACM-SIAM symposium on discrete algorithms*, pp. 2755–2771. SIAM, 2019a.

Yu Cheng, Ilias Diakonikolas, Rong Ge, and David Woodruff. Faster algorithms for high-dimensional robust covariance estimation, 2019b. URL https://arxiv.org/abs/1906.04661.

Yu Cheng, Ilias Diakonikolas, Rong Ge, and Mahdi Soltanolkotabi. High-dimensional robust mean estimation via gradient descent, 2020. URL https://arxiv.org/abs/2005.01378.

Yu Cheng, Ilias Diakonikolas, Rong Ge, Shivam Gupta, Daniel M. Kane, and Mahdi Soltanolkotabi. Outlier-robust sparse estimation via non-convex optimization, 2022. URL https://arxiv.org/abs/2109.11515.

Jules Depersin and Guillaume Lecué. Robust subgaussian estimation of a mean vector in nearly linear time, 2019. URL https://arxiv.org/abs/1906.03058.

Aditya Deshmukh, Jing Liu, and Venugopal V. Veeravalli. Robust mean estimation in high dimensions: An outlier fraction agnostic and efficient algorithm, 2022. URL https://arxiv.org/abs/2102.08573.

Sunipa Dev and Jeff Phillips. Attenuating bias in word vectors. In *The 22nd international conference on artificial intelligence and statistics*, pp. 879–887. PMLR, 2019.

Jacob Devlin, Ming-Wei Chang, Kenton Lee, and Kristina Toutanova. Bert: Pre-training of deep bidirectional transformers for language understanding, 2019. URL https://arxiv.org/abs/1810.04805.

Luc Devroye, Matthieu Lerasle, Gabor Lugosi, and Roberto I. Oliveira. Sub-gaussian mean estimators, 2015. URL `https://arxiv.org/abs/1509.05845`.

Ilias Diakonikolas and Daniel M Kane. *Algorithmic high-dimensional robust statistics*. Cambridge university press, 2023.

Ilias Diakonikolas, Gautam Kamath, Daniel M Kane, Jerry Li, Ankur Moitra, and Alistair Stewart. Being robust (in high dimensions) can be practical. In *International Conference on Machine Learning*, pp. 999–1008. PMLR, 2017a.

Ilias Diakonikolas, Daniel M. Kane, and Alistair Stewart. List-decodable robust mean estimation and learning mixtures of spherical gaussians, 2017b. URL `https://arxiv.org/abs/1711.07211`.

Ilias Diakonikolas, Daniel M. Kane, and Alistair Stewart. Statistical query lower bounds for robust estimation of high-dimensional gaussians and gaussian mixtures, 2017c. URL `https://arxiv.org/abs/1611.03473`.

Ilias Diakonikolas, Weihao Kong, and Alistair Stewart. Efficient algorithms and lower bounds for robust linear regression, 2018. URL `https://arxiv.org/abs/1806.00040`.

Ilias Diakonikolas, Gautam Kamath, Daniel Kane, Jerry Li, Ankur Moitra, and Alistair Stewart. Robust estimators in high-dimensions without the computational intractability. *SIAM Journal on Computing*, 48 (2):742–864, 2019a.

Ilias Diakonikolas, Gautam Kamath, Daniel Kane, Jerry Li, Jacob Steinhardt, and Alistair Stewart. Sever: A robust meta-algorithm for stochastic optimization. In *International Conference on Machine Learning*, pp. 1596–1606. PMLR, 2019b.

Ilias Diakonikolas, Sushrut Karmalkar, Daniel Kane, Eric Price, and Alistair Stewart. Outlier-robust high-dimensional sparse estimation via iterative filtering, 2019c. URL `https://arxiv.org/abs/1911.08085`.

Ilias Diakonikolas, Daniel M. Kane, Sushrut Karmalkar, Ankit Pensia, and Thanasis Pittas. Robust sparse mean estimation via sum of squares. In Po-Ling Loh and Maxim Raginsky (eds.), *Proceedings of Thirty Fifth Conference on Learning Theory*, volume 178 of *Proceedings of Machine Learning Research*, pp. 4703–4763. PMLR, 02–05 Jul 2022. URL `https://proceedings.mlr.press/v178/diakonikolas22e.html`.

Ilias Diakonikolas, Daniel M. Kane, Sushrut Karmalkar, Ankit Pensia, and Thanasis Pittas. Robust sparse estimation for gaussians with optimal error under huber contamination, 2024. URL `https://arxiv.org/abs/2403.10416`.

Steven Diamond and Stephen Boyd. CVXPY: A Python-embedded modeling language for convex optimization. *Journal of Machine Learning Research*, 17(83):1–5, 2016.

Yihe Dong, Samuel B. Hopkins, and Jerry Li. Quantum entropy scoring for fast robust mean estimation and improved outlier detection. In *NeurIPS*, 2019. URL `https://arxiv.org/abs/1906.11366`.

Cynthia Dwork and Jing Lei. Differential privacy and robust statistics. In *Proceedings of the forty-first annual ACM symposium on Theory of computing*, pp. 371–380, 2009.

Thomas L Griffiths and Mark Steyvers. Finding scientific topics. *Proceedings of the National academy of Sciences*, 101(suppl_1):5228–5235, 2004.

Shivam Gupta, Jasper CH Lee, and Eric Price. Finite-sample symmetric mean estimation with fisher information rate. In *The Thirty Sixth Annual Conference on Learning Theory*, pp. 4777–4830. PMLR, 2023.

Shivam Gupta, Samuel B. Hopkins, and Eric Price. Beyond catoni: Sharper rates for heavy-tailed and robust mean estimation, 2024. URL `https://arxiv.org/abs/2311.13010`.

Kaiming He, Xiangyu Zhang, Shaoqing Ren, and Jian Sun. Deep residual learning for image recognition, 2015. URL `https://arxiv.org/abs/1512.03385`.

Samuel B. Hopkins and Jerry Li. How hard is robust mean estimation?, 2019. URL `https://arxiv.org/abs/1903.07870`.

Samuel B. Hopkins, Gautam Kamath, Mahbod Majid, and Shyam Narayanan. Robustness implies privacy in statistical estimation. In *Proceedings of the 55th Annual ACM Symposium on Theory of Computing*, STOC 2023, pp. 497–506, New York, NY, USA, 2023. Association for Computing Machinery. ISBN 9781450399135. doi: 10.1145/3564246.3585115. URL `https://doi.org/10.1145/3564246.3585115`.

Andrew Howard, Mark Sandler, Grace Chu, Liang-Chieh Chen, Bo Chen, Mingxing Tan, Weijun Wang, Yukun Zhu, Ruoming Pang, Vijay Vasudevan, Quoc V. Le, and Hartwig Adam. Searching for mobilenetv3, 2019. URL `https://arxiv.org/abs/1905.02244`.

Wenpeng Hu, Jiajun Zhang, and Nan Zheng. Different contexts lead to different word embeddings. In Yuji Matsumoto and Rashmi Prasad (eds.), *Proceedings of COLING 2016, the 26th International Conference on Computational Linguistics: Technical Papers*, pp. 762–771, Osaka, Japan, December 2016. The COLING 2016 Organizing Committee. URL `https://aclanthology.org/C16-1073`.

PJ Huber. Robust estimation of a location parameter. *Ann. Math. Statist.*, 35:73–101, 1964.

Ayush Jain, Alon Orlitsky, and Vaishakh Ravindrakumar. Robust estimation algorithms don't need to know the corruption level, 2022. URL `https://arxiv.org/abs/2202.05453`.

Adam Klivans, Pravesh K. Kothari, and Raghu Meka. Efficient algorithms for outlier-robust regression, 2020. URL `https://arxiv.org/abs/1803.03241`.

Alex Krizhevsky. Learning multiple layers of features from tiny images. 2009. URL `https://api.semanticscholar.org/CorpusID:18268744`.

Kevin A Lai, Anup B Rao, and Santosh Vempala. Agnostic estimation of mean and covariance. In *2016 IEEE 57th Annual Symposium on Foundations of Computer Science (FOCS)*, pp. 665–674. IEEE, 2016.

Zhenzhong Lan, Mingda Chen, Sebastian Goodman, Kevin Gimpel, Piyush Sharma, and Radu Soricut. Albert: A lite bert for self-supervised learning of language representations, 2020. URL `https://arxiv.org/abs/1909.11942`.

Beatrice Laurent and Pascal Massart. Adaptive estimation of a quadratic functional by model selection. *Annals of statistics*, pp. 1302–1338, 2000.

Jasper CH Lee and Paul Valiant. Optimal sub-gaussian mean estimation in very high dimensions. In *13th Innovations in Theoretical Computer Science Conference (ITCS 2022)*, 2022.

Xiyang Liu, Weihao Kong, Sham Kakade, and Sewoong Oh. Robust and differentially private mean estimation, 2021a. URL `https://arxiv.org/abs/2102.09159`.

Zifan Liu, Jong Ho Park, Theodoros Rekatsinas, and Christos Tzamos. On robust mean estimation under coordinate-level corruption. In Marina Meila and Tong Zhang (eds.), *Proceedings of the 38th International Conference on Machine Learning*, volume 139 of *Proceedings of Machine Learning Research*, pp. 6914–6924. PMLR, 18–24 Jul 2021b. URL `https://proceedings.mlr.press/v139/liu21r.html`.

Gábor Lugosi. Mean estimation in high dimension. In *Proc. Int. Cong. Math*, volume 7, pp. 5500–5514, 2022.

Gabor Lugosi and Shahar Mendelson. Mean estimation and regression under heavy-tailed distributions–a survey, 2019. URL `https://arxiv.org/abs/1906.04280`.

Gábor Lugosi and Shahar Mendelson. Robust multivariate mean estimation: The optimality of trimmed mean. *The Annals*, 49(1):393–410, 2021.

Gábor Lugosi and Shahar Mendelson. Sub-gaussian estimators of the mean of a random vector, 2017. URL `https://arxiv.org/abs/1702.00482`.

27

Tomas Mikolov, Ilya Sutskever, Kai Chen, Greg S Corrado, and Jeff Dean. Distributed representations of words and phrases and their compositionality. *Advances in neural information processing systems*, 26, 2013.

Stanislav Minsker. Efficient median of means estimator, 2023a. URL `https://arxiv.org/abs/2305.18681`.

Stanislav Minsker. U-statistics of growing order and sub-gaussian mean estimators with sharp constants, 2023b. URL `https://arxiv.org/abs/2202.11842`.

Jeffrey Pennington, Richard Socher, and Christopher Manning. GloVe: Global vectors for word representation. In Alessandro Moschitti, Bo Pang, and Walter Daelemans (eds.), *Proceedings of the 2014 Conference on Empirical Methods in Natural Language Processing (EMNLP)*, pp. 1532–1543, Doha, Qatar, October 2014. Association for Computational Linguistics. doi: 10.3115/v1/D14-1162. URL `https://aclanthology.org/D14-1162`.

Adarsh Prasad, Arun Sai Suggala, Sivaraman Balakrishnan, and Pradeep Ravikumar. Robust estimation via robust gradient estimation, 2018. URL `https://arxiv.org/abs/1802.06485`.

Adarsh Prasad, Sivaraman Balakrishnan, and Pradeep Ravikumar. A unified approach to robust mean estimation, 2019. URL `https://arxiv.org/abs/1907.00927`.

Colin Raffel, Noam Shazeer, Adam Roberts, Katherine Lee, Sharan Narang, Michael Matena, Yanqi Zhou, Wei Li, and Peter J. Liu. Exploring the limits of transfer learning with a unified text-to-text transformer, 2023. URL `https://arxiv.org/abs/1910.10683`.

Stephen Robertson, Hugo Zaragoza, et al. The probabilistic relevance framework: Bm25 and beyond. *Foundations and Trends® in Information Retrieval*, 3(4):333–389, 2009.

Christopher G Small. A survey of multidimensional medians. *International Statistical Review/Revue Internationale de Statistique*, pp. 263–277, 1990.

Mingxing Tan and Quoc V. Le. Efficientnet: Rethinking model scaling for convolutional neural networks, 2020. URL `https://arxiv.org/abs/1905.11946`.

Brandon Tran, Jerry Li, and Aleksander Madry. Spectral signatures in backdoor attacks, 2018. URL `https://arxiv.org/abs/1811.00636`.

John W Tukey. Mathematics and the picturing of data. In *Proceedings of the International Congress of Mathematicians, Vancouver, 1975*, volume 2, pp. 523–531, 1975.

Yehuda Vardi and Cun-Hui Zhang. A modified weiszfeld algorithm for the fermat-weber location problem. *Mathematical Programming*, 90:559–566, 2001.

Roman Vershynin. Introduction to the non-asymptotic analysis of random matrices, 2011. URL `https://arxiv.org/abs/1011.3027`.

Wenhui Wang, Furu Wei, Li Dong, Hangbo Bao, Nan Yang, and Ming Zhou. Minilm: Deep self-attention distillation for task-agnostic compression of pre-trained transformers, 2020. URL `https://arxiv.org/abs/2002.10957`.

Banghua Zhu, Jiantao Jiao, and Jacob Steinhardt. When does the tukey median work? In *2020 IEEE International Symposium on Information Theory (ISIT)*, pp. 1201–1206. IEEE, 2020a.

Banghua Zhu, Jiantao Jiao, and Jacob Steinhardt. Robust estimation via generalized quasi-gradients, 2020b. URL `https://arxiv.org/abs/2005.14073`.

Banghua Zhu, Jiantao Jiao, and Jacob Steinhardt. Generalized resilience and robust statistics, 2020c. URL `https://arxiv.org/abs/1909.08755`.

A   Appendix

A.1   Updated Eigenvalue Threshold

Here we leverage a theorem in Vershynin (2011) to bound the complexity of aggregated high-dimensional Gaussian random variables. We will use it in a couple ways.

Theorem 2 (Vershynin (2011) Thm. 5.35). *Let A be a $n \times d$ matrix whose entries are independent standard normal random variables. Let $\|A\|_2$ denote the spectral norm of A. Then for every $t \geq 0$, with probability of at least $1 - 2\exp(-t^2/2)$, one has*

$$\sqrt{n} - \sqrt{d} - t \leq s_{\min}(A) \leq \|A\|_2 \leq \sqrt{n} + \sqrt{d} + t.$$

Where $s_{\min}(A)$ is the smallest singular value of A. The lower bound assumes $n > d$, if not the roles are reversed.

We prove the following implication.

Theorem 3 (restatement of Theorem 1). *Let X be a $n \times d$ matrix whose entries are independently drawn from $\mathcal{N}(\mu, I)$. Let $\Sigma = \frac{1}{n}(X - \bar{\mu})^T(X - \bar{\mu})$ be the sample covariance matrix of X, where $\bar{\mu} = \frac{1}{n}\sum_i X_i$ and X_i is the ith row of X. Then for every $t > 0$, with probability of at least $1 - 3\exp(-t^2/2)$, one has*

$$\|\Sigma\|_2 \leq \left(1 + \sqrt{d/n} + t/\sqrt{n} + \frac{\sqrt{d + \sqrt{2d}t + t^2}}{n}\right)^2.$$

Proof. Let $\bar{X} = X - \mu$ be the centered matrix, equivalent to each entry being drawn from $\mathcal{N}(0, I)$. Let $Z = X - \bar{\mu}$ be the matrix centered by the sample mean. Then $\|Z\|_2 = \|\bar{X} + [\mu - \bar{\mu}]\|_2 \leq \|\bar{X}\|_2 + \|\mu - \bar{\mu}\|_2$ by triangle inequality.

First, by Theorem 2, we have that $\|\bar{X}\|_2 \leq \sqrt{n} + \sqrt{d} + t$, with probability at least $1 - 2\exp(-t^2)$.

Second, to bound $\|\mu - \bar{\mu}\|_2$ we first decompose by coordinate $\|\mu - \bar{\mu}\|_2^2 = \sum_{j=1}^d (\mu_j - \bar{\mu}_j)^2$. Now consider d random variables $B_j = \mu_j - \bar{\mu}_j$ for $j = 1 \ldots d$, and further write $B_j = \frac{1}{n}\sum_{i=1}^n F_i$ where $F_i \sim \mathcal{N}(0, 1)$. As a result $B_j \sim \mathcal{N}(0, 1/n) = \frac{1}{\sqrt{n}}\mathcal{N}(0, 1)$, since the average of n normals is still normal with variance reduced by factor n. As a result B_j is a squared normal distribution, and $B = n\|\mu - \bar{\mu}\|^2 = n\sum_{j=1}^d B_j^2$ is a chi-squared distribution $\chi^2(d)$. Hence we have (Laurent & Massart, 2000)

$$\Pr[B \geq d + 2\sqrt{d}t + 2s^2] \leq \exp(-s^2).$$

Inside the probability expression, using $\sqrt{B/n} = \|\mu - \bar{\mu}\|$, and letting $t = \sqrt{2}s$, we can rewrite this as

$$\Pr\left[\|\mu - \bar{\mu}\| < \sqrt{(d + \sqrt{2}\sqrt{d}t + t^2)/n}\right] \geq 1 - \exp(-t^2/2).$$

So now if both of these events hold, which by union bound occurs with probability at least $1 - 3\exp(-t^2/2)$, we have that

$$\|Z\|_2 \leq \|\bar{X}\|_2 + \|\mu - \bar{\mu}\| \leq (\sqrt{n} + \sqrt{d} + t) + \sqrt{\frac{d + \sqrt{2d}t + t^2}{n}}$$

Notice that $\|\Sigma\|_2 = \|\frac{1}{n}Z^T Z\|_2 = \frac{\|Z\|_2^2}{n}$. Thus we have

$$\|\Sigma\|_2 = \frac{\|Z\|_2^2}{n} \leq \left(1 + \sqrt{d}/\sqrt{n} + t/\sqrt{n} + \frac{\sqrt{d + \sqrt{2d}t + t^2}}{n}\right)^2$$

$\square$

Note that the fourth term in this bound, coming from the error in $\|\mu - \bar\mu\|$, is a lower order effect. This is captured in the following corollary.

Corollary 3.1 (restatement of Corollary 1.1)**.** *Let X be a $n \times d$ matrix whose entries are independently drawn from $\mathcal{N}(\mu, I)$. Let $\Sigma = \frac{1}{n}(X - \bar\mu)^T(X - \bar\mu)$ be the sample covariance matrix of X, where $\bar\mu = \frac{1}{n}\sum_i X_i$ and X_i is the ith row of X. If one assumes $d/n \leq 16, n \geq 16, t \geq 5$, then with probability of at least $1 - 3\exp(-t^2/8)$, one has*

$$\|\Sigma\|_2 \leq \left(1 + \sqrt{d/n} + t/\sqrt{n}\right)^2.$$

Proof. Starting with the bound in Theorem 3 we have

$$\|\Sigma\|_2 \leq \left(1 + \sqrt{d/n} + t/\sqrt{n} + \frac{\sqrt{d + \sqrt{2d}t + t^2}}{n}\right)^2$$

$$= \left(1 + \sqrt{d/n} + t/\sqrt{n} + \frac{t}{\sqrt{n}} \cdot \frac{\sqrt{d/t^2 + \sqrt{2d}/t + 1}}{\sqrt{n}}\right)^2$$

$$= \left(1 + \sqrt{d/n} + \frac{t}{\sqrt{n}}\left(1 + \sqrt{(d/n)/t^2 + \sqrt{2}\sqrt{d/n}/t/\sqrt{n} + 1/n}\right)\right)^2$$

$$\leq \left(1 + \sqrt{d/n} + \frac{t}{\sqrt{n}}\left(1 + \sqrt{(16)/t^2 + \sqrt{2}\sqrt{16}/t/\sqrt{n} + 1/n}\right)\right)^2$$

$$\leq \left(1 + \sqrt{d/n} + \frac{t}{\sqrt{n}}\left(1 + \sqrt{16/25 + \sqrt{32}/(5\sqrt{n}) + 1/n}\right)\right)^2$$

$$\leq \left(1 + \sqrt{d/n} + \frac{t}{\sqrt{n}}\left(1 + \sqrt{16/25 + \sqrt{32}/(5 \cdot 4) + 1/16}\right)\right)^2$$

$$< \left(1 + \sqrt{d/n} + 2t/\sqrt{n}\right)^2$$

Adjusting t to $2t$ in the probability of failure, so it is $3\exp(-t^2/8)$ instead of $3\exp(-t^2/2)$, completes the proof. $\square$

A.2 Corrupted Gaussian Data Identity Covariance: Additional Noise Schemes

We examine the performance of robust mean estimators across additional corruption schemes. We still draw $X \sim (1-\eta)P + \eta Q$ where $P = \mathcal{N}_d(\mu, I)$ and Q describes the corrupted data distribution, where μ is the all-fives vector. We utilize the following additional corruption schemes:

Two Gaussian clusters shifted to variance shell. Consider corrupted data distribution $Q = 0.7\mathcal{N}_d(\mu^0, \frac{1}{10}I) \cup 0.3\mathcal{N}_d(\mu^1, \frac{1}{10}I)$ where $\|\mu - \mu^0\| = \sqrt{d}$, $\|\mu - \mu^1\| = \sqrt{d}$, and $\theta = 75°$ where θ is the angle between μ^0 and μ^1. The location of μ^0 is determined by a random rotation matrix to prevent any coordinate-axis specific biases. Results over this noise distribution are shown in Figure 16.

In Distribution Noise. Consider corrupted data distribution, Q, where for each corrupted data point $q_i \in Q$, each coordinate j of q_i is drawn from $\mathsf{Uniform}(\mu_j, \mu_j + 2)$. Here μ_j represents the jth coordinate of the true mean μ. Results over this noise distribution are shown in Figure 17.

Large Outlier Noise. Consider corrupted data distribution $Q = 0.7\mathcal{N}_d(\mu^0, \frac{1}{10}I) \cup 0.3\mathcal{N}_d(\mu^1, \frac{1}{10}I)$ where $\|\mu - \mu^0\| = 10\sqrt{d}$, $\|\mu - \mu^1\| = 20\sqrt{d}$, and $\theta = 75°$ where θ is the angle between μ^0 and μ^1. The location of μ^0 is determined by a random rotation matrix to prevent any coordinate-axis specific biases. Results over this noise distribution are shown in Figure 18.

Large Outlier Noise Mixes. Consider corrupted data distribution $Q = 0.5L \cup 0.5Q'$ where L is the large outlier corruption scheme previously described and Q' is a subtle corruption scheme. We examine two settings for Q': additive variance shell corruption with one cluster, shown in Figure 19, and DKK corruption, shown in Figure 20.
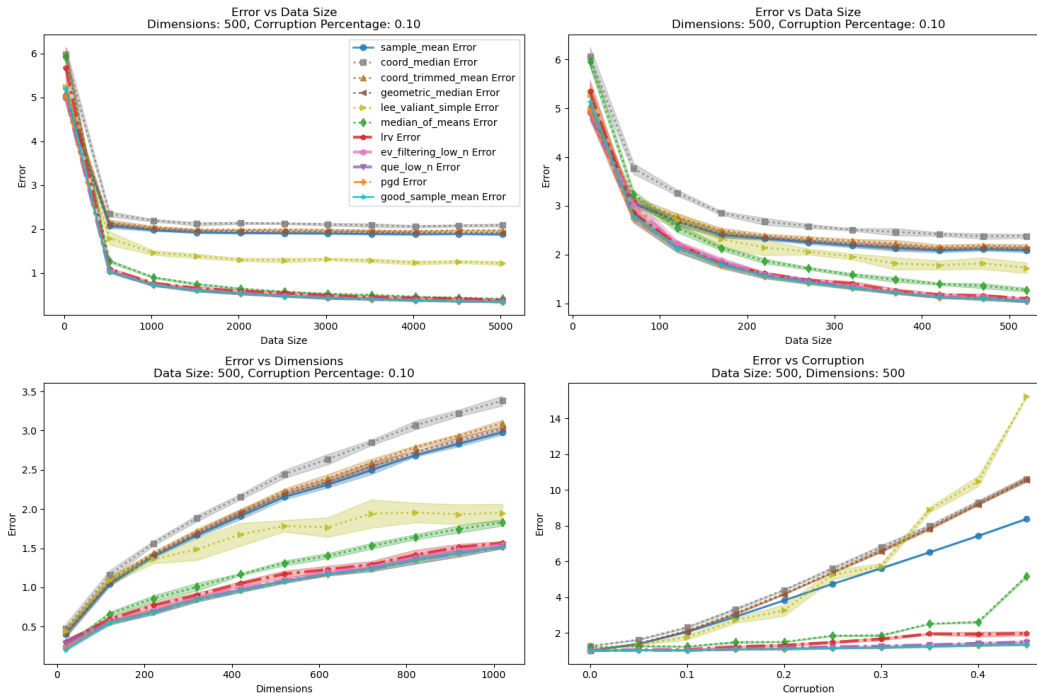

Figure 16: Corrupted Gaussian Identity Covariance: Two Variance Shell Clusters

Across all of these distributions, including those with large outliers, ev_filtering_low_n, QUE_low_n, PGD, and LRV perform the best, suggesting that their performance is not overly sensitive to the noise distribution. However, we note that across schemes with large outliers, PGD sees areas of higher variance and slightly worse performance, and LRV degrades worse as η increases with large outliers. This downgrade in performance can be remedied by first preprocessing data by removing large outliers through a naive pruning method, but this step doesn't appear necessary for other methods. We remark that LRV requires outlier weights to be clipped to avoid numerical instability issues under large outlier schemes. Otherwise, it will degrade poorly over large outliers and large η as predicted outliers will be assigned near-zero weights. We also see again that median_of_means significantly outperforms other simple estimators, especially under large data size, although its performance degrades poorly under certain conditions, such as with larger η. With large outliers, lee_valiant_simple nearly matches good_sample_mean error across conditions, achieving much better performance than it does across subtle noise distributions. As it additionally outperforms coord_trimmed_mean, this suggests that lee_valiant_simple may operate as a more effective naive pruning method, as seen in the LLM experiments.

Dependence on true mean We additionally verify that performance does not depend on the choice of true mean, μ. We recreate experiments over Additive Variance Shell Noise and DKK Noise over different choices of μ. We replicate the same experimental setup as before, but draw every coordinate of μ from $\mathcal{N}(0, 50)$ at every iteration in the experiment rather than fixing μ as the all-fives vector. As a reminder, this occurs for every choice of the independent variable over every run. If performance depended on μ, we would expect to achieve high variance results. Instead, we find nearly identical results to the original experiments across both distributions. These results are shown in Figure 21 and Figure 22.
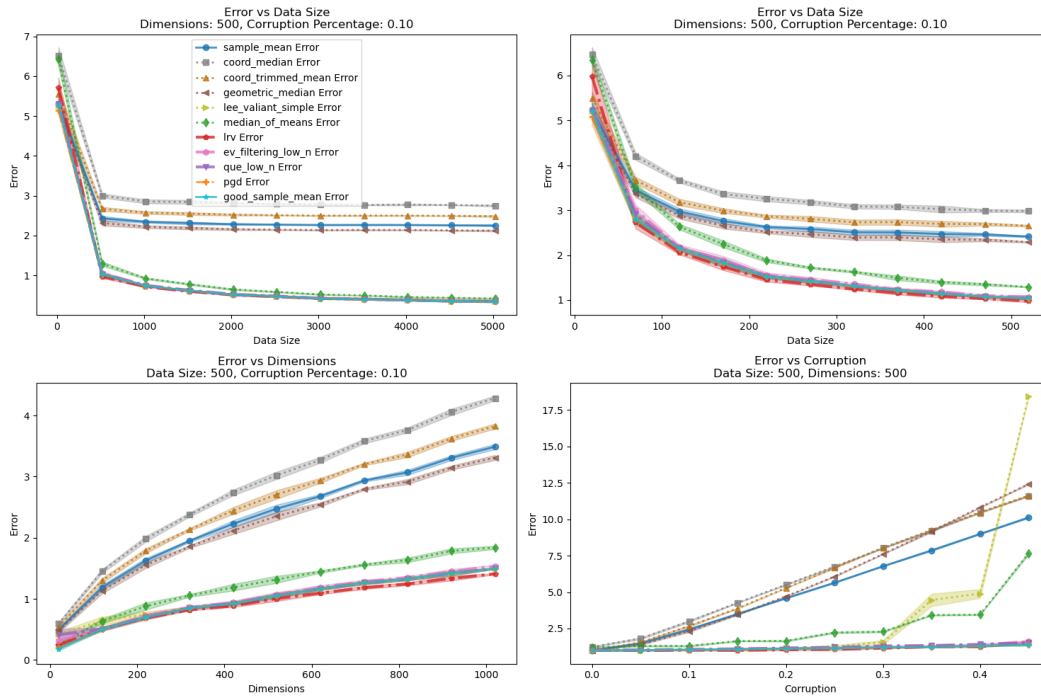
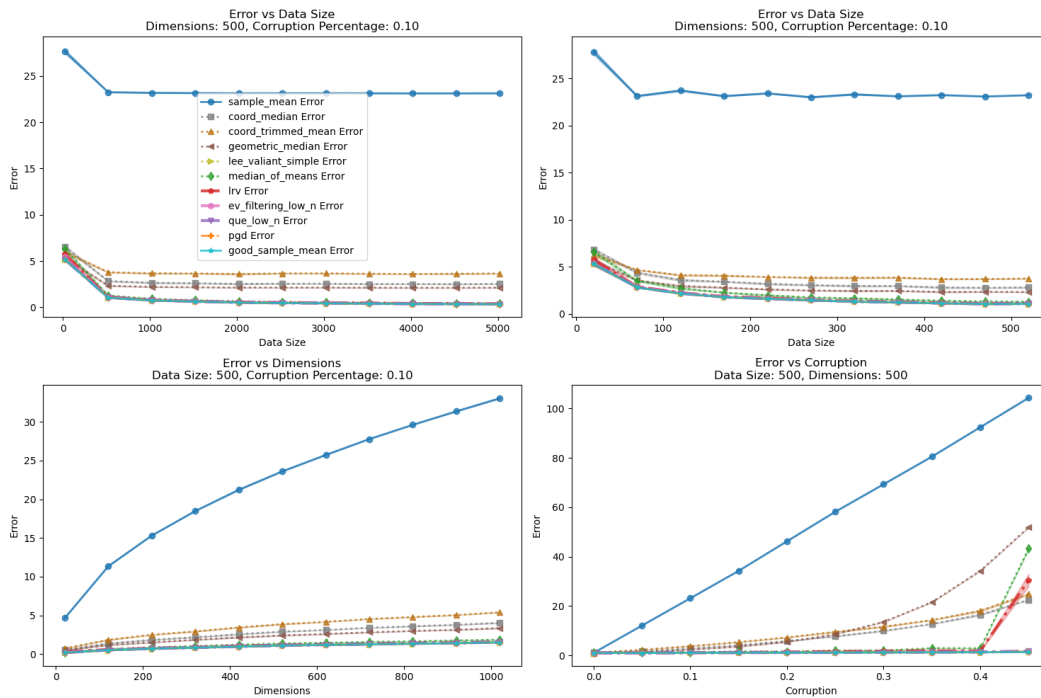Figure 17: Corrupted Gaussian Identity Covariance: In Distribution Noise

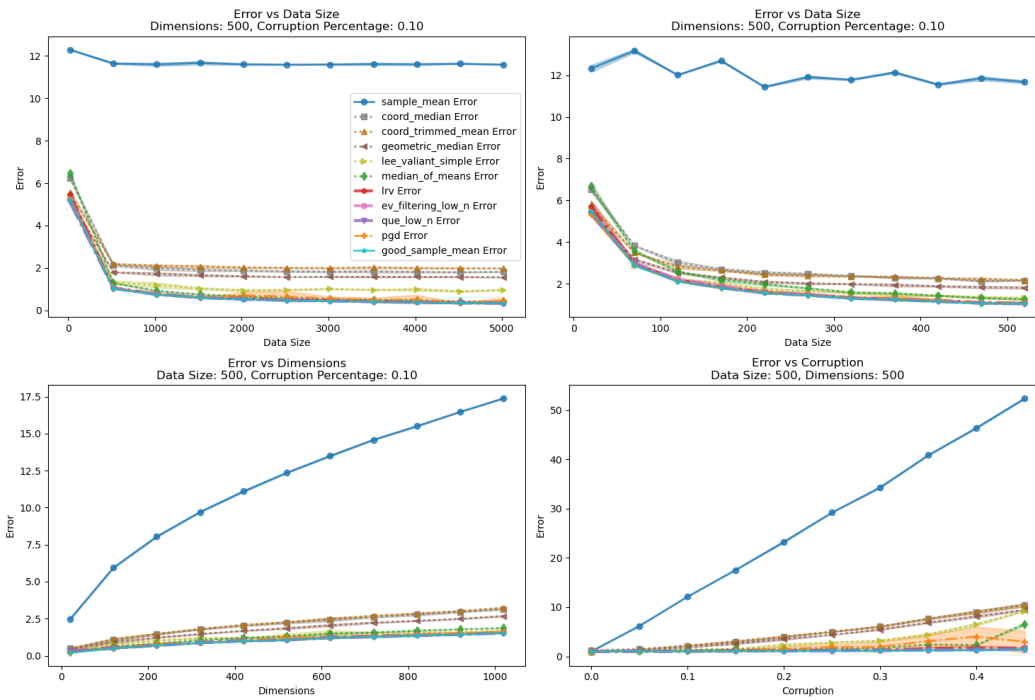Figure 18: Corrupted Gaussian Identity Covariance: Large Outliers

Figure 19: Corrupted Gaussian Identity Covariance: Large Outliers w/ Additive Variance Shell Noise
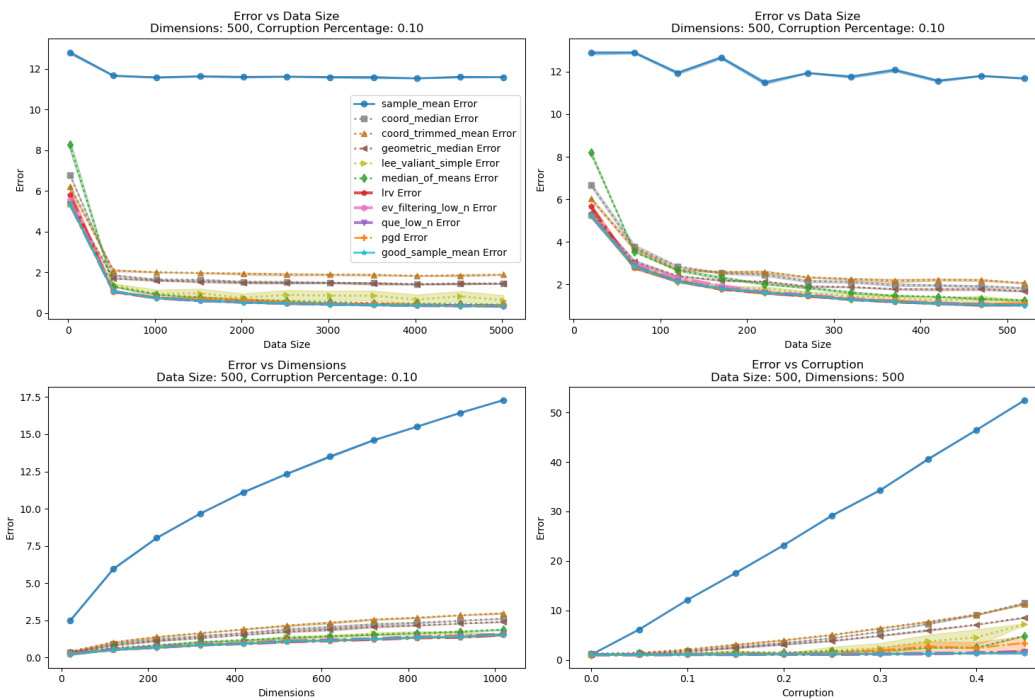

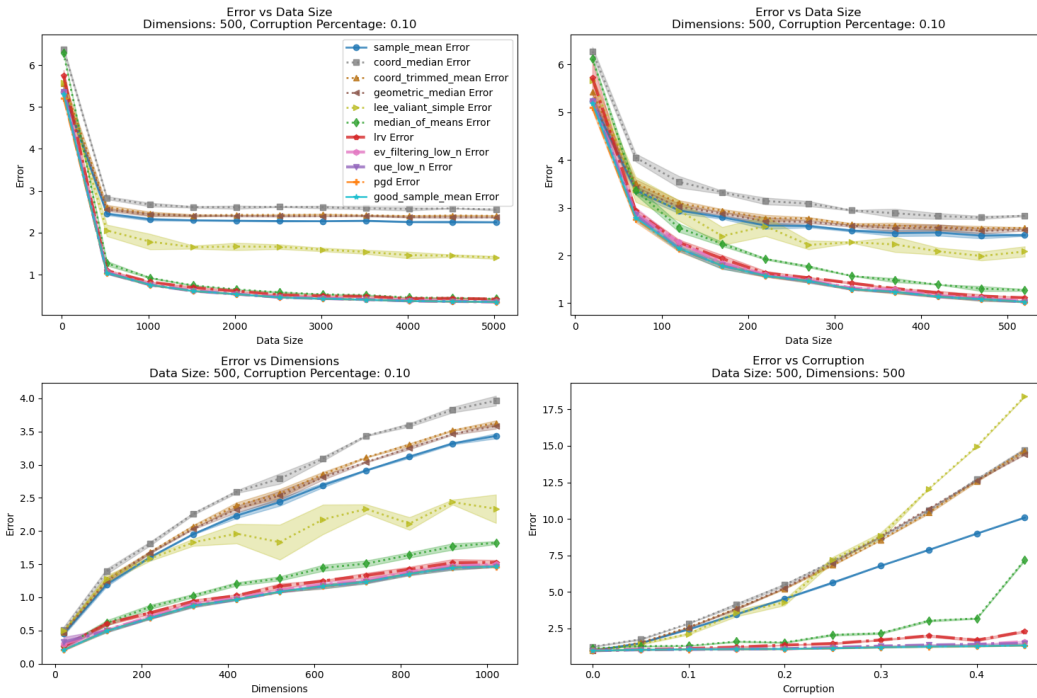Figure 20: Corrupted Gaussian Identity Covariance: Large Outliers w/ DKK Noise

Figure 21: Dependence On True Mean: Identity Covariance, Additive Variance Shell Noise
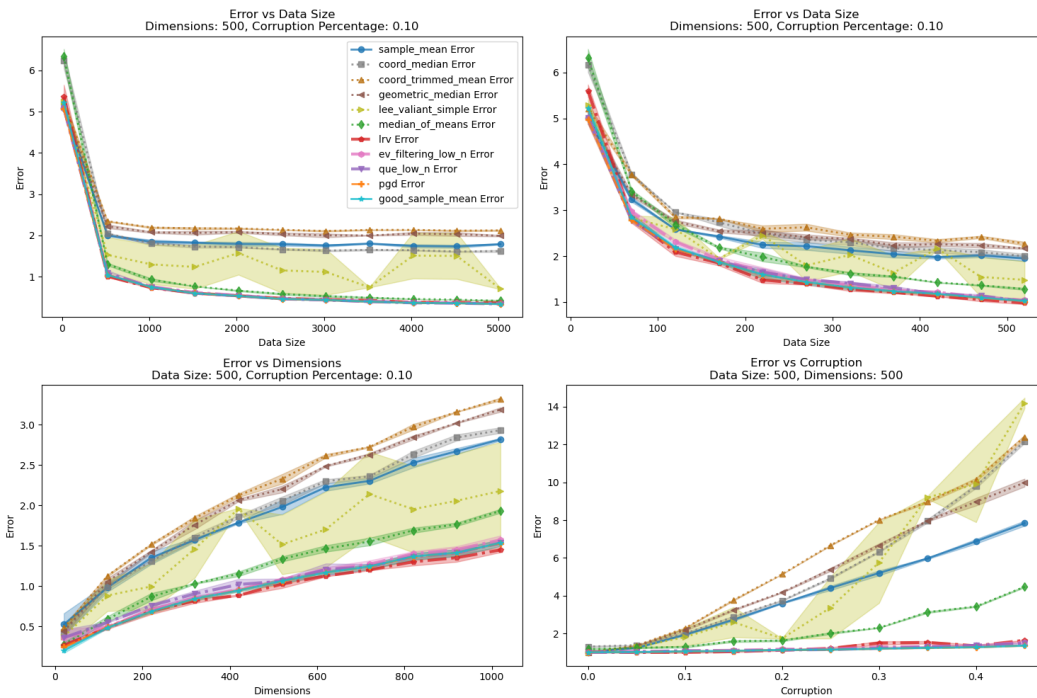

Figure 22: Dependence On True Mean: Identity Covariance, DKK Noise

A.3 Corrupted Gaussian Data Unknown Spherical Covariance: Additional Corruption Schemes

We examine the unknown spherical covariance case across additional corruption schemes. We utilize the same uncorrupted distribution as before, $P = \mathcal{N}_d(\mu, \sigma^2 I)$ where μ is the all-fives vector and $\sigma = 5$. We find similar performance across the distributions we test.

Adapting noise distributions to spherical covariance As in the Gaussian noise shifted to variance shell case, we utilize the well know Gaussian concentration inequality that for data $X \sim \mathcal{N}_d(\mu, \sigma I)$, $\mathbb{E}_{x \sim X}[\|x - \mu\|^2] = \sigma^2 d$. This observation is used to adapt noise distributions in the identity covariance case to this case. For two additive variance shell clusters, each cluster has mean μ^i for $i \in [0, 1]$ where $\|\mu - \mu^i\| = \sigma\sqrt{d}$, with other conditions remaining the same; results are shown in Figure 23. For DKK noise, half the noise is drawn over the hypercube where every coordinate is $-\sigma$ or 0 away from the true mean at that coordinate with equal probability. The other half is drawn from the product distribution where the first coordinate is either 11σ or $-\sigma$ away from the true mean at that coordinate with equal probability, the second coordinate is -3σ or $-\sigma$ away from the corresponding true mean coordinate with equal probability, and all remaining coordinates are $-\sigma$ away from the true mean. Results are shown in Figure 24. For in distribution corruption, we draw each coordinate j of a corrupted data point from $\mathsf{Uniform}(\mu_j, \mu_j + 2\sigma)$; results are shown in Figure 25. We also perform subtractive corruption, using the same scheme as in the identity covariance case; results are shown in Figure 26.
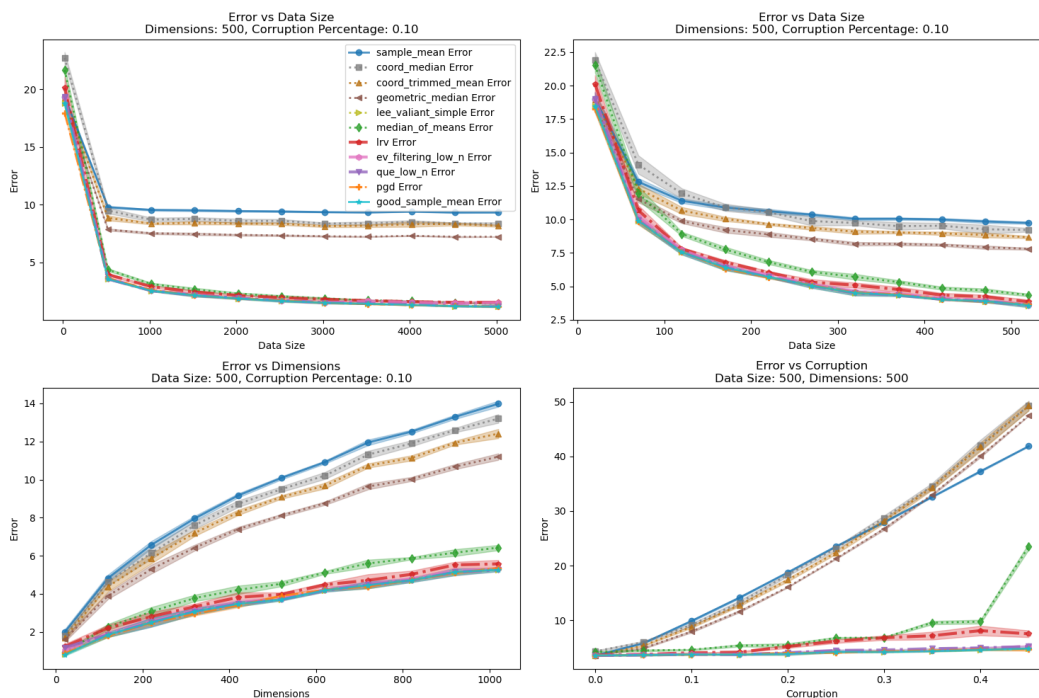

Figure 23: Corrupted Gaussian Large Spherical Covariance: Two Variance Shell Clusters

We find similar results to the identity covariance case across the best estimators, again observing the near optimal performance of QUE_low_n and PGD, along with the slightly worse but still near optimal performance of LRV. As a result of using the scaling data heuristic, ev_filtering_low_n degrades slightly. This is especially noticeable with DKK noise, where it does not converge to good_sample_mean error as data size increases. QUE_low_n appears to be less sensitive to the trace scaling heuristic, retaining its performance in these experiments. There is some variance among other estimators. Notably, lee_valiant_simple performs near optimally across two variance shell corruption and in distribution noise with spherical covariance (its performance in these plots is hidden amongst the best estimators which approximately match good_sample_mean error), whereas it performs comparably worse across analogous noise distributions for identity covariance
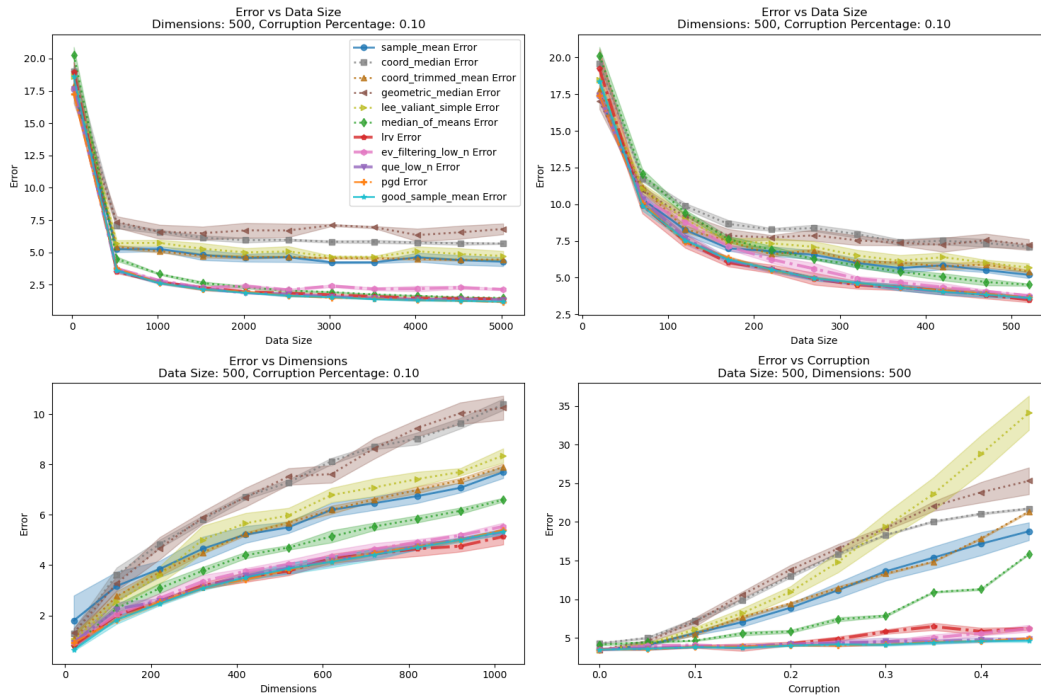
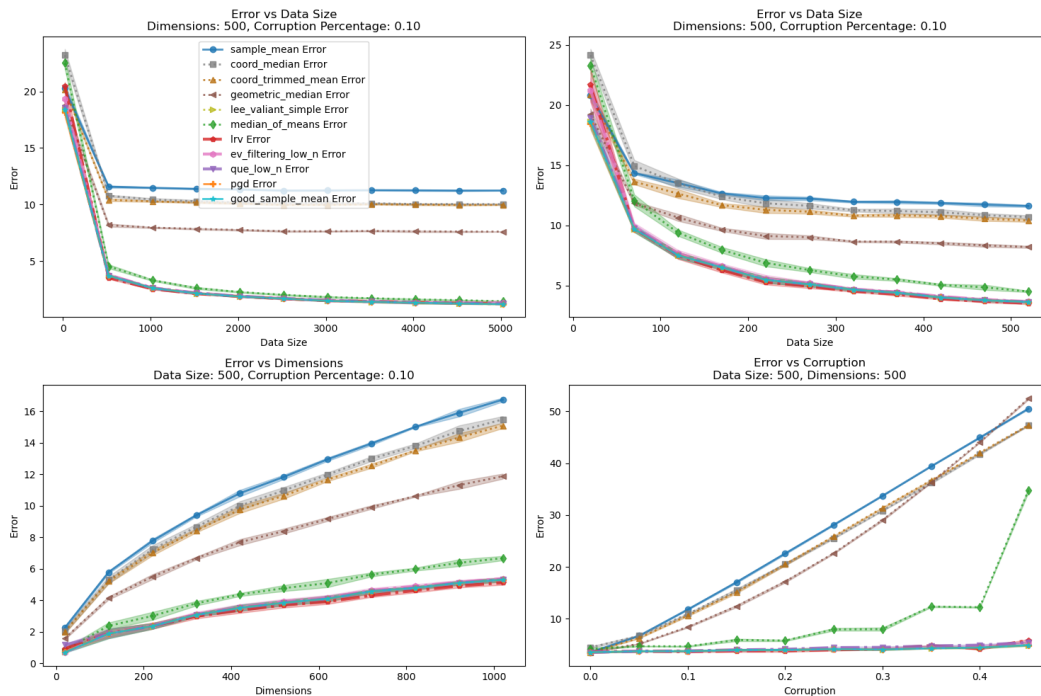Figure 24: Corrupted Gaussian Large Spherical Covariance: DKK Noise

Figure 25: Corrupted Gaussian Large Spherical Covariance: In Distribution Noise

data. Still, lee_valiant_simple does not generally perform better in the spherical covariance case compared to the (known) identity covariance case; performing consistently worse than sample_mean compared to outperforming sample_mean except with large η under identity covariance.
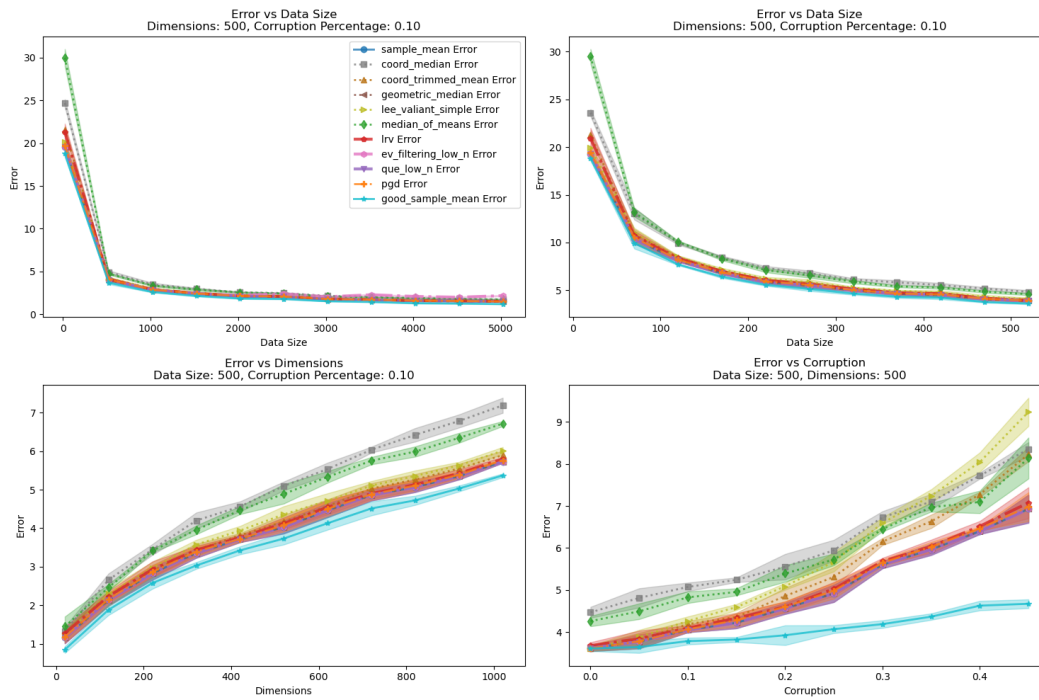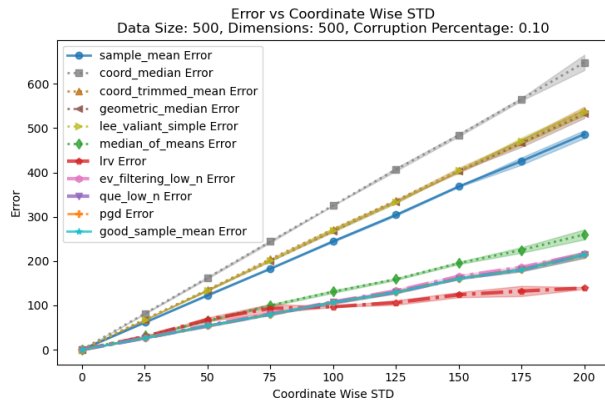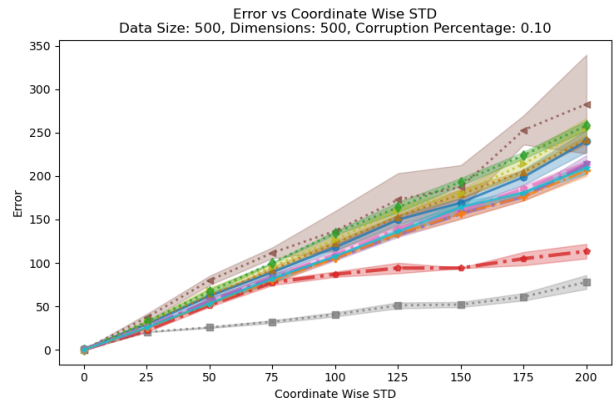
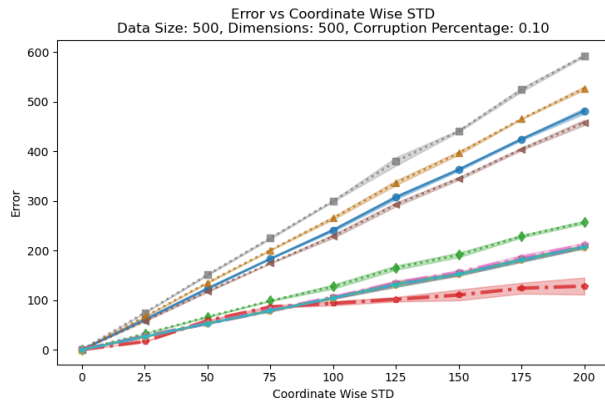Figure 26: Corrupted Gaussian Large Spherical Covariance: Subtractive Noise

Varying σ We rerun several experiments as we vary σ from $\sigma = 0.1$ to $\sigma = 200$ – the coordinate wise standard deviation of the true covariance matrix – and fix other variables as their default values. In particular, we examine Additive Variance Shell Noise, DKK Noise, In Distribution Uniform Noise, and Two Variance Shell Clusters Noise. Results are shown in Figure 27. As expected, error tends to increase linearly with σ. Generally, relative performance of the algorithms remains the same, with ev_filtering_low_n, QUE_low_n, and PGD nearly identically matching good_sample_mean error throughout. Surprisingly, LRV error does not grow linearly with σ, consistently outperforming even good_sample_mean with large enough choices of σ. A similar trend is also seen for coord_median, but only across DKK Noise, in which it is noticeably the best estimator with larger values of σ.
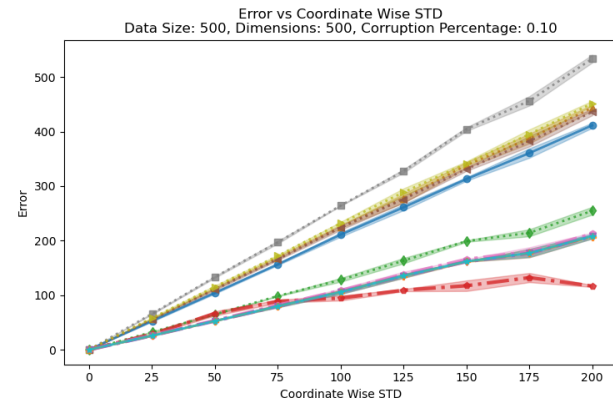
(a) Additive Variance Shell Noise

(b) DKK Noise

(c) In Distribution Noise

(d) Two Variance Shell Clusters

Figure 27: Corrupted Gaussian Large Spherical Covariance: Varying Coordinate-Wise Standard Deviation σ

A.4 Corrupted Gaussian Data Unknown Non Spherical Covariance

A.4.1 Unknown Diagonal Covariance

Here we consider the performance of mean estimators on corrupted Gaussian data with unknown diagonal non-spherical covariance. We draw uncorrupted data from $\mathcal{N}_d(\mu, \Sigma)$ where μ is the all fives-vector and Σ has large diminishing covariance. In particular, the diagonal elements uniformly decrease from 25 to 0.1.

Noise Distributions We adapt the variance shell additive noise distribution to cluster outliers to be a standard deviation away from the true mean along every coordinate axis. That is, consider corrupted data distribution $Q = \mathcal{N}_d(\mu', \frac{1}{10}I)$ with $|\mu'_j - \mu_j| = \Sigma_j$, where Σ_j is the jth diagonal element in Σ, μ'_j is the jth coordinate of μ', and μ_j is the jth coordinate of the true mean μ; results are shown in Figure 28. We adapt in distribution uniform noise to draw each coordinate j of a corrupted data point from $\mathsf{Uniform}(\mu_j, \mu_j + \Sigma_j)$; results are shown in Figure 29. For large outlier noise we weight the distance of clusters from μ by $\sqrt{\frac{\mathrm{Tr}(\Sigma)}{d}}$. That is, consider corrupted data distribution $Q = 0.7\mathcal{N}_d(\mu^0, \frac{1}{10}I) \cup 0.3\mathcal{N}_d(\mu^1, \frac{1}{10}I)$ where $\|\mu - \mu^0\| = 10\sqrt{\frac{\mathrm{Tr}(\Sigma)}{d}}\sqrt{d}$, $\|\mu - \mu^1\| = 20\sqrt{\frac{\mathrm{Tr}(\Sigma)}{d}}\sqrt{d}$, and $\theta = 75°$ where θ is the angle between μ^0 and μ^1.; results are shown in Figure 30. We also utilize subtractive noise which already works in this case; results are shown in Figure 31.
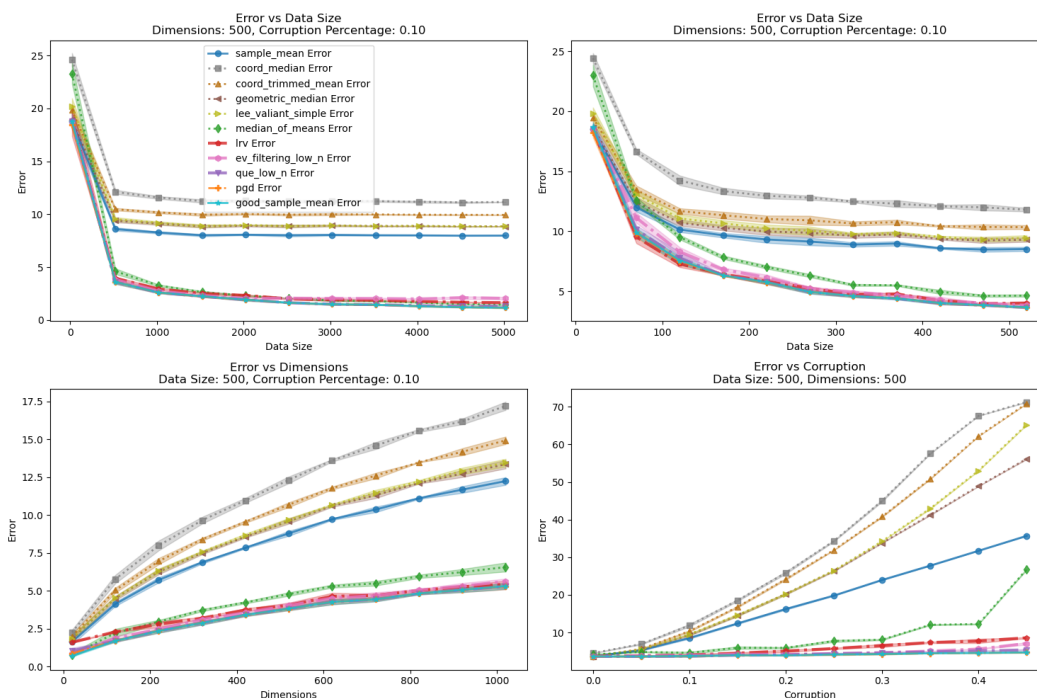

Figure 28: Corrupted Gaussian Large Diminishing Diagonal Covariance: Additive Variance Shell Noise

Again, we find that QUE_low_n and PGD nearly match good_sample_mean error across distributions, with LRV doing slightly worse but still significantly outperforming sample_mean. ev_filtering_low_n still does among the best here, but, as in the large spherical covariance case, sees slight degradation as a result of the scaling data heuristic. In particular, error does not clearly converge to good_sample_mean error as n increases over Additive Variance Shell Noise and In Distribution Noise. QUE_low_n does not encounter this issue despite employing the same heuristic to generalize to non-identity covariance data, suggesting that it is more robust to distributional assumptions. Additionally, median_of_means performs best among simpler estimators, outperforming the sample_mean with $n \approx d$ and performing similarly to good_sample_mean with sufficiently large n.
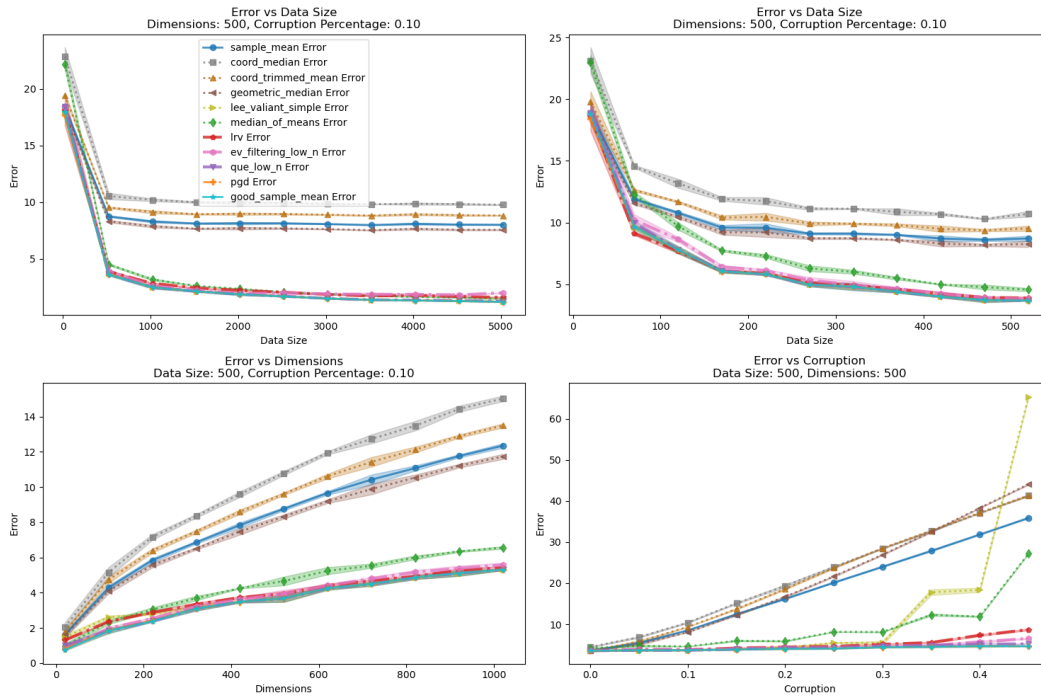
Figure 29: Corrupted Gaussian Large Diminishing Diagonal Covariance: In Distribution Noise
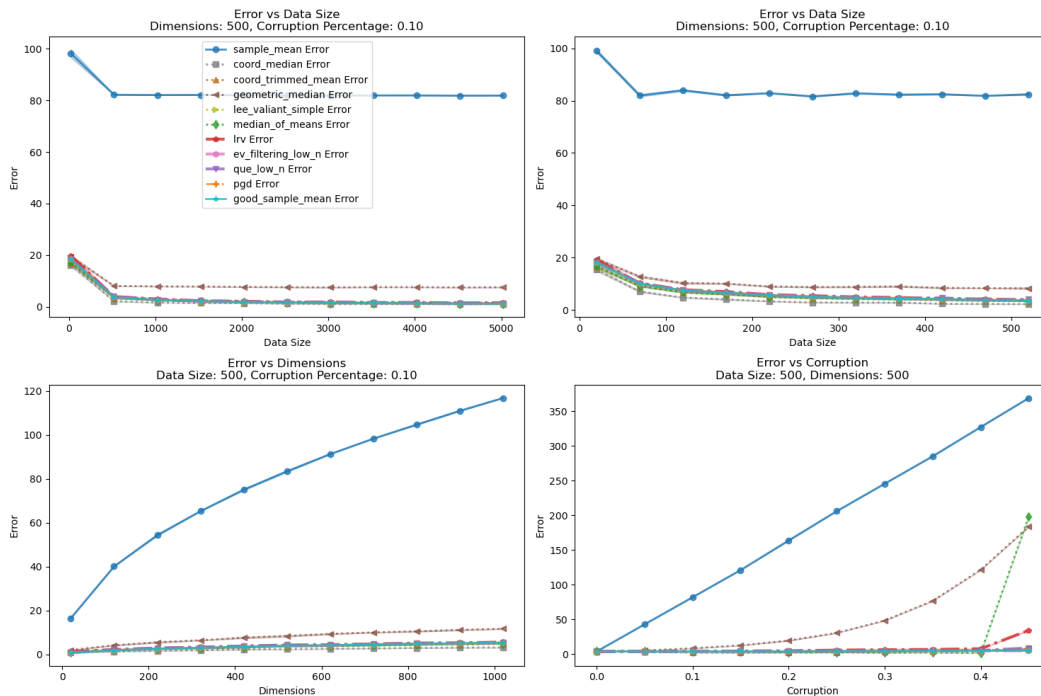
Figure 30: Corrupted Gaussian Large Diminishing Diagonal Covariance: Large Outliers

Varying top Eigenvalue   We rerun Additive Variance Shell Noise and In Distribution Noise as we vary the squareroot of the top eigenvalue of the true covariance matrix, labeled as σ, from $\sigma = 0.1$ to $\sigma = 200$. In particular, the diagonal of the covariance will uniformly decrease from σ^2 to 0.1. For every choice of σ,
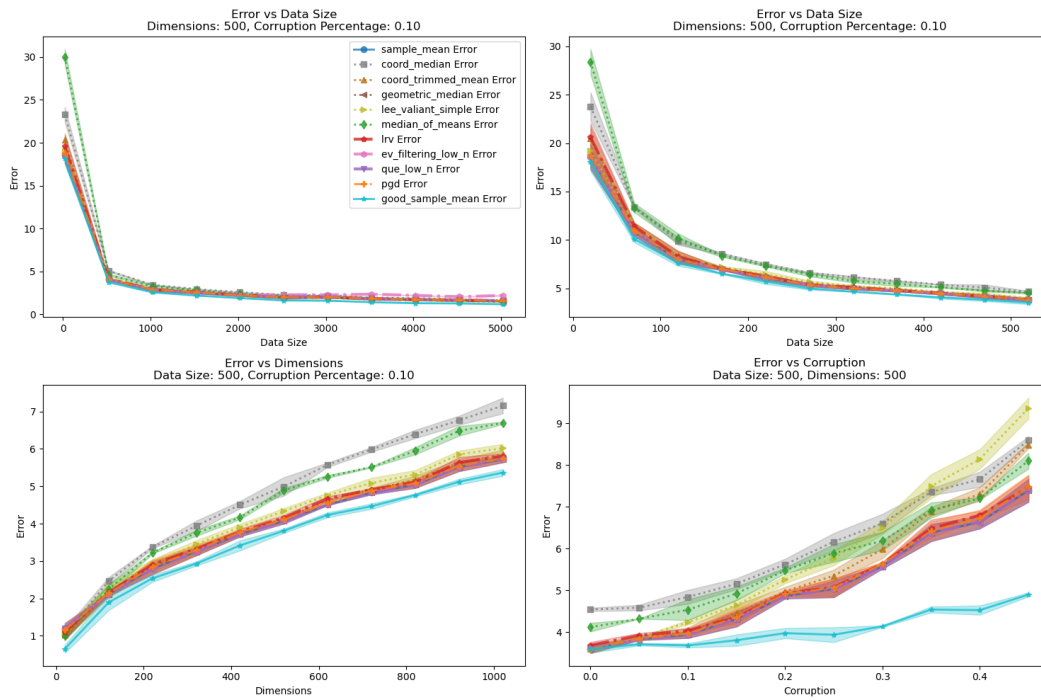
Figure 31: Corrupted Gaussian Large Diminishing Diagonal Covariance: Subtractive Noise

the noise is scaled as described previously. These results are shown in Figure 32. Like in the spherical case, we find that the relative performance of algorithms remains nearly identical throughout choices of σ.
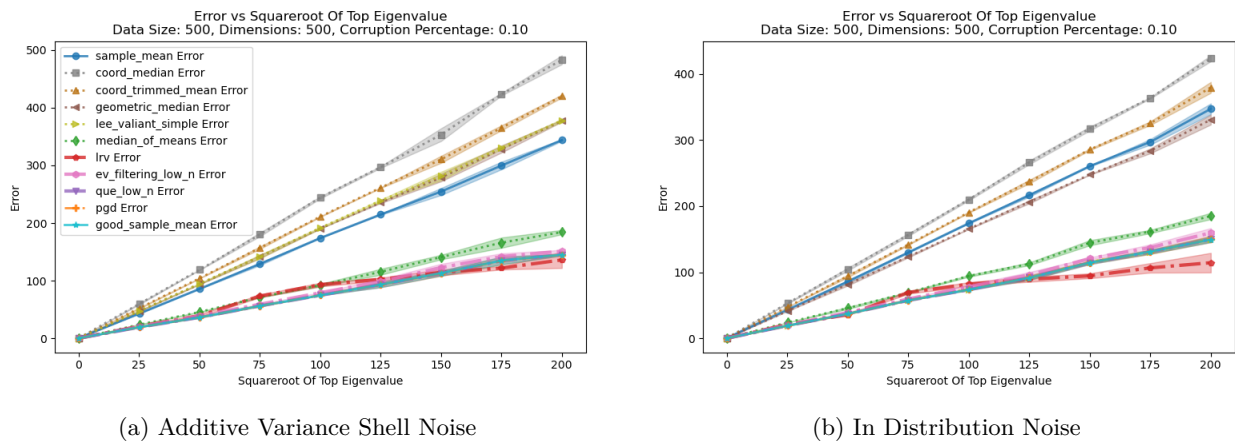
(a) Additive Variance Shell Noise

(b) In Distribution Noise

Figure 32: Corrupted Gaussian large diminishing diagonal covariance: Varying the square root of the top eigenvalue: σ

A.4.2 Unconstrained Covariance

So far, we have only examined inlier data with diagonal covariance matrices. However, in line with the intuition that there is nothing inherently special about the standard orthonormal basis, we hope for a robust estimator to work well regardless of the choice of coordinate axis. Since the covariance matrix is always symmetric, it is also diagonalizable by taking the eigenvectors as the orthonormal basis. Then, any possible data distribution over unconstrained covariance can be framed as a data distribution over a diagonal matrix by using these eigenvectors as the orthonormal basis. As a result, any robust estimator that does not leverage the standard orthonormal basis should perform equally well on unconstrained covariance. However, this does not necessarily hold for the estimators that we examine. We employ a trace estimate to adapt ev_filtering_low_n and QUE_low_n to the unknown covariance case. coord_median, coord_trimmed_mean, and median_of_means all directly utilize coordinate wise calculations. LRV utilizes a trace estimate when downweighting points. In this section, we evaluate the performance of robust mean estimators over data with non-diagonal covariance matrices.

Rotated Data Noise Because the covariance matrix is always symmetric, it is diagonalizable, and experiments over unconstrained covariance can be framed as an ablation on noise distributions over inliers with diagonal covariances. We reuse data and noise distributions, but randomly rotate everything before estimation, resulting in unconstrained true covariances and appropriately difficult noise distributions. Random rotation is implemented by generating a standard normal matrix and utilizing its QR decomposition. We examine the performance on Rotated Identity Covariance with DKK Noise in Figure 33; Rotated Identity Covariance with Subtractive Noise in Figure 34; Rotated Large Spherical Covariance with Additive Variance Shell Noise (with coordinate-wise standard deviation $\sigma = 5$) in Figure 35; and Rotated Large Diminishing Covariance with Additive Variance Shell Noise (with squareroot of the top eigenvalue $\sigma = 5$) in Figure 36. As in the original experiments, we set the true mean, μ, to be the all-fives vector.
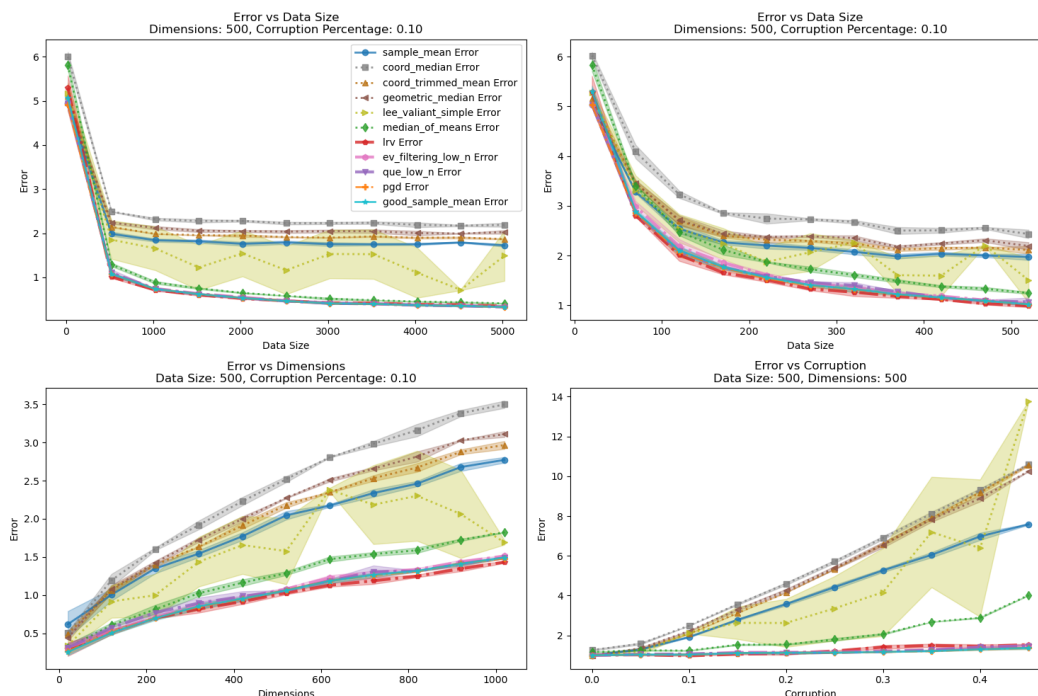
Figure 33: Corrupted Rotated Identity Covariance - DKK Noise

We find nearly identical results among the best estimators to the corresponding non-rotated data experiment. While many of these algorithms induce a bias to the coordinate axis, they are not enough to significantly skew results in the distributions that we examine. There is some variation between coord_median and coord_trimmed_mean with the corresponding non-rotated data experiments, but no major changes in their

Figure 34: Corrupted Rotated Identity Covariance - Subtractive Noise

Figure 35: Corrupted Rotated Large Spherical Covariance - Additive Variance Shell Noise

trends. There is no such variation for QUE_low_n, ev_filtering_low_n, or median_of_means among the settings that we test.

Figure 36: Corrupted Rotated Large Diminishing Covariance - Additive Variance Shell Noise

A.5 Hyperparameter Tuning

In this section we tune the hyperparameters of some of the most interesting algorithms, median_of_means, LRV, ev_filtering_low_n, and PGD. We utilize the best hyperparameters in this section across all other experiments. In general, we find that none of these algorithms are overly sensitive to choices of hyperparamaters, as long as they lay within a reasonable range.

We evaluate performance over a subset of 4 corrupted data distributions previously discussed: Identity Covariance with DKK Noise; Identity Covariance with In Distribution Noise; Large Spherical Covariance with Variance Shell Additive Noise; Large Diminishin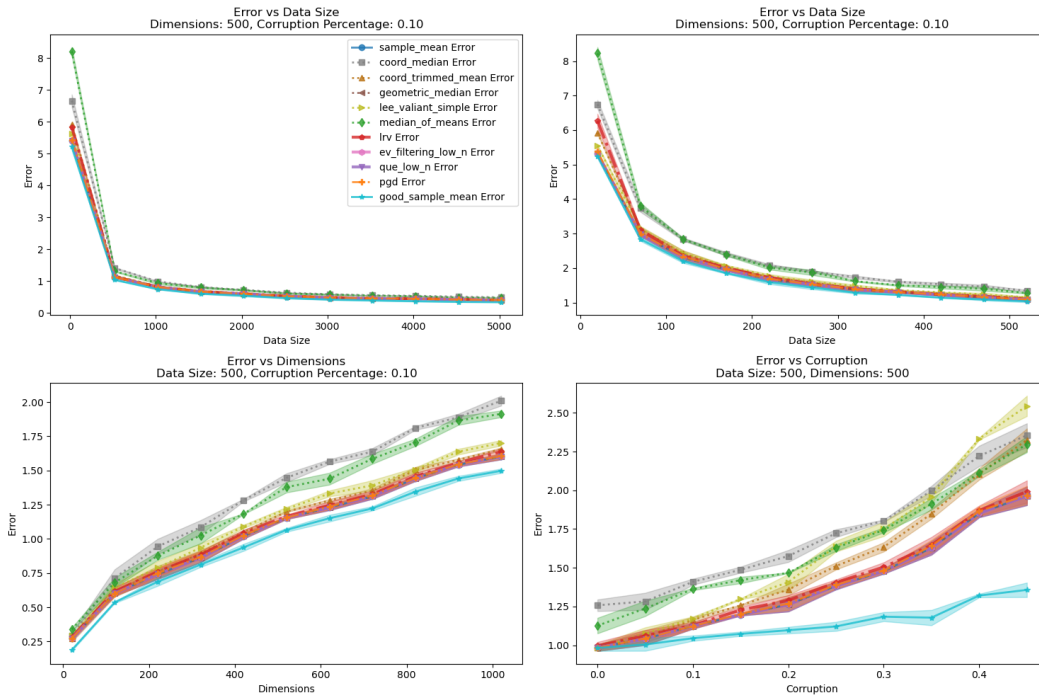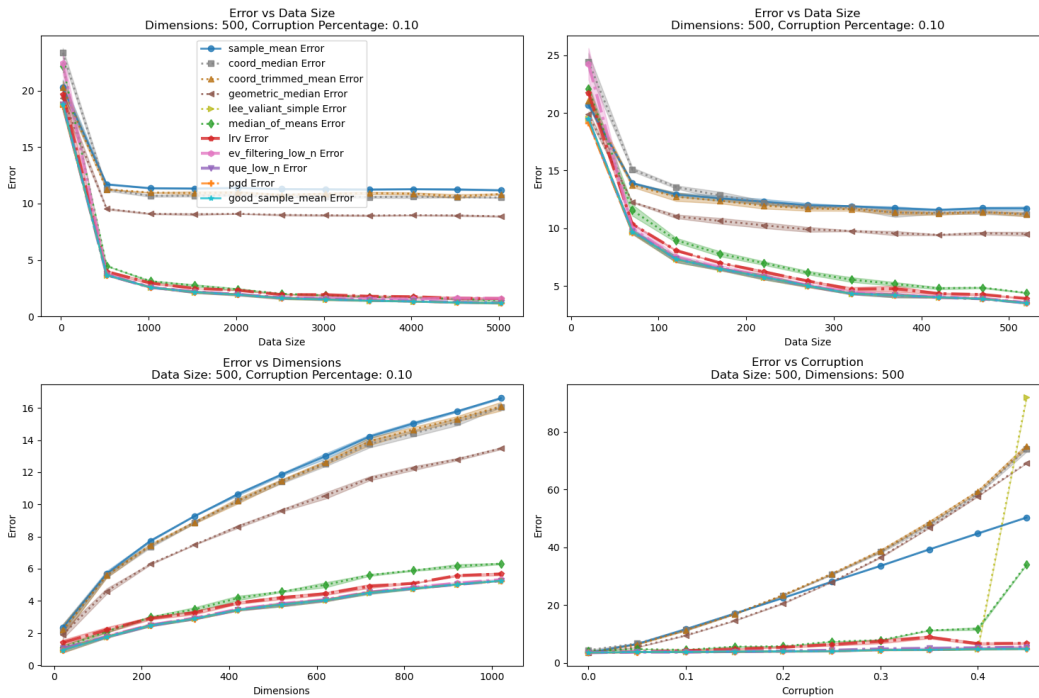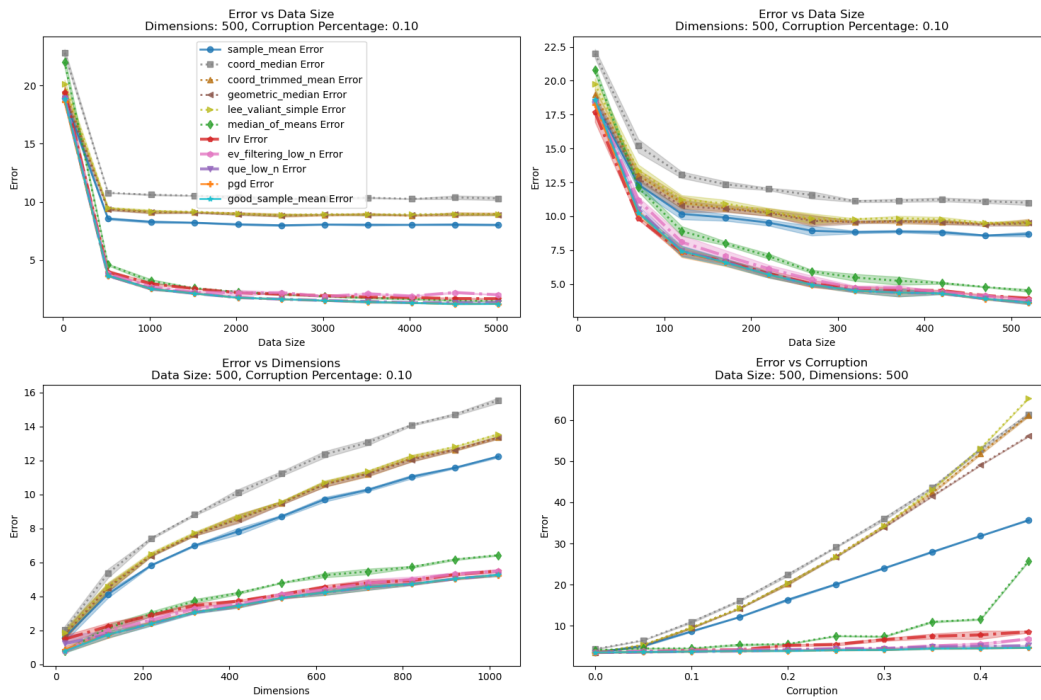g Covariance with Variance Shell Additive Noise. We manually pick the hyperparameters that achieve the best performance across these distributions, or when similar use default ones from the corresponding paper.

Median of how many means? Here we explore the parameter k in median_of_means algorithm. This parameter controls the number of chunks that we split the data into; then we take the median of k means determined by these chunks. We vary k in the set $[3, 5, 10, 15, 20, 30]$. For the case where $n < k$, we simply set $k = n$. These results are shown in Figures 37, 38, 39, 40. We find that although there is not always an obvious choice for k, that $k = 10$ tends to perform well throughout most settings. However, we find that this and larger choices of k are more prone to error as η increases than smaller choices of k. Approximately when $\eta > 0.15$, $k = 3$ becomes the best choice of k. However, with smaller corruption, such as $\eta = 0.10$ which we generally test, $k = 3$ performs notably worse, making $k = 10$ a better choice. Since we utilize $\eta = 0.1$ as a default value, we set $k = 10$ throughout our experiments.
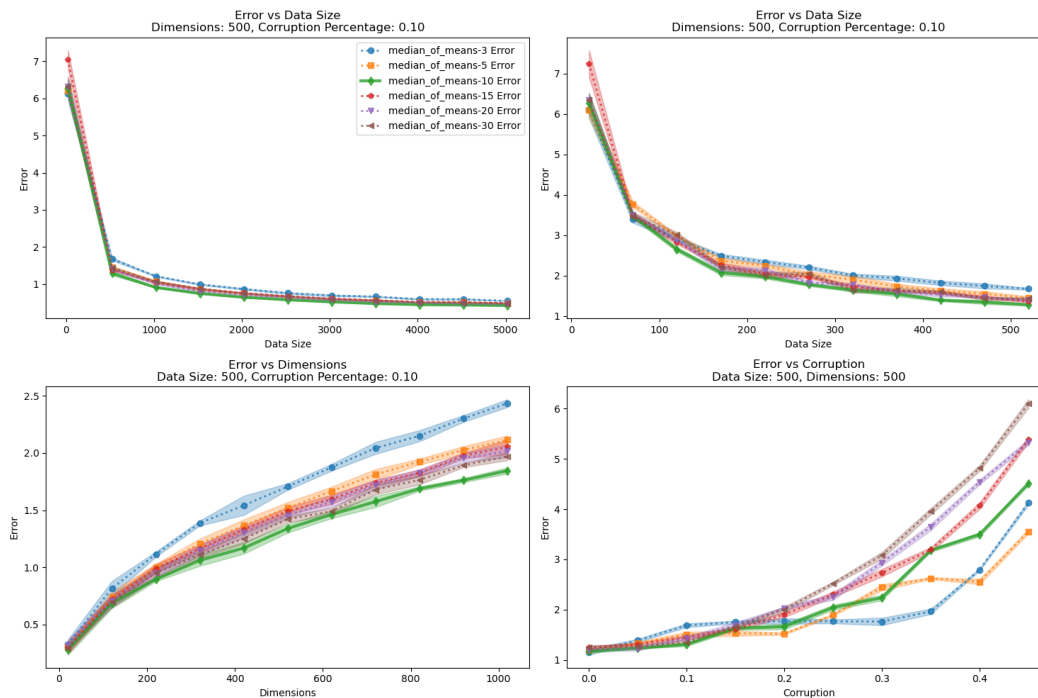
Figure 37: Median Of Means - Number of Chunks k: Identity Covariance, DKK Noise
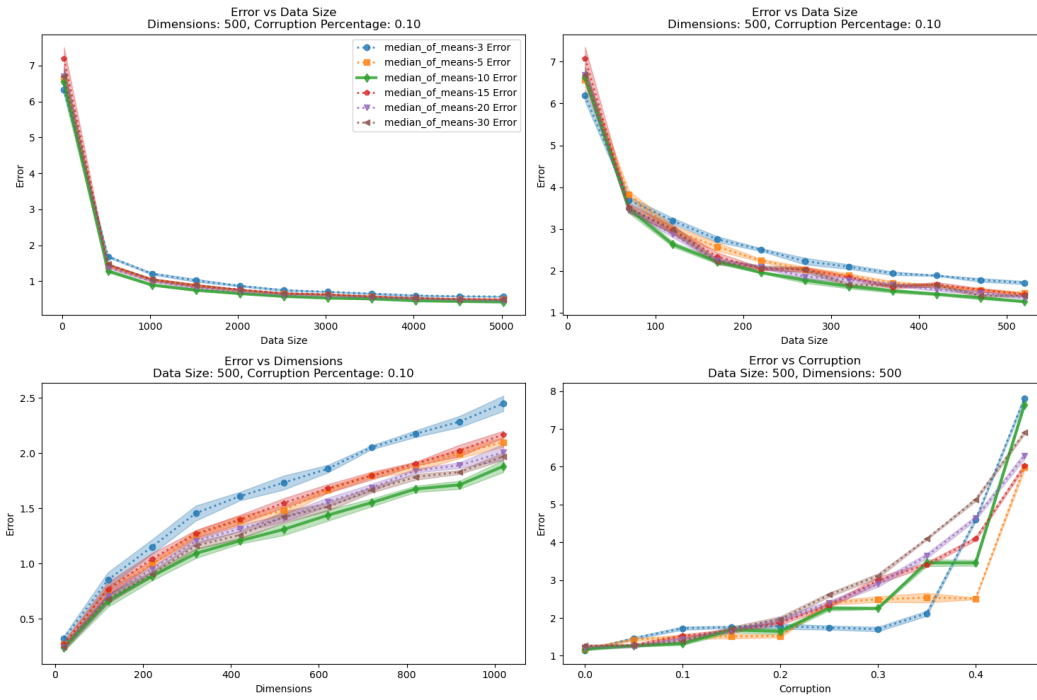
Figure 38: Median Of Means - Number of Chunks k: Identity Covariance, In Distribution Noise
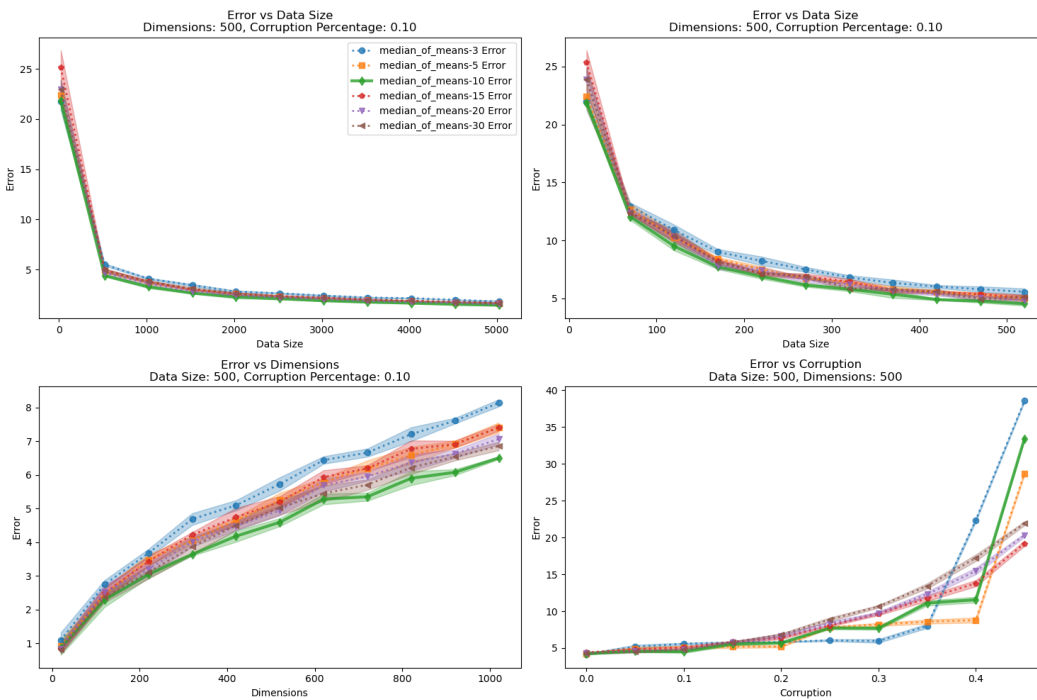
Figure 39: Median Of Means - Number of Chunks k: Large Spherical Covariance, Additive Variance Shell Noise
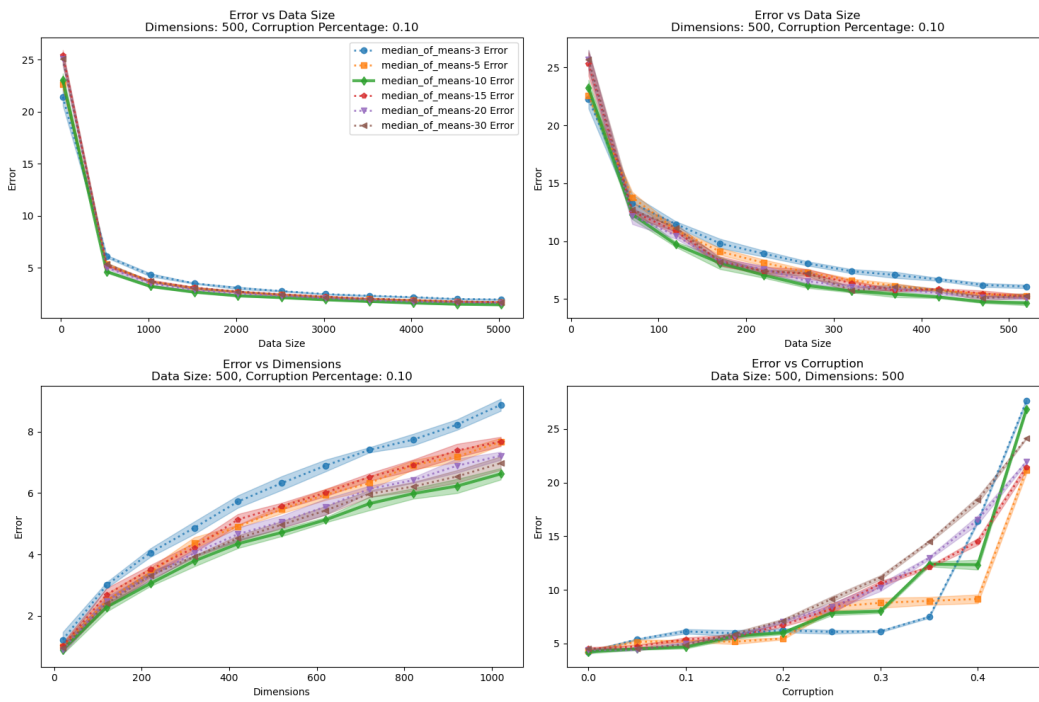
Figure 40: Median Of Means - Number of Chunks k: Large Diminishing Covariance, Additive Variance Shell Noise

LRV Weighting Procedure Here we explore the weighting procedure in LRV. First, we examine the parameter C in the weighting procedure for LRV. This parameter is used when we calculate weights for each point, x_i as $w_i = \exp(-\|x_i - a\|^2 / (C * s^2))$. We vary C in the set $[0.1, 0.5, 1, 5, 10, 20, 50]$. Results are shown in Figures 41, 42, 43, 44. We notice that performance may degrade with choices of C that are too high or too low, such as with $C = 0.5$ and 50. We also notice that smaller choices of C tend to degrade worse with greater corruption. To strike a balance, we select $C = 1$ throughout our experiments, which consistently performs among the best throughout the hyperparameter trials that we test, and is the default value used the original author's implementation of LRV. Although there are cases where larger choices of C noticeably outperform $C = 1$, this is not robust as such choices may perform meaningfully worse over different noise distributions. For example, $C = 20$ noticeably outperforms $C = 1$ over Large Diminishing Covariance with Additive Variance Shell Noise, especially with larger η, but performs much worse over Identity Covariance with DKK Noise and Large Spherical Covariance with Additive Variance Shell Noise.
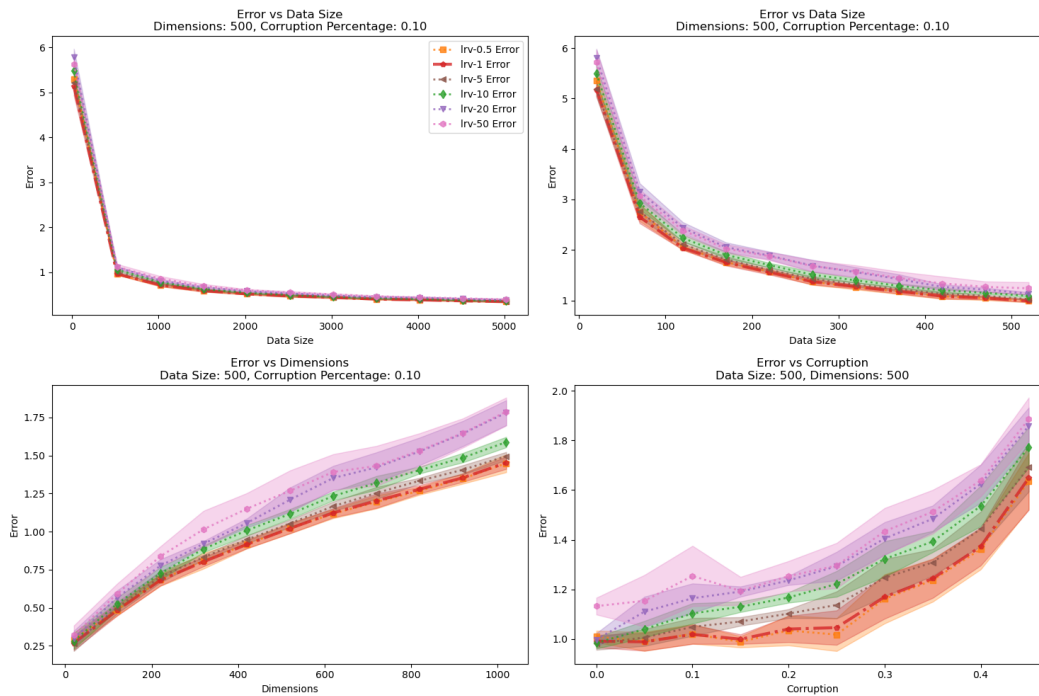
Figure 41: LRV - Choice Of C: Identity Covariance, DKK Noise
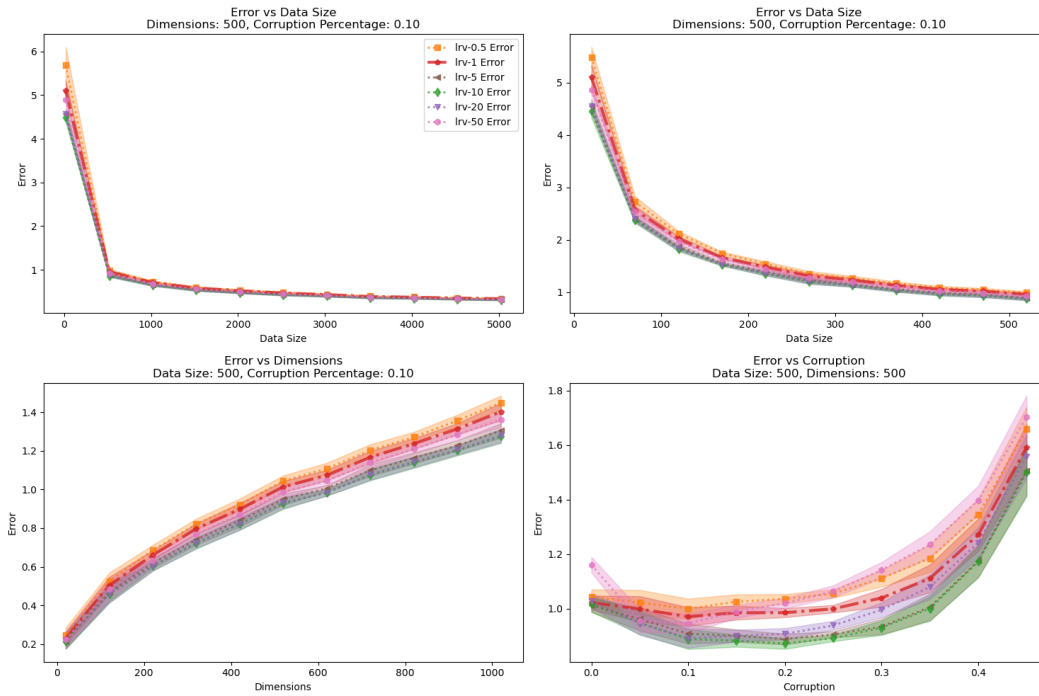
Figure 42: LRV - Choice Of C: Identity Covariance, In Distribution Noise
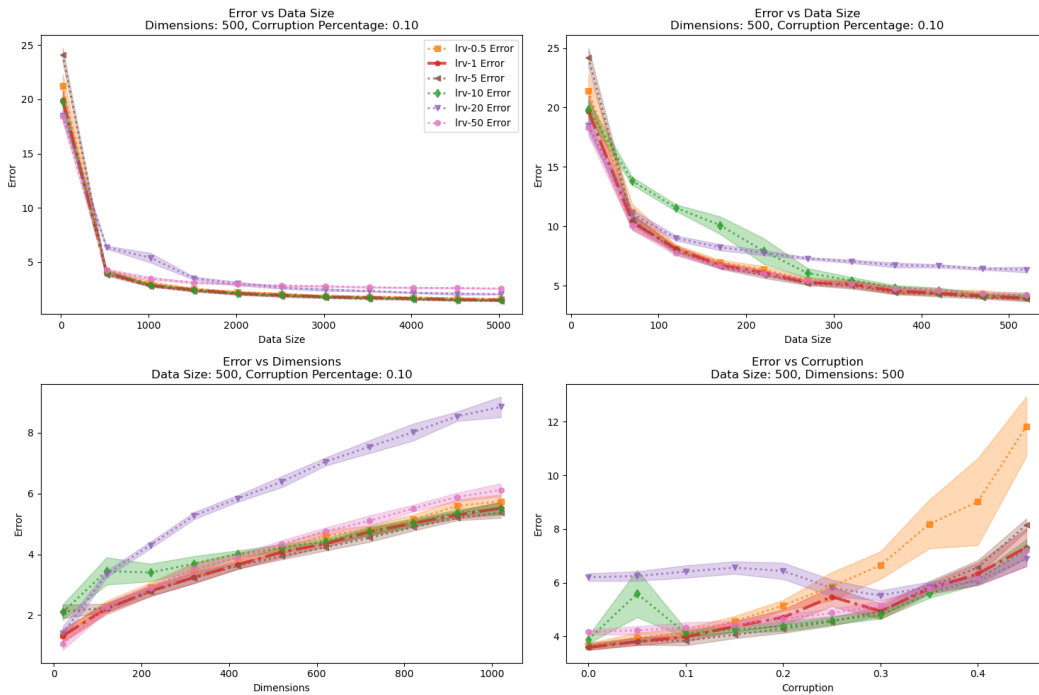
Figure 43: LRV - Choice Of C: Large Spherical Covariance, Additive Variance Shell Noise
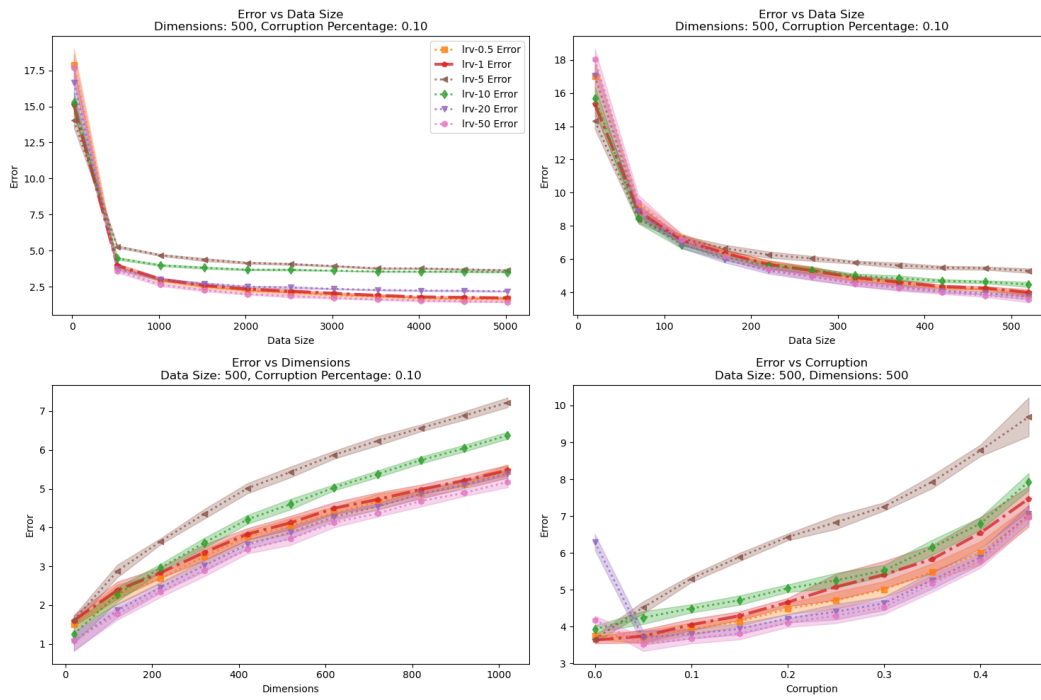
Figure 44: LRV - Choice Of C: Large Diminishing Covariance, Additive Variance Shell Noise

We additionally compare the weighting procedure of LRV that we consider with one meant for more general distributions discussed by Lai et al. (2016). Rather than downweighting outliers, this alternate procedure completely prunes outliers by calculating a point, μ', analogous to the coordinate wise median, finding a ball centered at μ' that contains $1 - \tau$ percentage of data points, and throwing away all points outside of this ball. Results are shown in Figures 45, 46, 47, 48. This general weighting procedure performs meaningfully worse than the Gaussian weighting procedure and degrades significantly worse with larger corruption across all of the distributions considered. However, it achieves similar results as data size increases. Since we focus on the low data size regime and synthetic data with Gaussian inliers, we only evaluate LRV with Gaussian-based outlier downweighting.
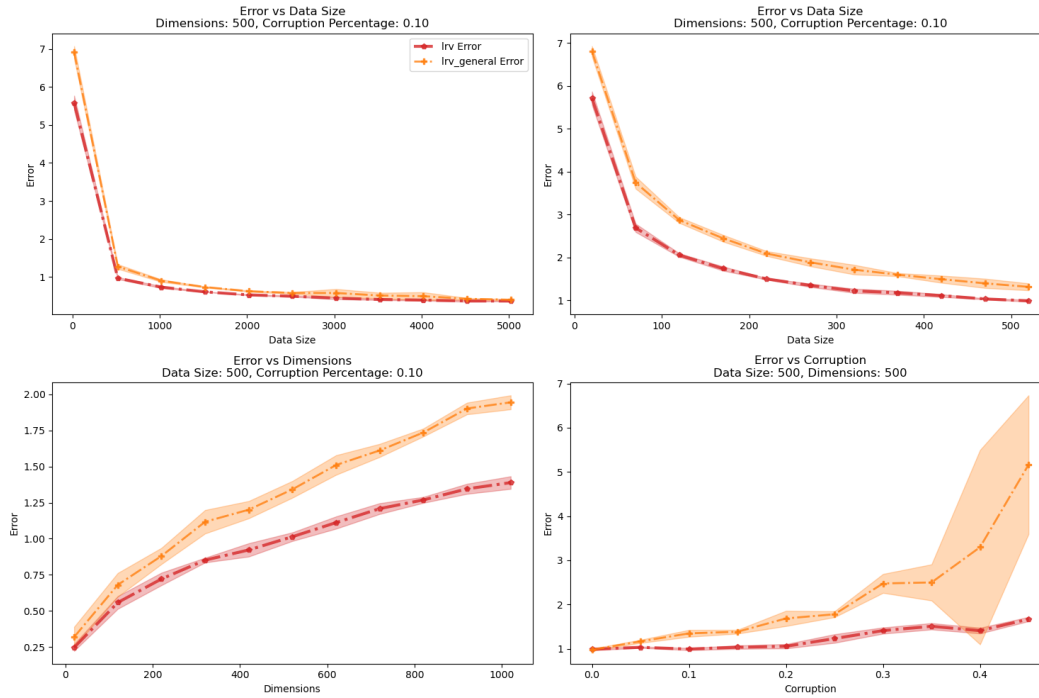
Figure 45: LRV - Gaussian Vs General Weighting: Identity Covariance, DKK Noise
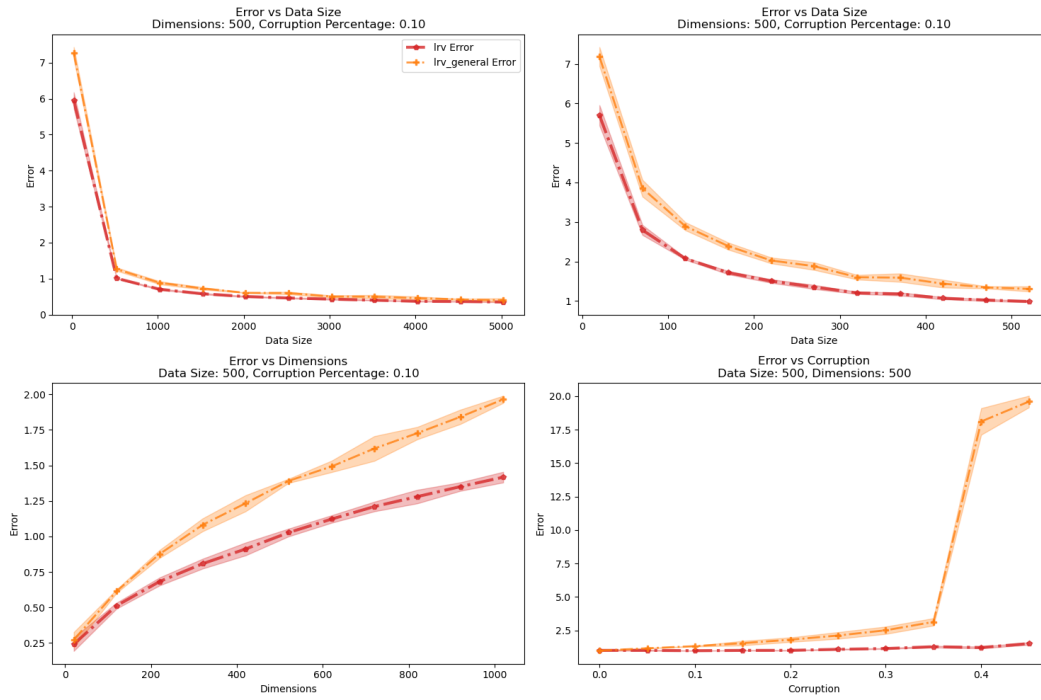
Figure 46: LRV - Gaussian Vs General Weighting: Identity Covariance, In Distribution Noise
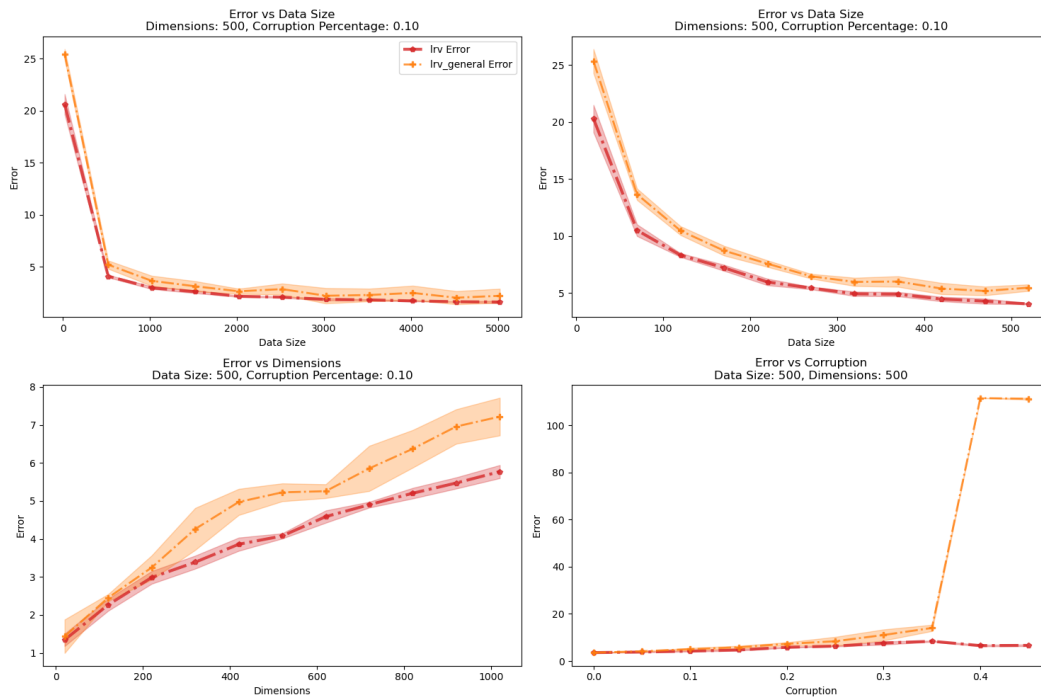
Figure 47: LRV - Gaussian Vs General Weighting: Large Spherical Covariance, Additive Variance Shell Noise
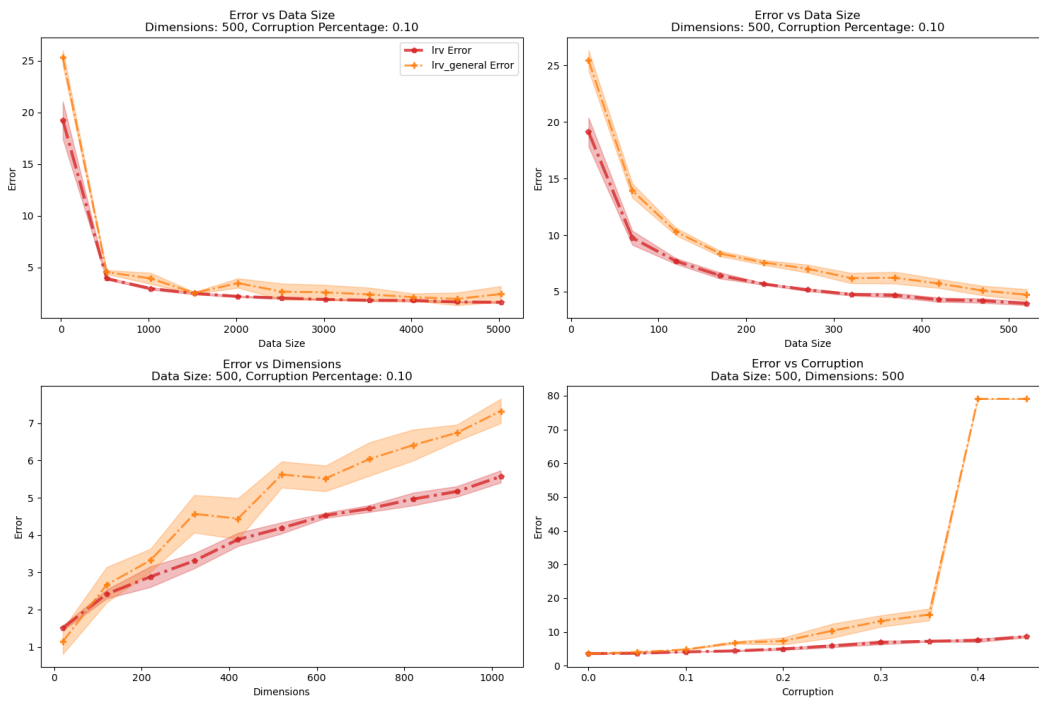
Figure 48: LRV - Gaussian Vs General Weighting: Large Diminishing Covariance, Additive Variance Shell Noise

Eigenvalue Pruning Tail Threshold Here we explore the pruning routine in ev_filtering_low_n. First, we examine the parameter γ in the pruning threshold for ev_filtering_low_n. γ weights the expectation that the Gaussian concentration inequality gives for how many points will surpass a certain value; larger values correspond to less aggressive pruning. We vary γ in the set $[0.5, 1, 2.5, 5, 10, 20, 50]$. Results are shown in Figures 49, 50, 51, 52. We find that using values of γ that are too small result in significantly worse error. Setting $\gamma = 0.5$ or $\gamma = 1$ both achieve performance identical to sample_mean because the pruning threshold is too sensitive, performing significantly worse than all other choices of γ, as it determines all data to be outliers. We note that when all data is determined to be outliers, we simply return sample_mean. However, using reasonably sized γ results in mostly similar performance across distributions. Notably, larger values of γ tend to perform better over large diminishing covariance with additive variance shell noise, especially with larger n. We select $\gamma = 5$ throughout our experiments.
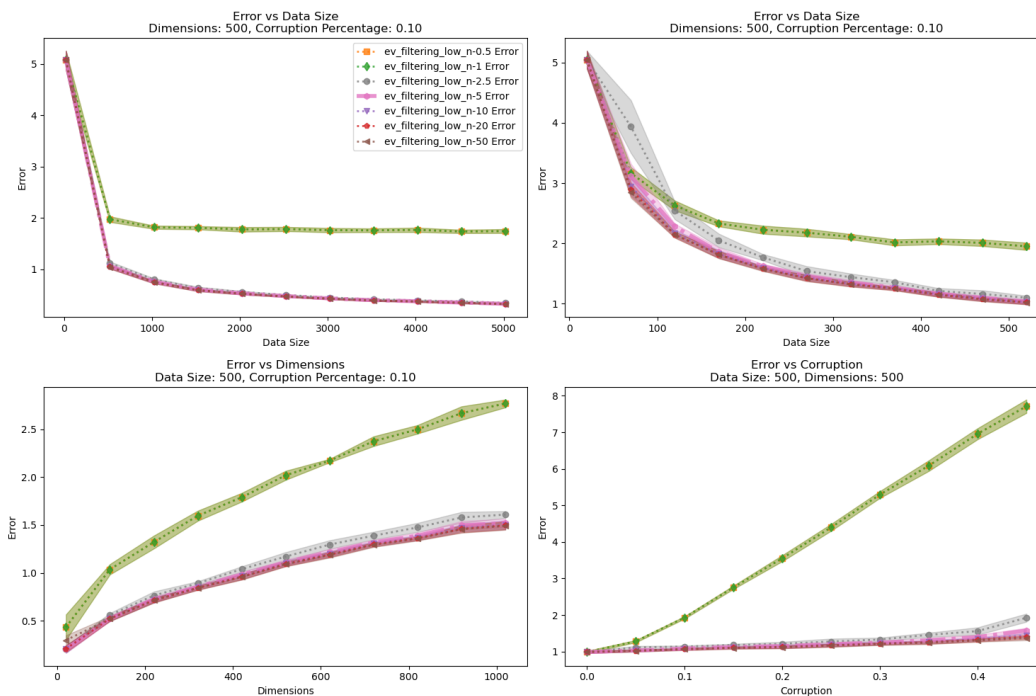
Figure 49: Eigenvalue Pruning - Choice Of γ: Identity Covariance, DKK Noise
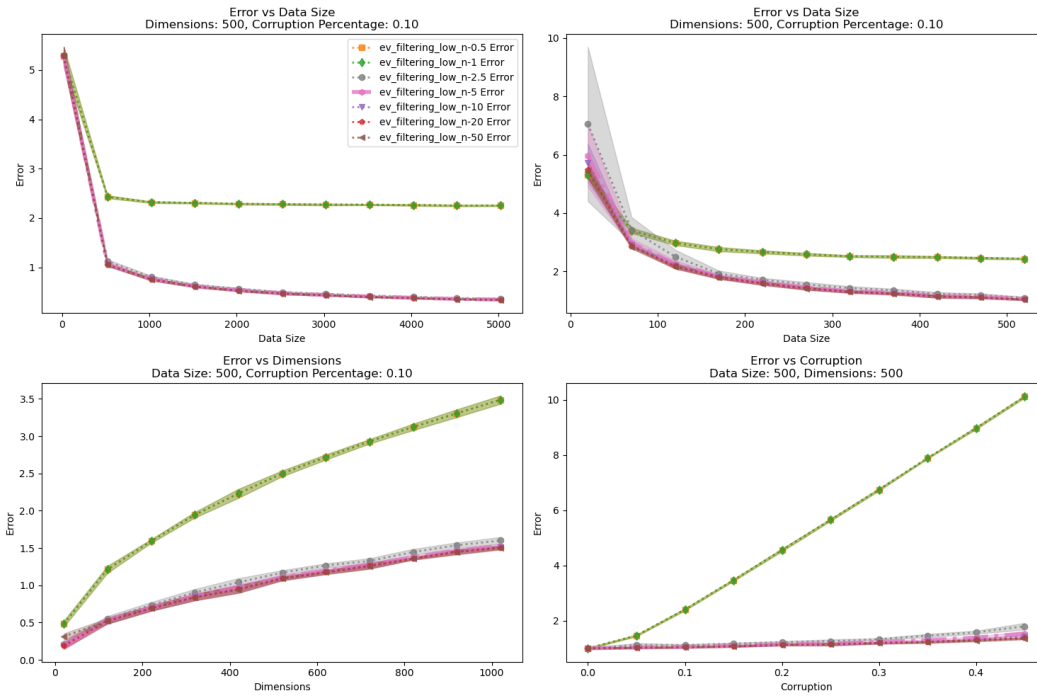
Figure 50: Eigenvalue Pruning - Choice Of γ: Identity Covariance, In Distribution Noise
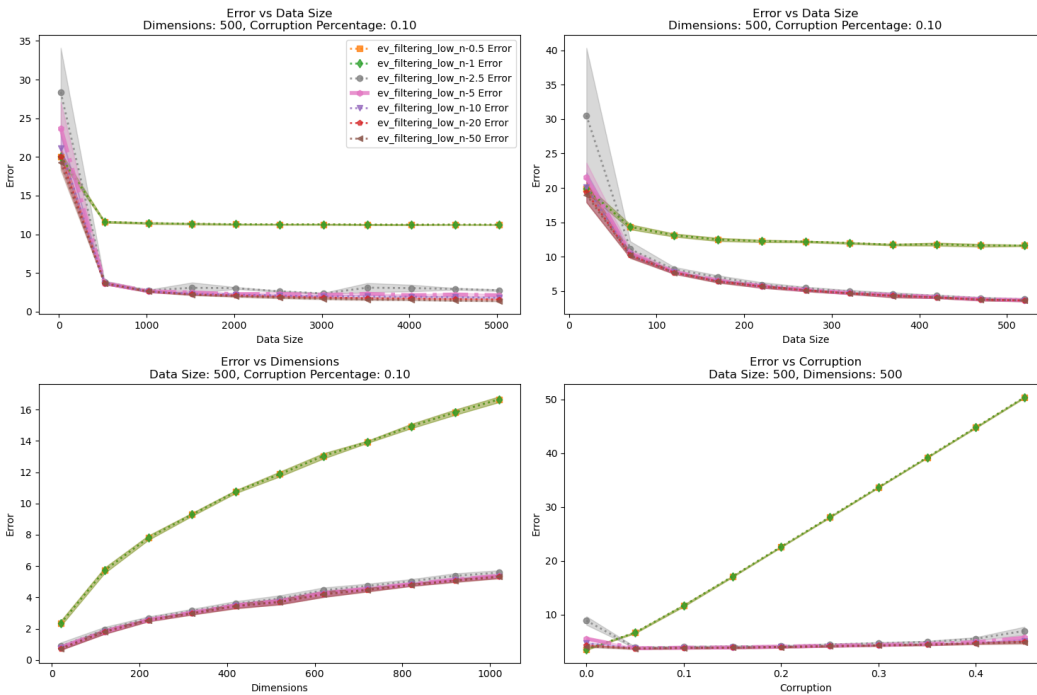
Figure 51: Eigenvalue Pruning - Choice Of γ: Large Spherical Covariance, Additive Variance Shell Noise
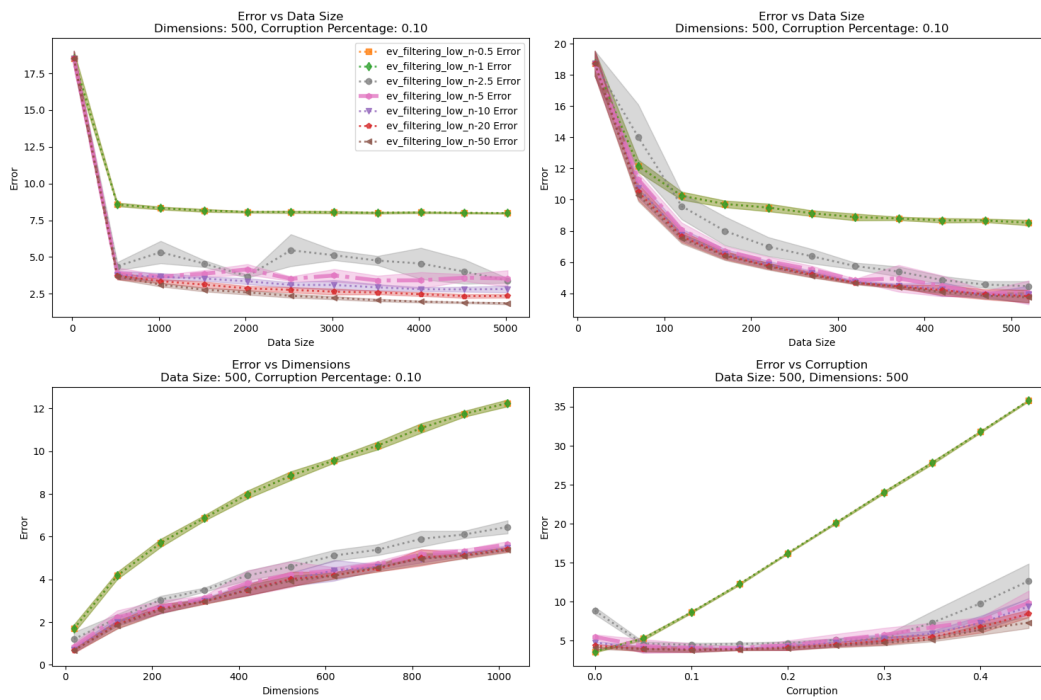
Figure 52: Eigenvalue Pruning - Choice Of γ: Large Diminishing Covariance, Additive Variance Shell Noise

We also explore ev_filtering_low_n using two alternate pruning methods not explicitly based on the Gaussian assumption as the current one is: randomized pruning and fixed pruning,. Randomized Pruning removes points based on a random scaling of the largest deviation in the dataset. Define T as the largest deviation of a point projected onto the top eigenvector from the median of the projected points. Draw Z from the distribution on $[0,1]$ with probability density function $2x$. Then, prune all points whose projected distance onto the top eigenvector is at least TZ. This randomized pruning method is derived from the mean estimation algorithm for unknown covariance distributions by Diakonikolas et al. (2017a). Fixed Pruning simply prunes the 0.5τ percentage of points whose projection onto the top eigenvector is furthest from the median of the projected points at every iteration. This is identical to the pruning method in QUE_low_n, with projected deviations being used as "outlier scores", instead of the quantum entropy scores used in QUE_low_n. Results are shown in Figures 53, 54, 55, 56. We find that both randomized and fixed pruning are able to match or slightly outperform the standard Gaussian pruning method. However, we note that unlike in QUE_low_n, fixed pruning could potentially result in catastrophic error. In particular, if corruption is uniformly distributed across $O(d)$ orthogonal clusters, then ev_filtering_low_n may take $O(d)$ runs to return an outlier, since it can only prune in one direction at once. But with fixed pruning, each iteration will prune too many outliers in each direction. We only evaluate Gaussian pruning to follow the conventions of Diakonikolas et al. (2017a).
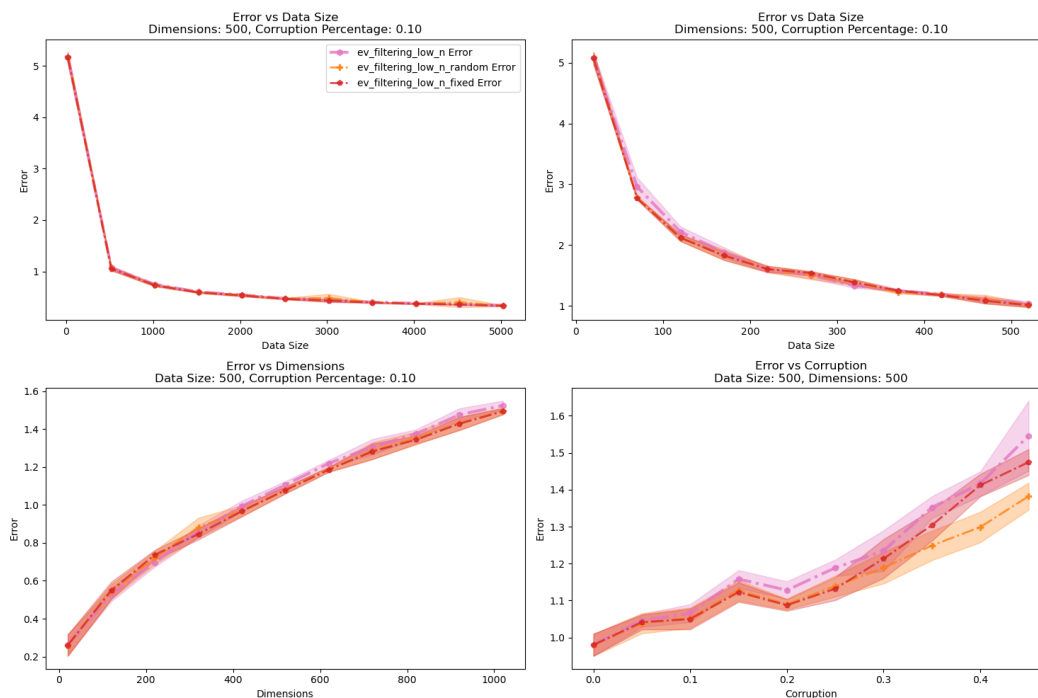
Figure 53: Eigenvalue Pruning - Pruning Method: Identity Covariance, DKK Noise
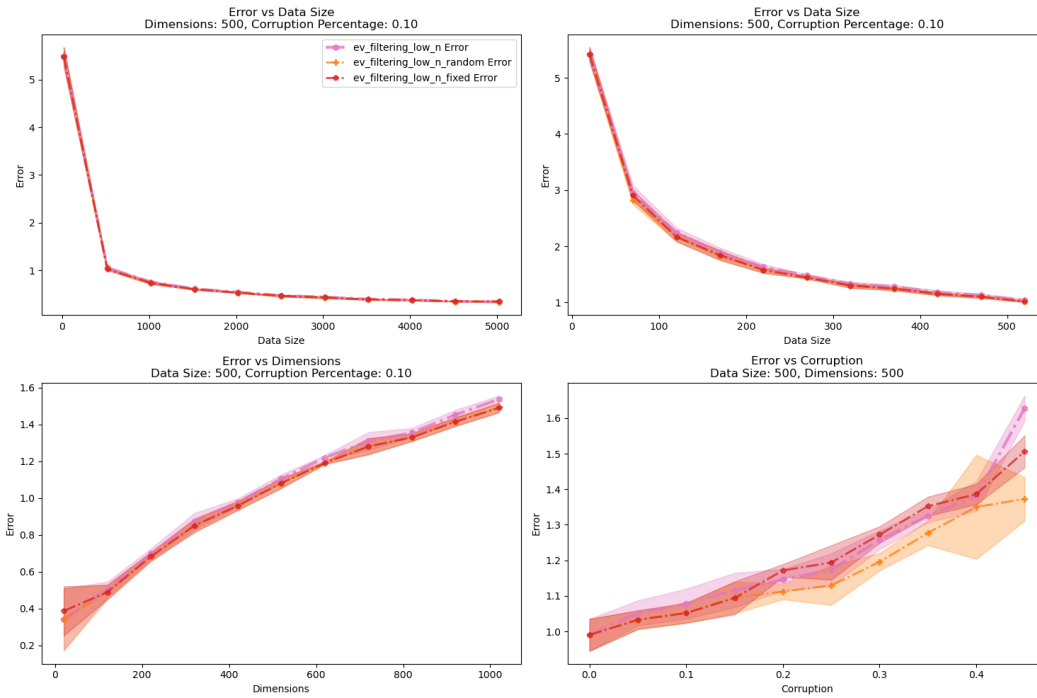
Figure 54: Eigenvalue Pruning - Pruning Method: Identity Covariance, In Distribution Noise
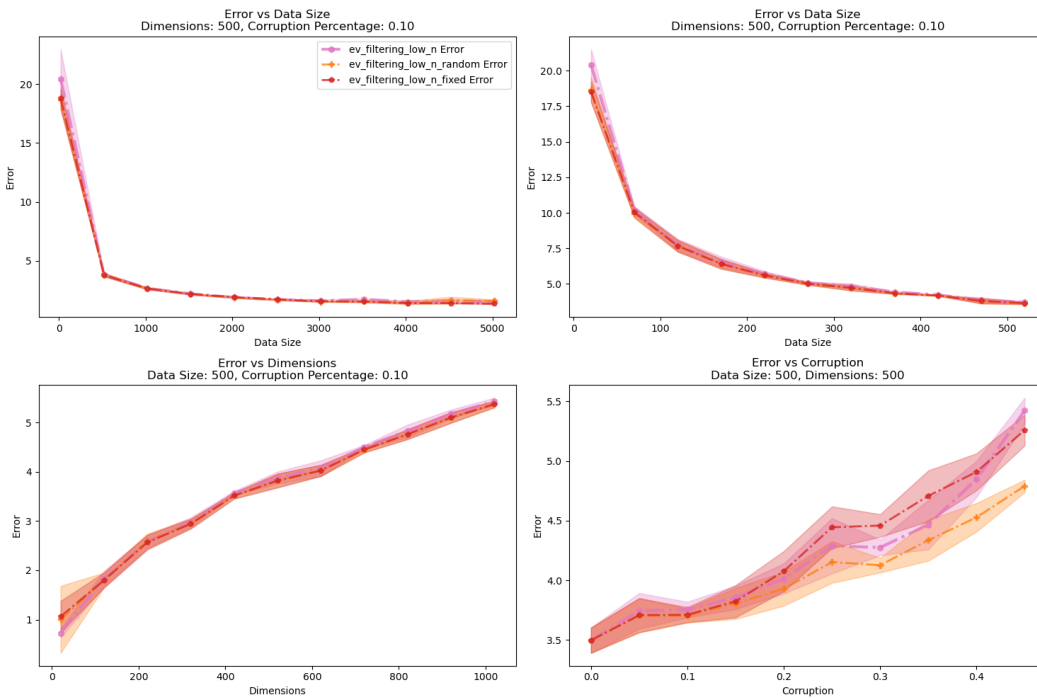
Figure 55: Eigenvalue Pruning - Pruning Method: Large Spherical Covariance, Additive Variance Shell Noise
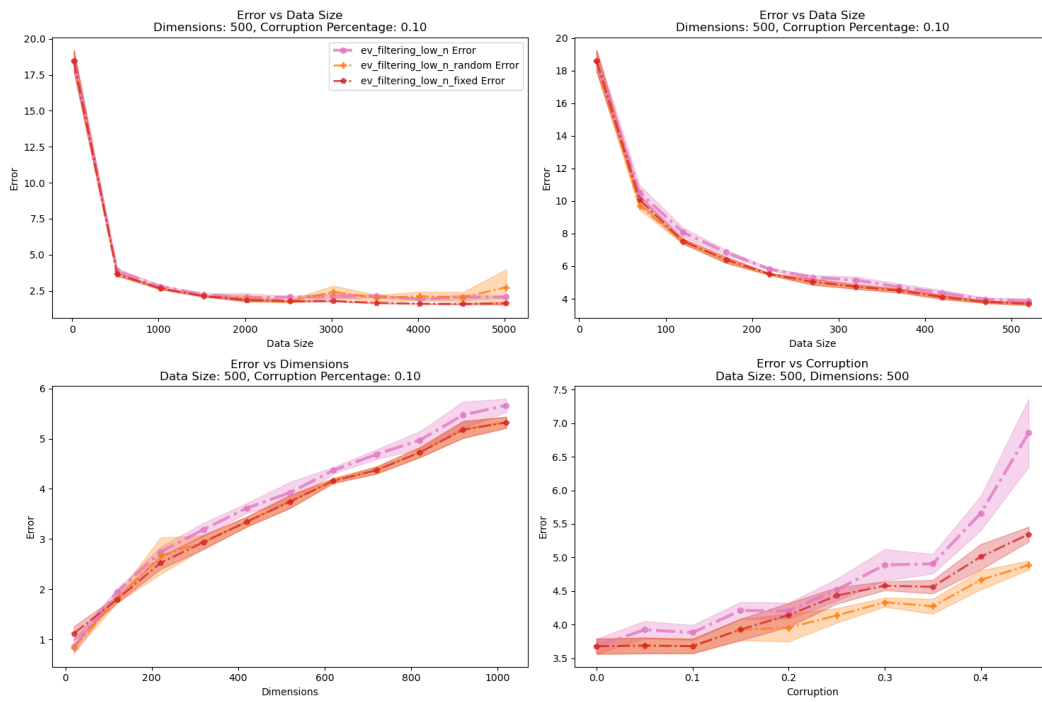
Figure 56: Eigenvalue Pruning - Pruning Method: Large Diminishing Covariance, Additive Variance Shell Noise

Projected Gradient Descent Iterations Here we explore the number of iterations parameter, γ for PGD. We choose values for γ in the set $[1, 5, 10, 15, 20]$. Results are shown in Figures 57, 58, 59, 60. We find that low choices of γ result in significantly worse performance, while higher choices perform roughly equally. Notably, when γ is set equal to 10, PGD performs much worse over Identity Covariance with DKK Noise, especially under large n, despite this choice of γ performing among the best across other distributions. This suggests that larger choices of γ may be necessary for PGD to be robust across different corruption schemes. We note that the runtime of PGD increases approximately linearly with respect to γ, so there is a meaningful tradeoff when using larger values of γ. We set $\gamma = 15$ across our experiments because it is the lowest γ that performs among the best across the distributions tested.
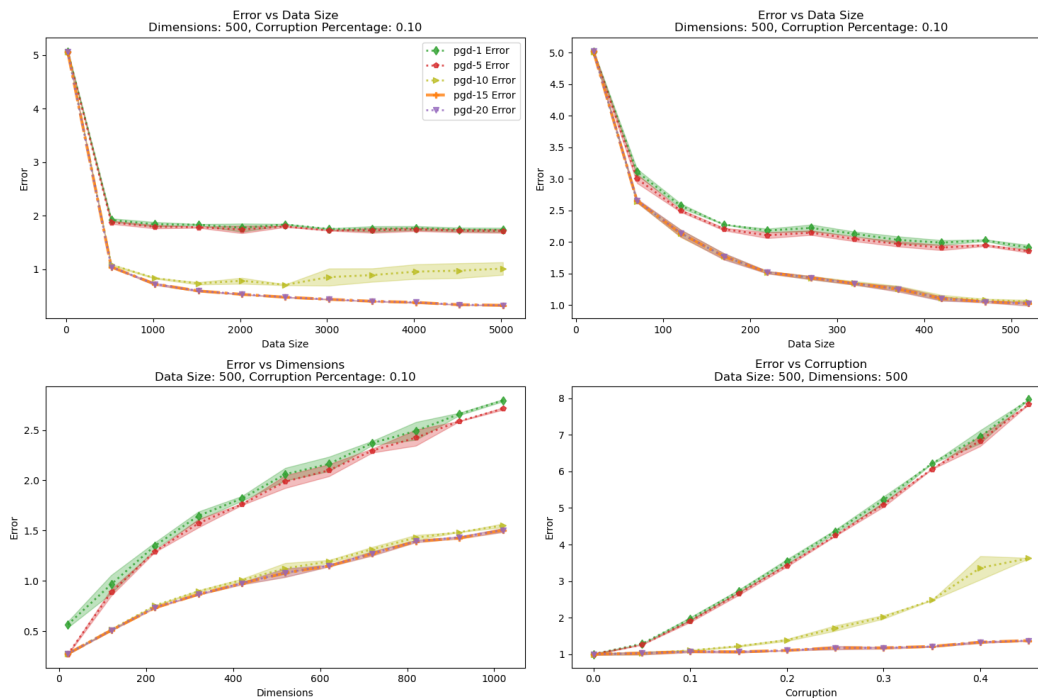
Figure 57: Projected Gradient Descent - Number Of Iterations γ: Identity Covariance, DKK Noise
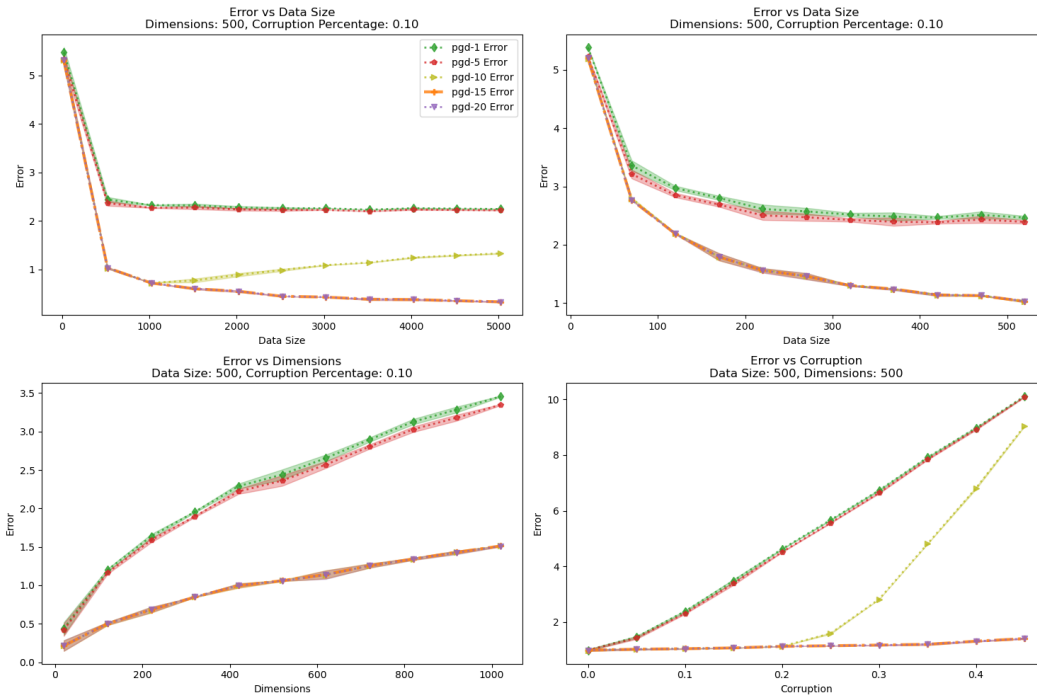
Figure 58: Projected Gradient Descent - Number Of Iterations γ: Identity Covariance, In Distribution Noise
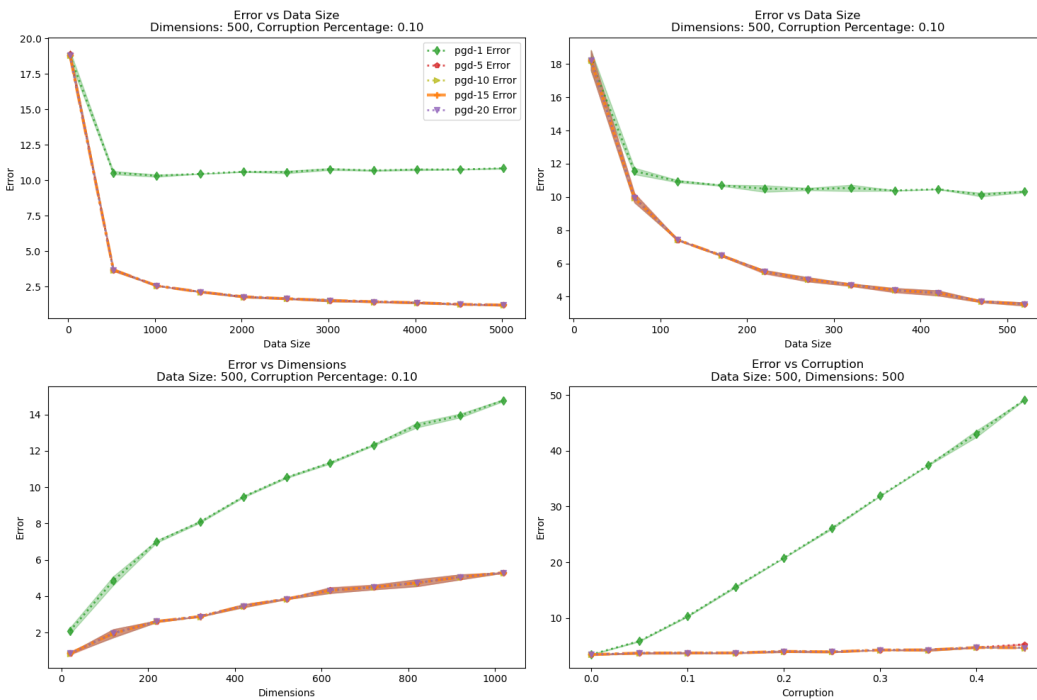
Figure 59: Projected Gradient Descent - Number Of Iterations γ: Large Spherical Covariance, Additive Variance Shell Noise
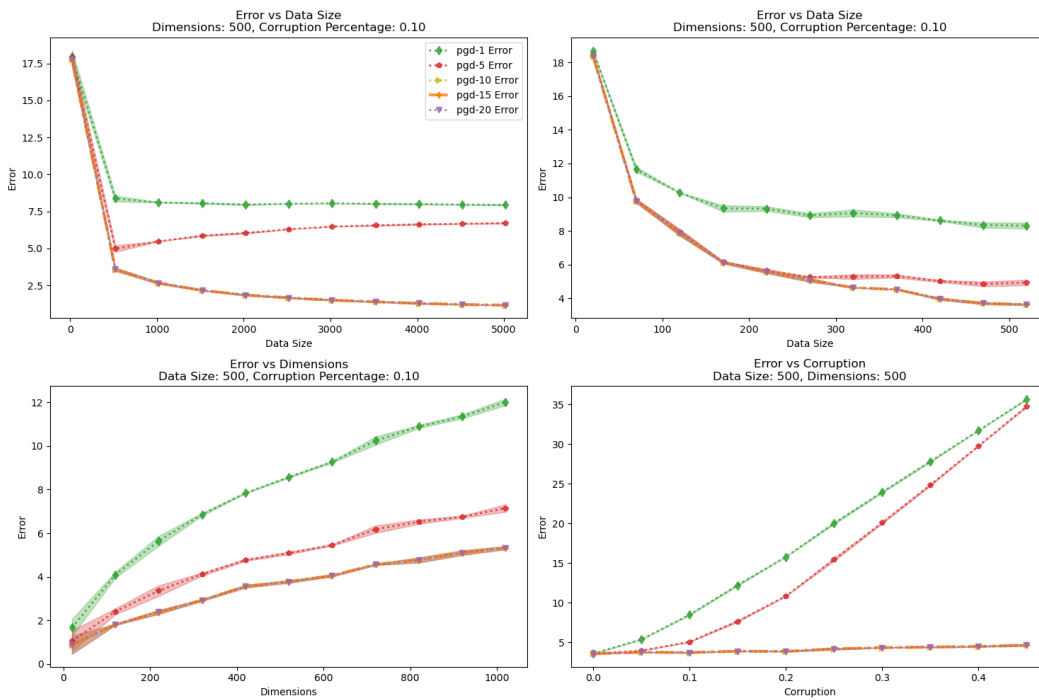
Figure 60: Projected Gradient Descent - Number Of Iterations γ: Large Diminishing Covariance, Additive Variance Shell Noise

A.6 Robustness To Expected Corruption

(a) Identity Covariance - DKK Noise

(b) Identity Covariance - Subtractive Noise

(c) Large Spherical Covariance - Additive Variance Shell Noise

(d) Large Diminishing Covariance - Additive Variance Shell Noise
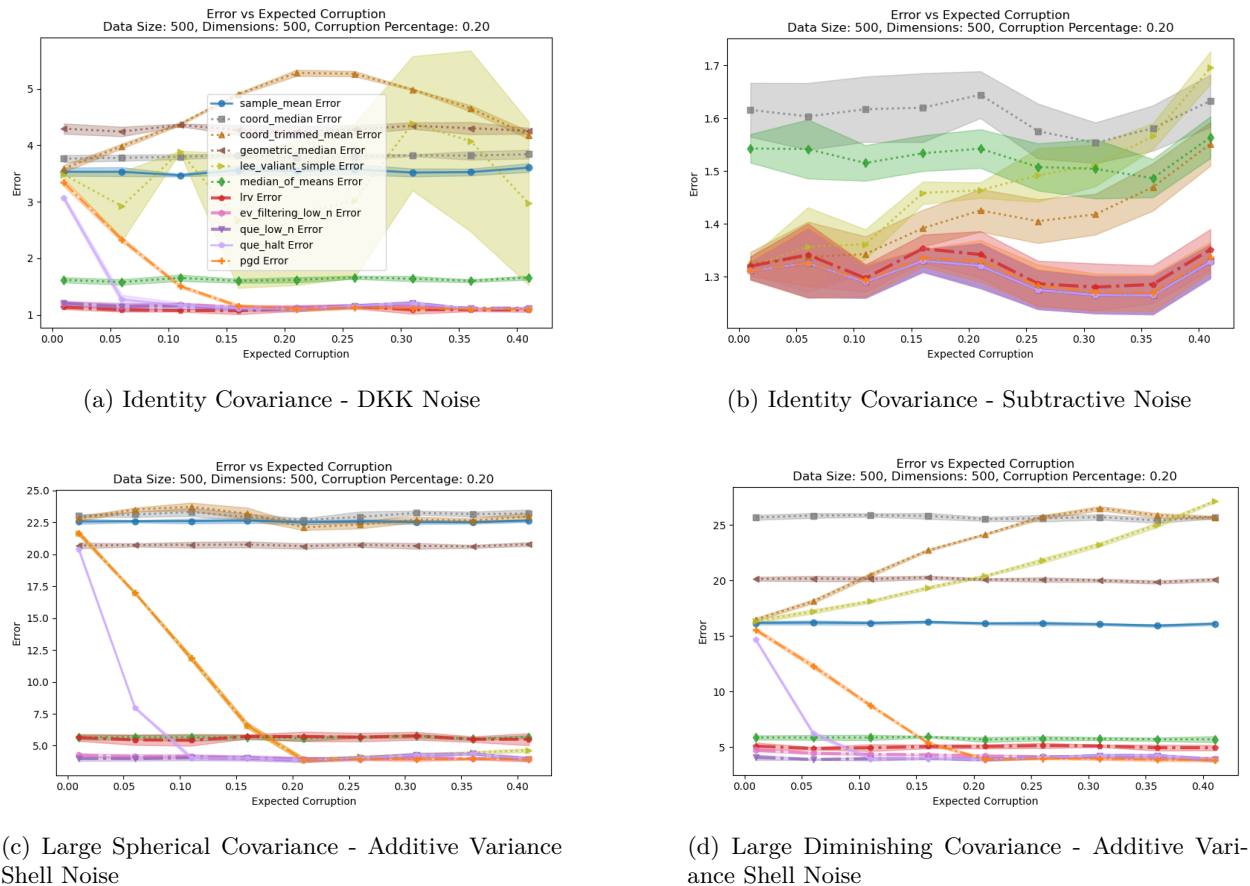
Figure 61: Robustness To Expected Corruption: Error vs Expected Corruption τ

We examine robustness to expected corruption, τ. This is a hyperparameter for ev_filtering_low_n, QUE_low_n, PGD, lee_valiant_simple, and coord_trimmed_mean. In ev_filtering_low_n, τ only plays a soft role as a slack term in the filtering step. In QUE_low_n, τ controls the number of points that are pruned in every iteration of the algorithm, but the number of iterations is unbounded. In lee_valiant_simple, and coord_trimmed_mean, τ explicitly controls the amount of data that is pruned in total. In PGD, τ controls the space of feasible outlier weights. We evaluate error as expected corruption, τ, varies from $\tau = 0.01$ to $\tau = 0.46$ with true corruption fixed as $\eta = 0.20$. Otherwise, the experiment setup remains the same as seen previously. As in Appendix A.5, we replicate experiments over Identity Covariance with DKK Noise and with Subtractive Noise; Large Spherical Covariance with Additive Variance Shell Noise; and Large Diminishing Covariance with Additive Variance Shell Noise. These results are shown in Figure 61, with all estimators included for reference. We include QUE_low_n with and without early halting.

We find that most estimators perform nearly identically regardless of the choice of τ, except for PGD, which performs nearly identically when τ is an upper bound on true corruption η but degrades with underestimates of η. QUE_low_n without early halting performs well throughout choices of τ. With smaller choices of τ, it will prune significantly less points at each iteration, but will run for more iterations until the corruption detection threshold is passed, while for larger choices of τ, it will prune more points at each iteration, but will run for less iterations until the corruption detection threshold is passed. QUE_low_n with early halting, which is used throughout the real world experiments, sees degradation with underestimates of τ, but identical performance with overestimates. ev_filtering_low_n also performs nearly identically regardless of the choice of τ, as expected by the soft dependency of the pruning threshold on τ. lee_valiant_simple and coord_trimmed_mean both degrade noticeably as τ increases over Identity Covariance data with Subtractive

Noise and Large Diminishing Covariance data with Additive Variance Shell Noise; in both cases yielding error worse than `sample_mean` the more points they prune. Surprisingly, over Large Spherical Covariance with Additive Variance Shell Noise, `lee_valiant_simple` nearly exactly matches the performance of `PGD`, except with slightly worse degradation with large overestimates of τ.

A.7 Image Embedding Experiments

We evaluate algorithms on the problem of estimating the mean of embeddings of images generated by deep pretrained image models. As in the LLM experiment, we first examine the problem of mean estimation of image embeddings belonging to the same category, reporting LOOCV error. We then examine a corrupted distribution where images belonging to one category are considered inliers and those belonging to another are considered outliers. We utilize a set of images of cats and dogs from the CIFAR10 dataset (Krizhevsky, 2009). We embed these images using 4 deep pretrained image models of varying embedding dimensions: ResNet-18, ResNet-50 (He et al., 2015), MobileNet V3 (Howard et al., 2019), and EfficientNet B0 (Tan & Le, 2020). ResNet-18 has an embedding dimension of 512, MobileNet V3 has one of 960, EfficientNet B0 has one of 1280, and ResNet-50 has one of 2048.

Common Category Images Here we examine LOOCV error vs data size on embeddings of images of cats. We vary data size from $n = 10$ to $n = 1000$. Otherwise, experiments are run identically to the LLM experiment, fixing expected corruption $\eta = 0.1$, employing the trace scaling heuristic on `ev_filtering_low_n` and `QUE_low_n`, the halting heuristic on `QUE_low_n`, and averaging results over 5 runs. We note that, as in the LLM experiments, employing the halting heuristic on `ev_filtering_low_n` does not improve performance. Results are shown in Figure 62.

As in the LLM experiment, we observe that no algorithm significantly outperforms `sample_mean`, despite the nontrivial LOOCV error in each setting. As in the LLM experiment, `ev_filtering_low_n` tends to perform worse than other algorithms, which is unsurprising given its sensitivity to knowledge of the true covariance. Other robust mean estimation algorithms, including `QUE_low_n`, perform near identically to `sample_mean`.

Corrupted Images For the corrupted case, we draw data $X \sim (1-\eta)P + \eta Q$, where the inlier distribution, P, consists of embeddings of images of cats, and the outlier distribution, Q, consists of embeddings of images of dogs. We fix data size $n = 1000$ to focus on the $n \approx d$ and $n < d$ regime. Otherwise, the experimental setup is identical to in the LLM experiments. Results are shown in Figure 63.

These results demonstrate similar trends to the LLM experiment. One key difference is that `coord_trimmed_mean` performs much worse than `sample_mean` here, compared to the LLM experiment where it tends to slightly outperform `sample_mean`. This suggests that naive pruning does not work well in this setting as outliers are not obvious, reinforcing that this is a difficult setting for robust mean estimation. Nonetheless, several robust mean estimators are able to perform well in this case. In particular, `QUE_low_n` is again the strongest performer, noticeably outperforming all other estimators and nearly matching `good_sample_mean` error across settings. Notably, this strong performance occurs even with n much less than d, with relative performance remaining the same even with $n = 1000$ and $d = 2048$ in the ResNet-50 embedding case. Among the best estimators in the synthetic data case, `PGD` tends to perform similarly to `sample_mean`, except with large enough corruption across MobileNet V3 embeddings where it outperforms `sample_mean`; `LRV` tends to perform similarly to `sample_mean` except under low corruption, where it noticably degrades; and `ev_filtering_low_n` fails catastrophically throughout. As in the LLM experiments, `median_of_means` outperforms robust estimators that tend to perform better in the synthetic data cases. However, `lee_valiant_simple` no longer performs near optimally, suggesting its sensitivity to distributional assumptions, as expected due to its general poor performance over synthetic data experiments.

Corruption vs Data Size We repeat experiments over the same corrupted data scheme but examine error vs data size. We fix true corruption $\eta = 0.1$, set expected corruption $\tau = \eta$, and vary data size n. We examine the performance of all estimators with data size ranging from $n = 100$ to $n = 5000$. We additionally provide a zoomed in plot, examining the performance of estimators excluding `ev_filtering_low_n`, `coord_median`, and

(a) ResNet-18 Embeddings

(b) MobileNet V3 Embeddings

(c) EfficientNet B0 Embeddings

(d) ResNet-50 Embeddings
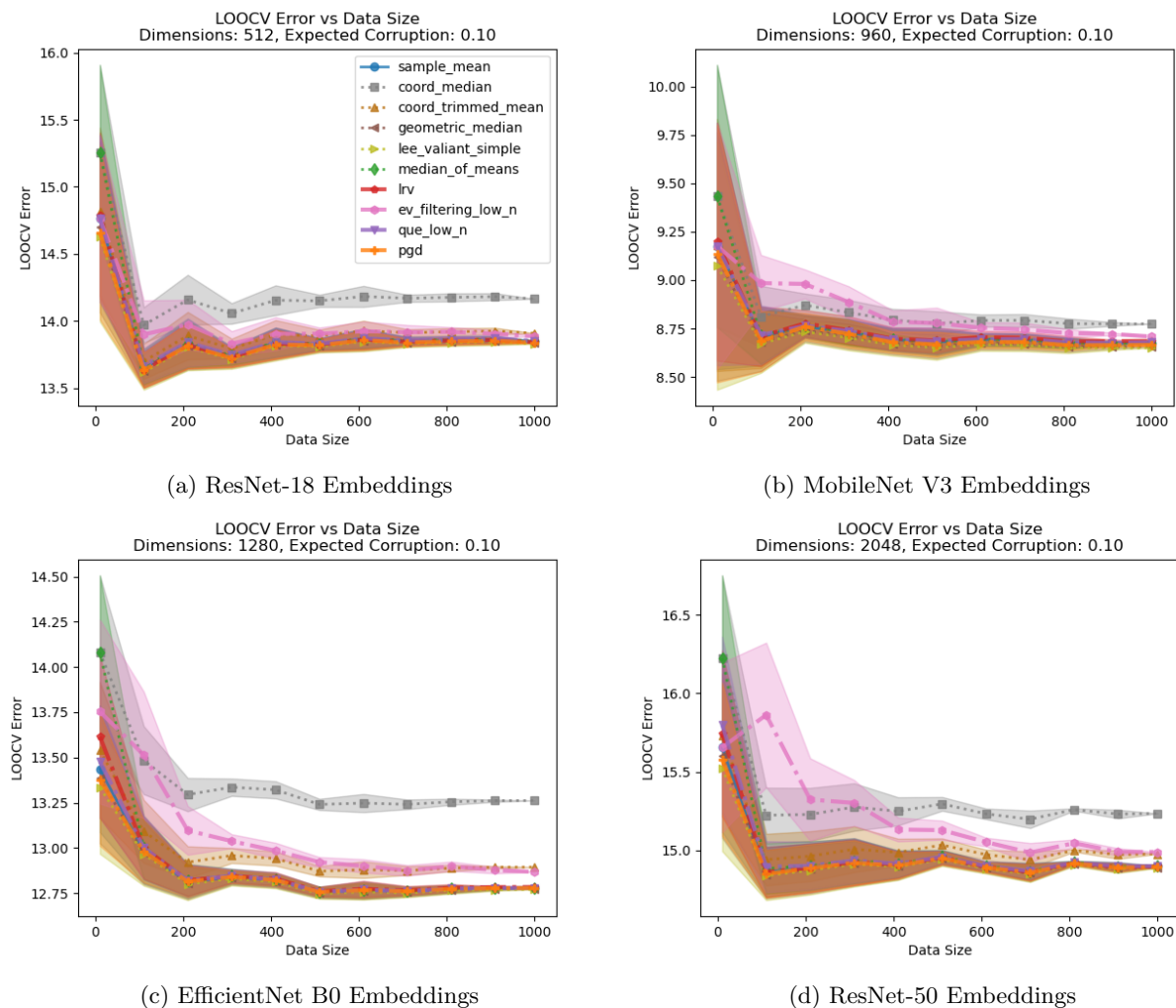
Figure 62: LOOCV Error on Cat Image Embeddings

coord_trimmed_mean– which all fail catastrophically – with data size from $n = 100$ to $n = 1000$. Results are shown in Figure 64.

We find that the relative performance of algorithms remains similar across data sizes. Particularly, even with very large n, such as $n = 5000$ and $d = 512$ under ResNet-18 Embeddings, only QUE_low_n and median_of_means consistently outperform sample_mean. PGD, LRV, and lee_valiant_simple tend to perform slightly worse than sample_mean. ev_filtering_low_n fails catastrophically regardless of data size, though the error stabilizes with larger n. These results suggest that the weakness of robust mean estimators over real world data distributions is not just confined to the low data size regime. Yet again, we find that QUE_low_n is the best performer, outperforming all other estimators and achieving near optimal performance throughout settings. Additionally, median_of_means does not show this same sensitivity to distributional assumptions as other estimators, and as in the synthetic data experiments, tends to perform near optimally with large enough n.
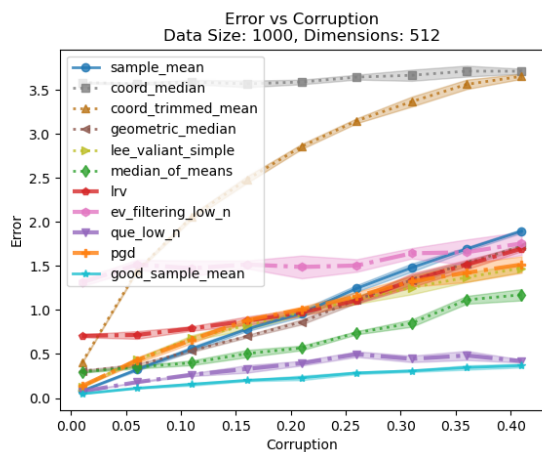
(a) ResNet-18 Embeddings
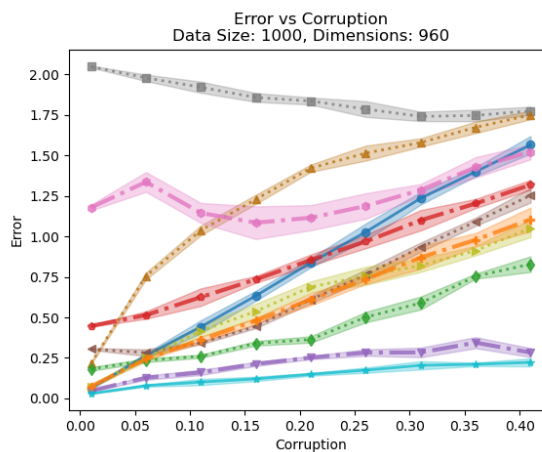
(b) MobileNet V3 Embeddings
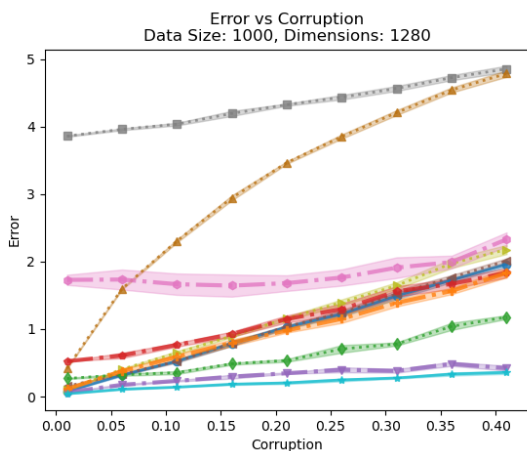
(c) EfficientNet B0 Embeddings
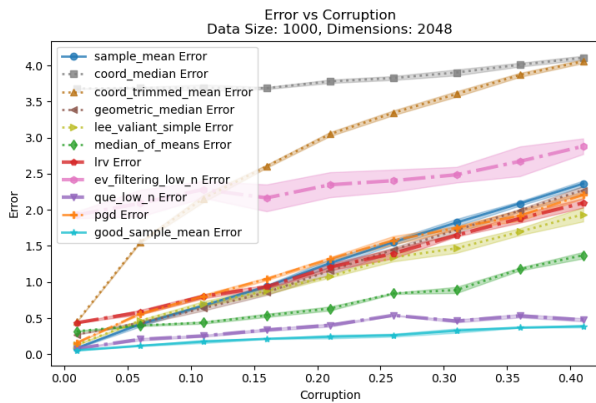
(d) ResNet-50 Embeddings

Figure 63: Error on Cat Image Embeddings Corrupted with Dog Image Embeddings
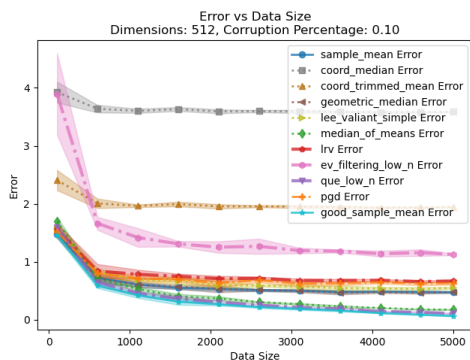
(a) ResNet-18 Embeddings
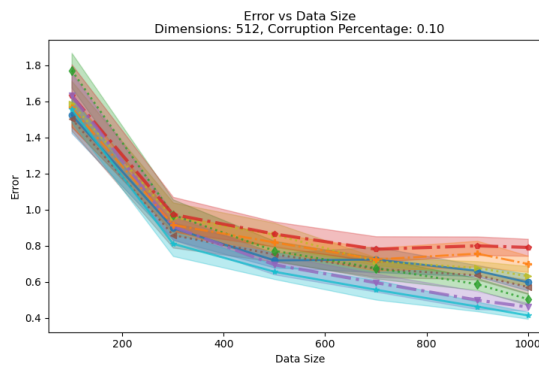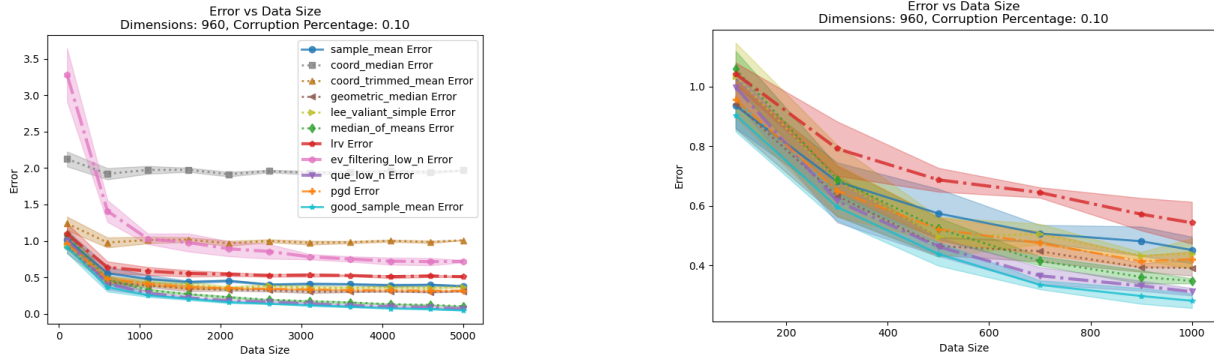
(b) MobileNet V3 Embeddings
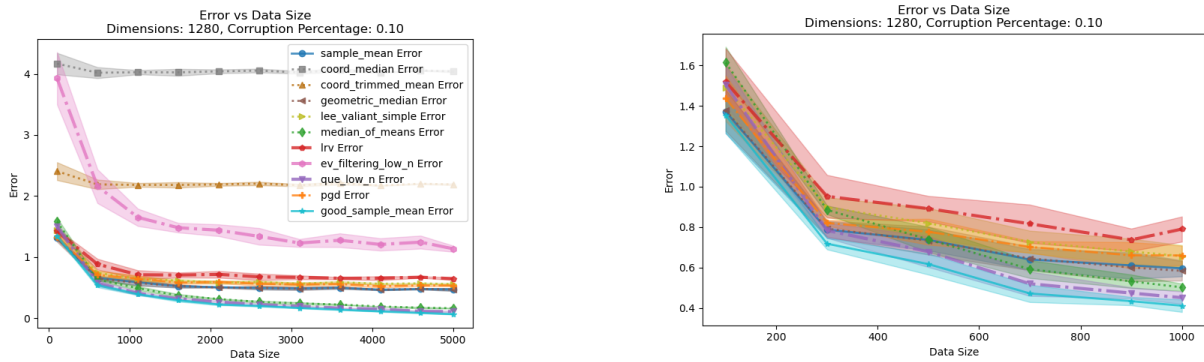
(c) EfficientNet B0 Embeddings
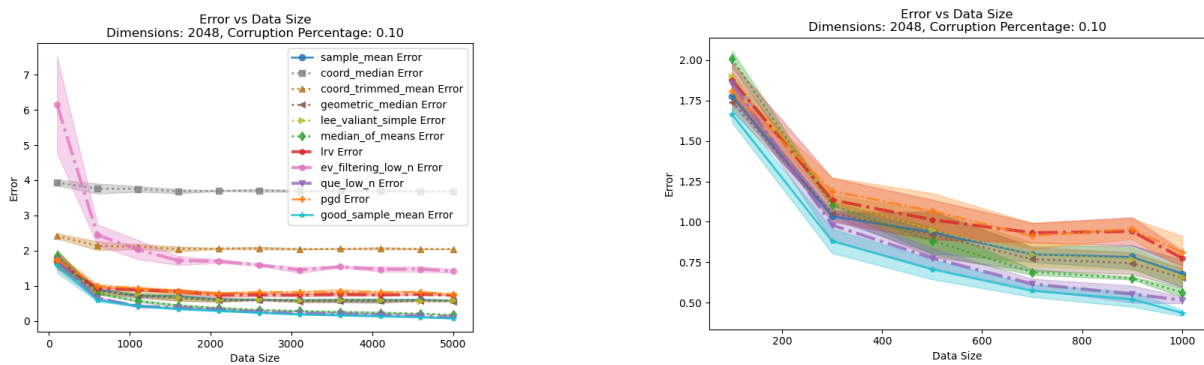
(d) ResNet-50 Embeddings

Figure 64: Error Vs Data Size on Corrupted Image Data

(a) 50 Dimensional Embeddings

(b) 100 Dimensional Embeddings

(c) 200 Dimensional Embeddings

(d) 300 Dimensional Embeddings
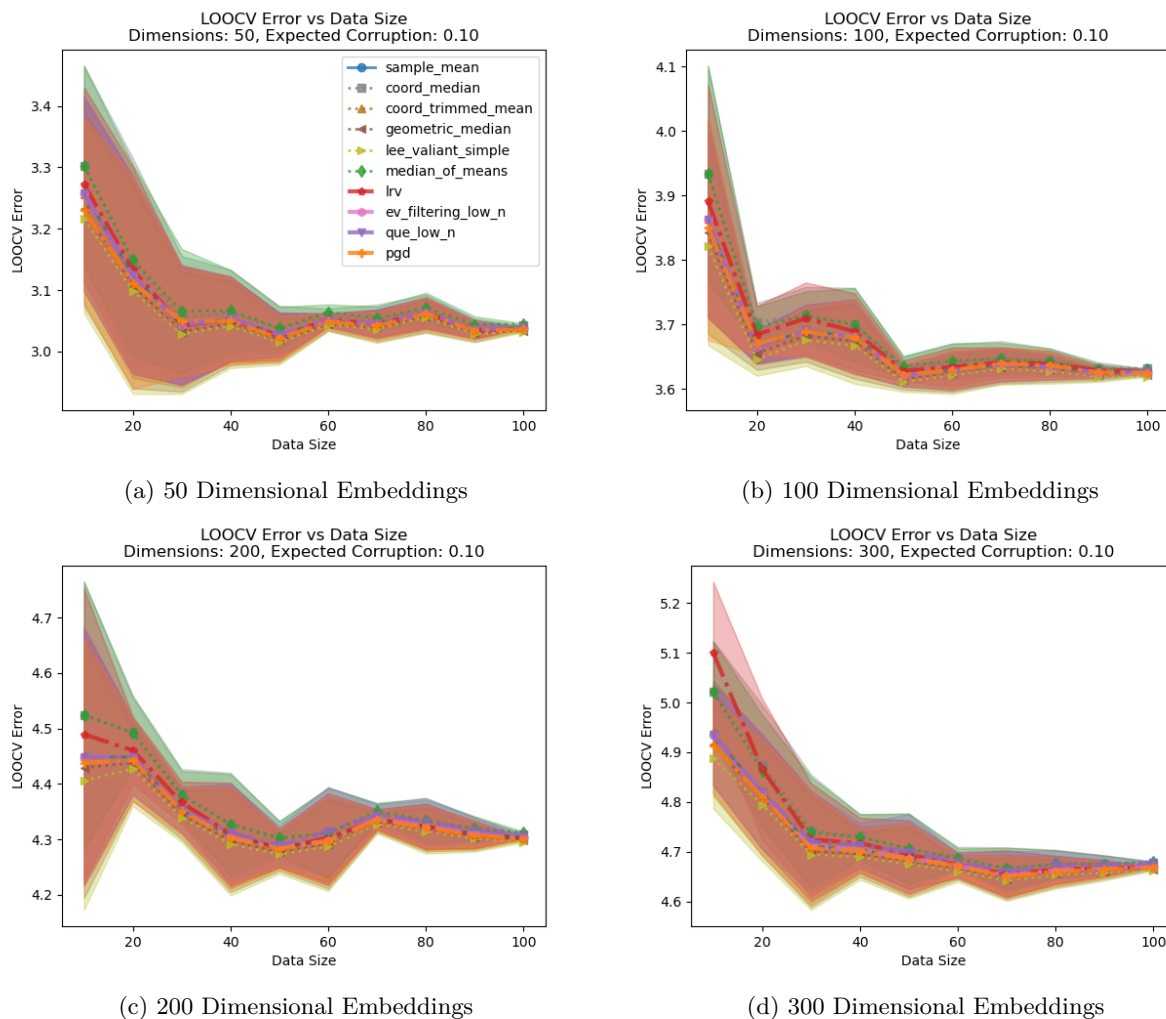
Figure 65: LOOCV Error on "Pleasant" GloVe Embeddings

A.8   Word Embedding Experiments

We further evaluate algorithms on the problem of estimating the mean of non attention based embeddings of words. As in the LLM experiment, we first examine the problem of mean estimation over words belonging in the same category, reporting LOOCV error. We then examine a corrupted distribution where words belonging to one category are considered inliers and those belonging to another are considered outliers. We examine four different pretrained GloVe (Pennington et al., 2014) models from GluonNLP[6] generating 50, 100, 200, and 300 dimensional embeddings. We utilize datasets of 100 pleasant words and 100 unpleasant words from Aboagye et al. (2023). The very limited data size available under this setting provides a valuable real world test for robust estimators under low data size.

Common Category Words   Here we examine LOOCV error vs data size on embeddings of "pleasant" words. Experiments are run identically to the LLM experiment, employing the trace scaling heuristic on ev_filtering_low_n and QUE_low_n, the halting heuristic on QUE_low_n, and averaging results over 5 runs. Results are shown in Figure 65.

---

[6]https://github.com/dmlc/gluon-nlp/

(a) 50 Dimensional Embeddings

(b) 100 Dimensional Embeddings

(c) 200 Dimensional Embeddings

(d) 300 Dimensional Embeddings
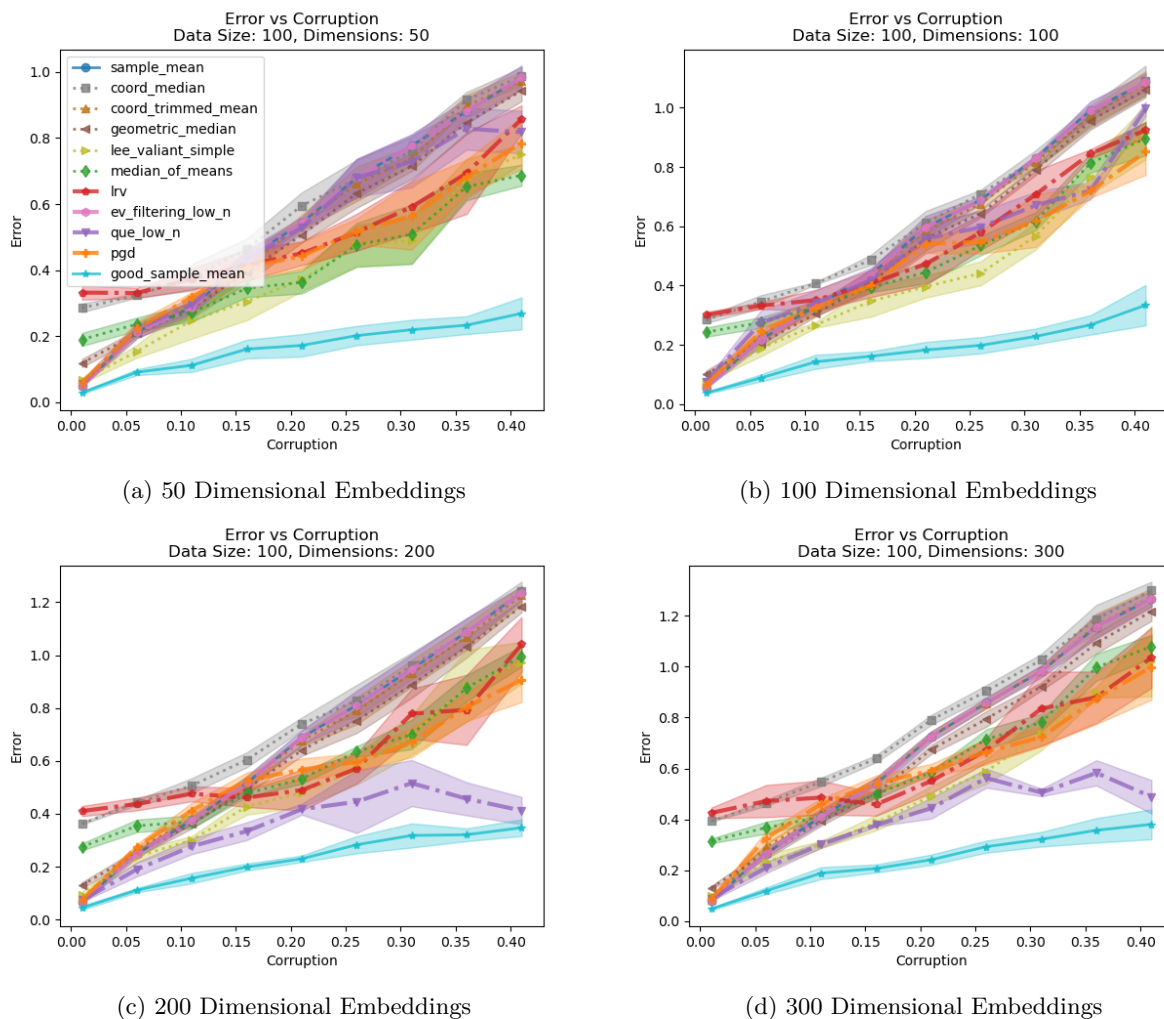
Figure 66: Error on "Pleasant" Embeddings Corrupted with "Unpleasant" Embeddings

As in the LLM experiment, we observe that no algorithm significantly outperforms sample_mean, despite the nontrivial LOOCV error in each setting. Moreover, we observe that median_of_means consistently achieves error slightly worse than sample_mean, which is not seen in the LLM experiments, suggesting the algorithm's sensitivity to distributional assumptions. However, unlike in the LLM experiment ev_filtering_low_n does not fail catastrophically here, instead nearly matching sample_mean. This is not unexpected given ev_filtering_low_n, and the trace estimate techniques sensitivity to distributional assumptions will sometime work – including this case. LRV also tends to perform worse than other algorithms, though this gap is not as large as in the LLM experiment.

Corrupted Words For the corrupted case, we draw data $X \sim (1-\eta)P + \eta Q$, where the inlier distribution, P, consists of embeddings of "pleasant" words, and the outlier distribution, Q, consists of embeddings of "unpleasant" words. This models a more extreme version of the case where ill-defined words may be placed in a category, inducing bias. This is a notable problem for word vectors, which do not take context into account (Hu et al., 2016). The experimental setup is identical to in the LLM experiments. Results are shown in Figure 66.

While these results are different from the LLM experiment, they demonstrate similar trends. In particular, QUE_low_n is again the strongest performer, noticeably outperforming all other estimators across the 200 and 300 dimensional cases, and never performing worse than sample_mean in the 50 and 100 dimensional

(a) 50 Dimensional Embeddings

(b) 100 Dimensional Embeddings

(c) 200 Dimensional Embeddings

(d) 300 Dimensional Embeddings
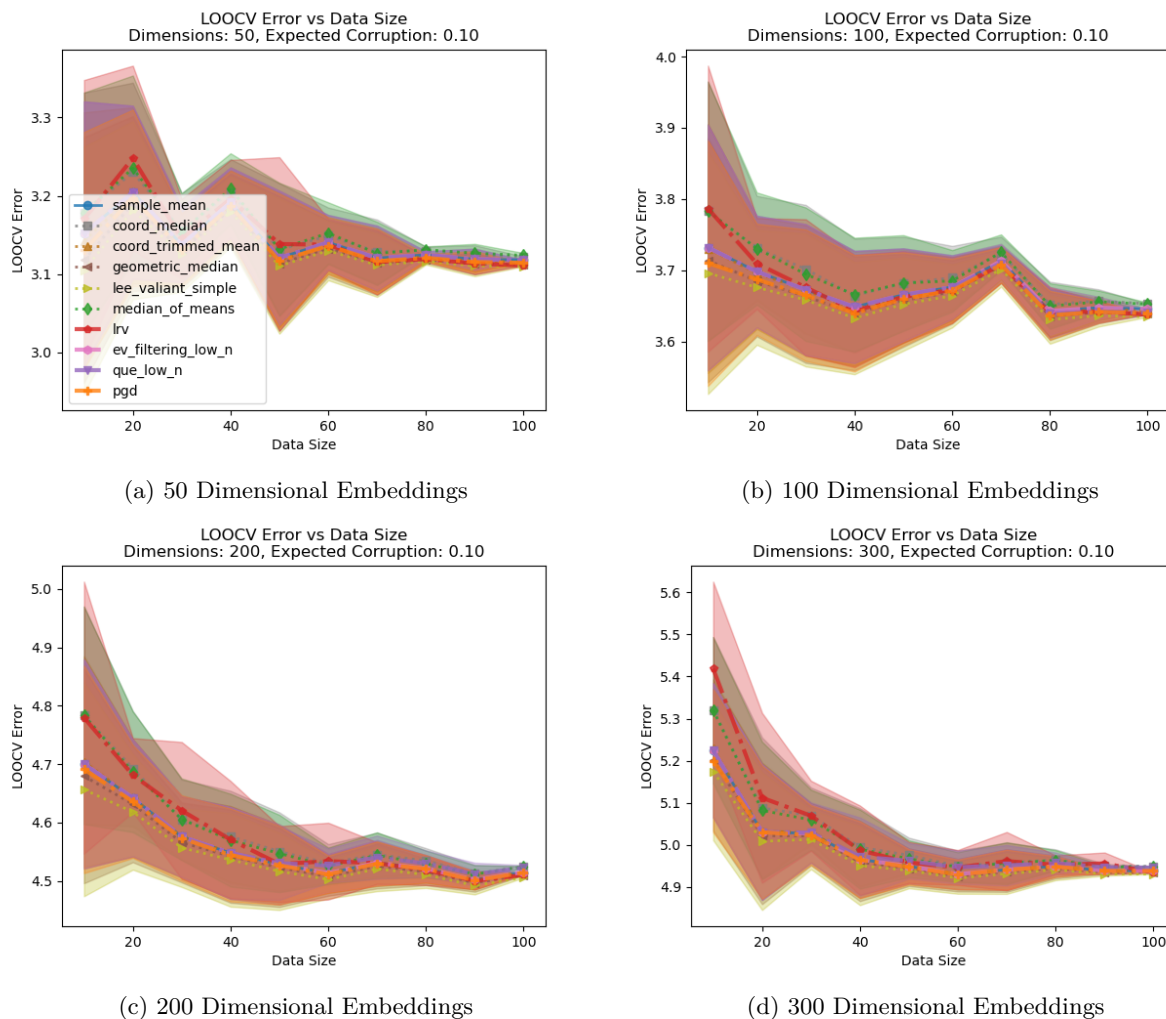
Figure 67: LOOCV Error on "Unpleasant" GloVe Embeddings

cases. Notably, this strong performance occurs even with n much less than d. Unlike the LLM experiments, here QUE_low_n never approaches good_sample_mean, and is beat by other estimators in the 50 and 100 dimensional cases. lee_valiant_simple, which tended to perform similarly to QUE_low_n and nearly match good_sample_mean in the LLM experiments, does not perform as well in this case. It always beats sample_mean but does not come close to matching good_sample_mean and performs similarly to other estimators. Likewise, median_of_means does not perform as strongly here as in the LLM experiments and even performs worse than sample_mean over very low corruption. Supported by synthetic data results, this suggests the sensitivity of median_of_means and lee_valiant_simple to distributional assumptions. As in the LLM experiments, LRV tends to perform much worse than sample_mean under low corruption and outperform sample_mean slightly with higher corruption; PGD tends to outperform sample_mean slightly; and coord_median, coord_trimmed_mean, and geometric_median tend to perform similarly or slightly worse than sample_mean. As in the LOOCV experiments, ev_filtering_low_n simply matches sample_mean here.

Additional Experiments We perform additional experiments, swapping the roles of "pleasant" and "unpleasant" embeddings. We report LOOCV error vs data size on embeddings of "unpleasant" words in Figure 67. We report corrupted error vs data size on embeddings of "unpleasant" words corrupted with "pleasant" words in Figure 68. We observe the same trends as in the previous word embedding experiments.

(a) 50 Dimensional Embeddings

(b) 100 Dimensional Embeddings

(c) 200 Dimensional Embeddings

(d) 300 Dimensional Embeddings
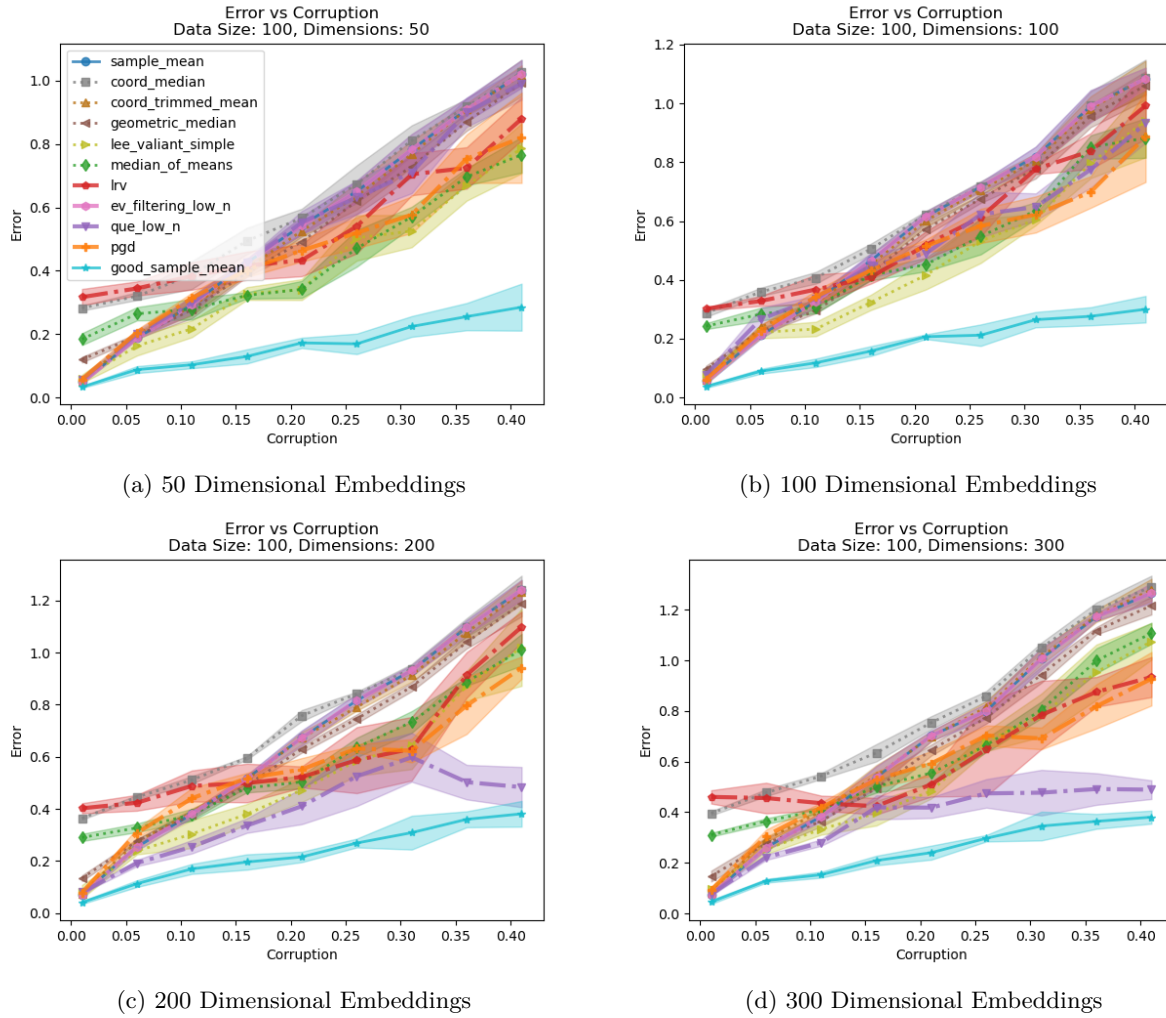
Figure 68: Error on "Unpleasant" Embeddings Corrupted with "Pleasant" Embeddings

A.9   LLM Experiment Ablations

Eigenvalue Pruning Method Comparison   We compare the performance of different pruning subroutines for ev_filtering_low_n over a selection of LLM experiments: LOOCV and Corruption Error over MiniLM and BERT embeddings. We evaluate Gaussian pruning, used throughout this paper, along with randomized pruning and fixed pruning, described in Appendix A.5. We retain the same conditions as in the original experiments, first scaling data utilizing the sample trace. We also include sample_mean and QUE_low_n in our plots for the sake of comparison, noting that QUE_low_n and ev_filtering_low_n with fixed pruning only differ in their method of scoring outliers. These results are shown in Figure 69. We notice that both randomized and fixed pruning methods do indeed perform better than the Gaussian pruning method. In particular, fixed pruning has the best LOOCV error over MiniLM and matches the error of sample_mean over BERT, whereas Gaussian pruning fails dramatically. However, this performance does not translate into the corrupted case, where all three pruning routines lead to significant error compared to even sample_mean, except with large η where it sample_mean's error approaches that of these methods. Additionally, as discussed in Appendix A.5, ev_filtering_low_n with fixed pruning is not robust to noise distributions that require several runs of the algorithm to prune i.e. cases where noise lays in multiple orthogonal clusters. Notably, QUE_low_n outperforms all variations of ev_filtering_low_n in the corrupted data case, reinforcing the observation that the outlier detection method of QUE_low_n is more robust to distributional assumptions than that of ev_filtering_low_n.

(a) LOOCV Error - MiniLM

(b) LOOCV Error - BERT

(c) Corrupted Error - MiniLM

(d) Corrupted Error - BERT
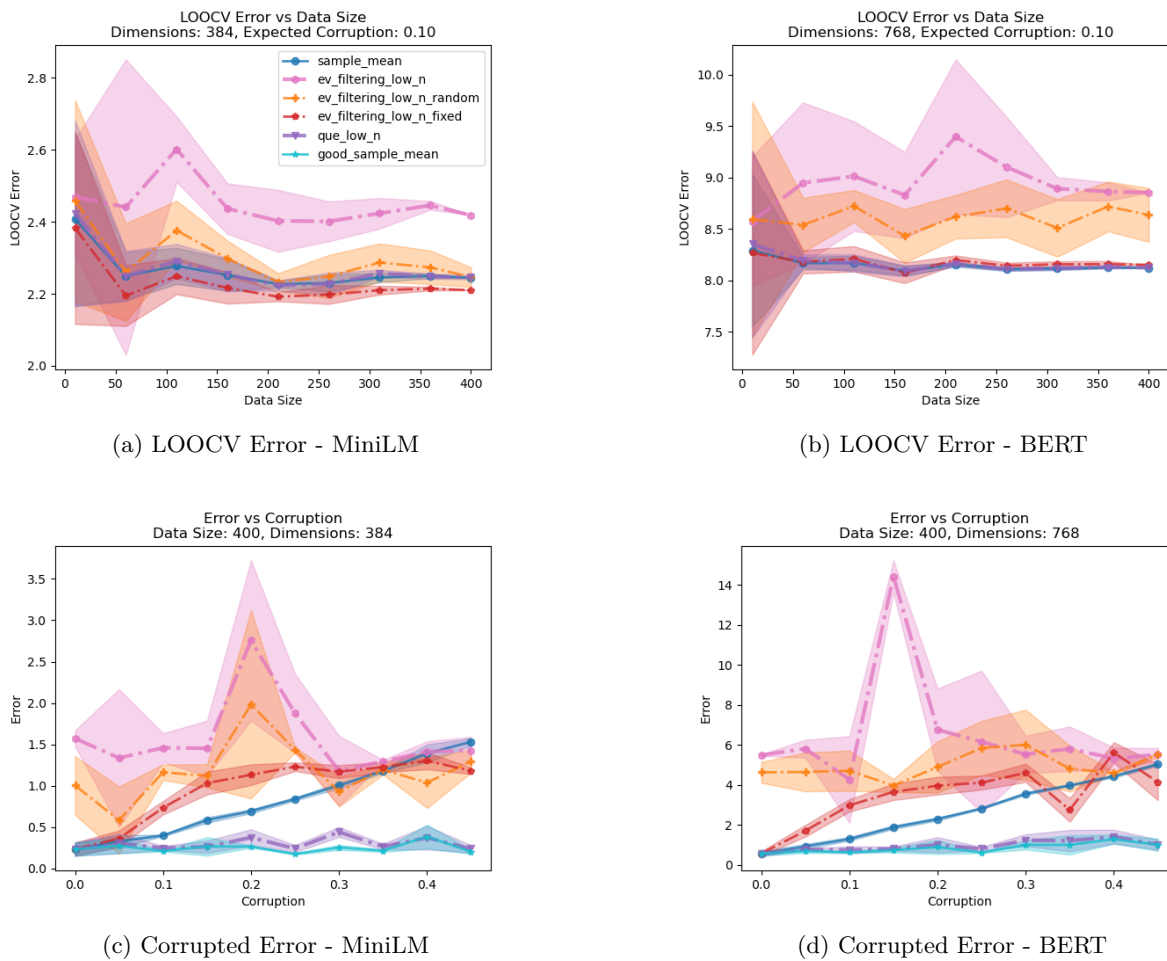
Figure 69: Eigenvalue Pruning - Pruning Method: LLM Comparison

LRV Weighting Procedure   Here we compare the two different weighting procedures for LRV described in Appendix A.5: Gaussian weighting, based on downweighting outliers, and general (non-Gaussian) weighting, based on completely pruning outliers. We evaluate these two methods over the same subselection of LLM experiments: LOOCV and Corruption Error over MiniLM and BERT embeddings. These results are shown in Figure 70. We notice that general weighting outperforms Gaussian weighting in LOOCV error, with this difference being especially noticeable across BERT embeddings. However, this performance increase is not seen in either corrupted case, where Gaussian weighting notably outperforms general weighting, except with small η. This suggests that, at least under low data size, LRV is not robust to general distributions, even using a general outlier weighting procedure.
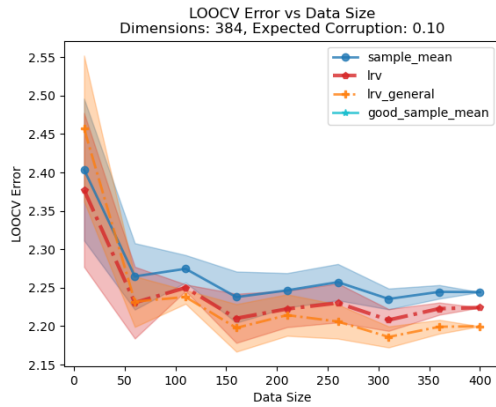
(a) LOOCV Error - MiniLM
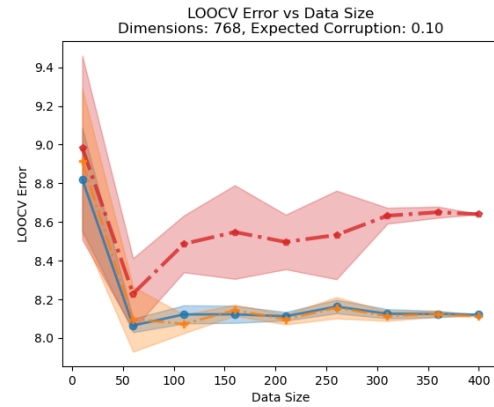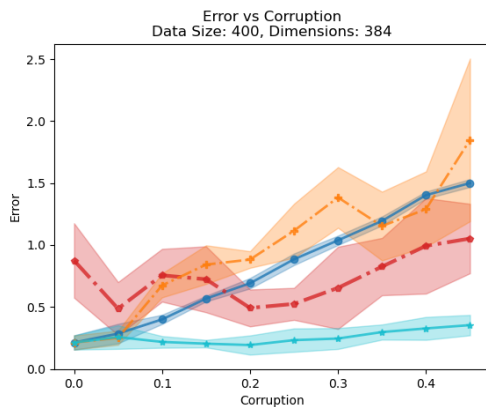
(b) LOOCV Error - BERT

(c) Corrupted Error - MiniLM
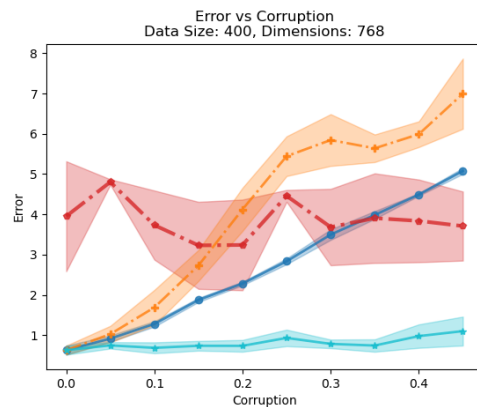
(d) Corrupted Error - BERT

Figure 70: LRV - Gaussian Vs General Weighting: LLM Comparison

Additional Experiments   We recreate the experiments in Section 5 over two different settings. First, we examine LOOCV Error over embeddings of the word field that correspond to the "field of study" definition rather than to the "field of land" definition. These results are shown in Figure 71. Second, we examine corrupted embeddings $X \sim (1 - \eta)P + \eta Q$, where inlier data, P, consists of embeddings of the word "field" corresponding to the "field of study" definition and outlier data, Q, consists of embeddings of the word "field" corresponding to the "field of land" definition; inverting the inlier and outlier data originally examined. These results are shown in Figure 72. While the LOOCV error plots are not identical to the original experiment, corresponding to the expected differences in structure between the distributions of P and Q, we find the same overall trends across the 4 plots. We additionally observe the same overall trends for corrupted data compared to the original experiment. However, lee_valiant_simple, which was consistently the best algorithm alongside QUE_low_n for corrupted data originally, breaks down for MiniLM here; always performing notably worse than good_sample_mean. Supported by the general poor performance of lee_valiant_simple over synthetic data experiments, this reinforces the unpredictable sensitivity of lee_valiant_simple to distributional assumptions. QUE_low_n does not see any such degradation, performing near optimally across all cases, as it does in the original LLM experiment.
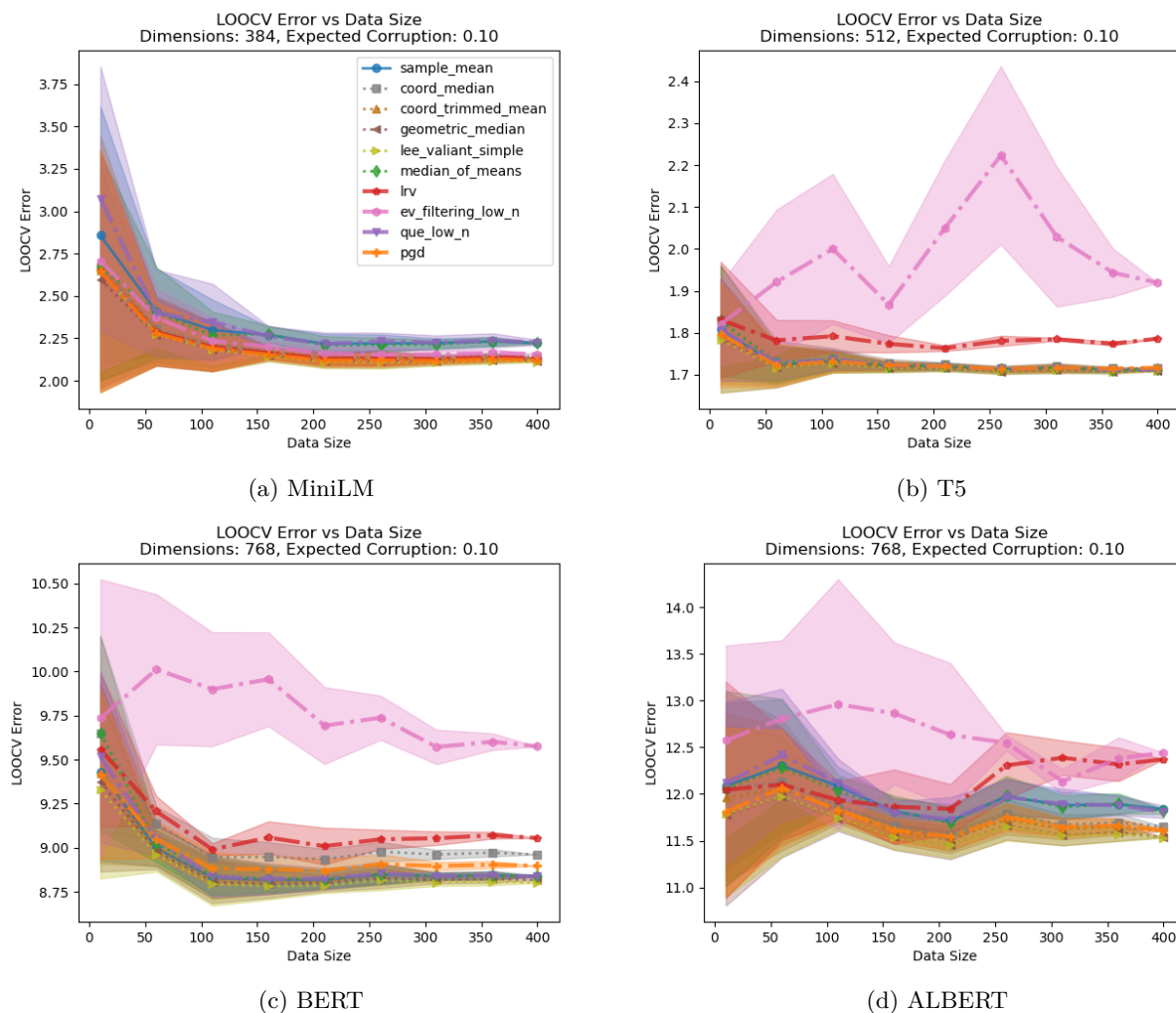
Figure 71: LOOCV Error on "Field Of Study" Embeddings

(a) MiniLM

(b) T5

(c) BERT

(d) ALBERT
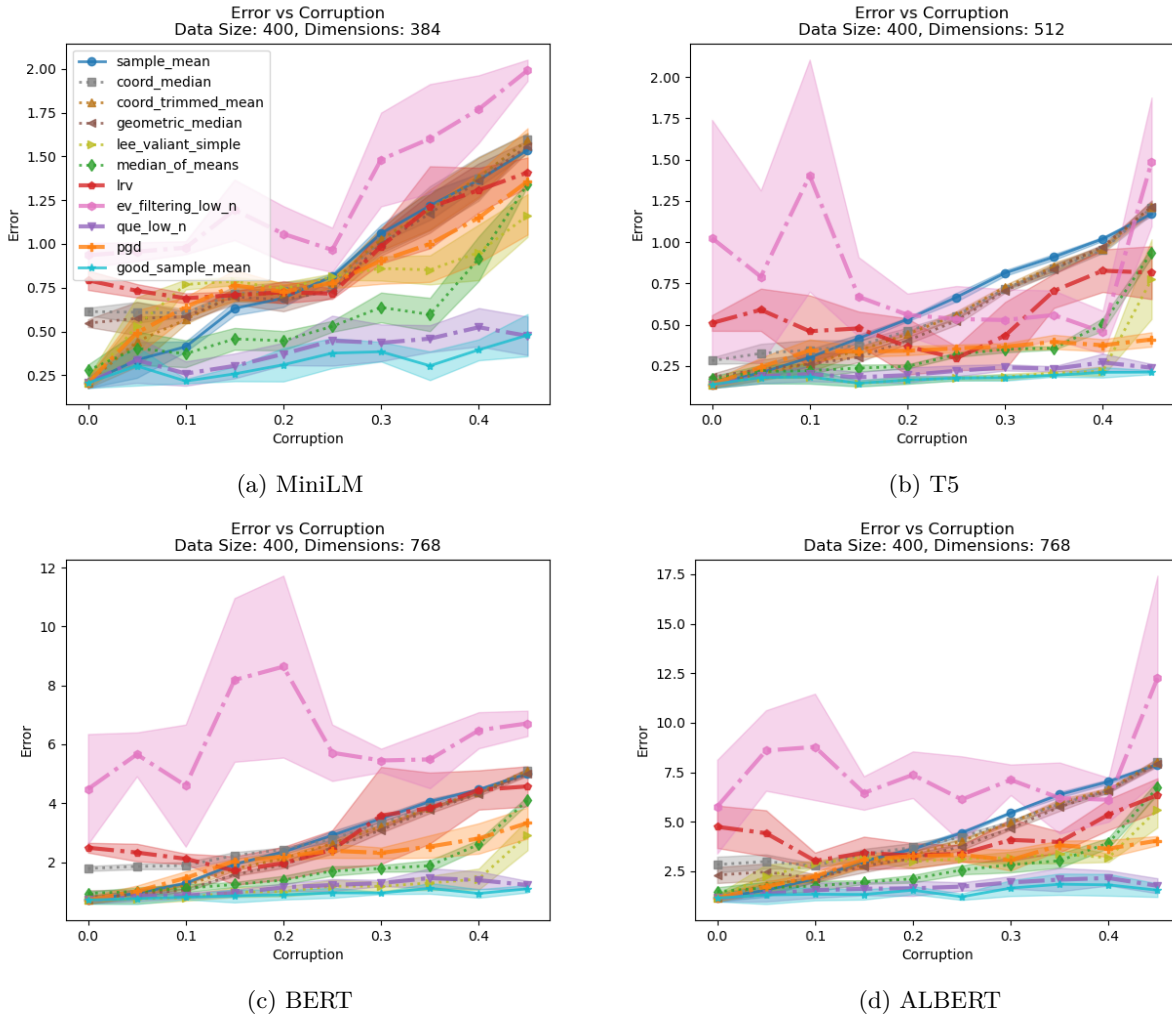
Figure 72: Error on "Field of Study" Embeddings Corrupted with "Field of Land" Embeddings

A.10 Dataset Generation

We generate a dataset of 400 sentences for each definition of the word *field* using ChatGPT-4o, accessed in June 2024. Attention based embeddings for the word *field* are extracted from these sentences for use in our LLM experiments. We used the following two prompts to obtain the sentences:

Field of Study

> *I am running an experiment where I examine embeddings of the word "field" with two different contexts. Please generate 400 unique sentences using the word "field" in context with the following definition: "a particular branch of study or sphere of activity or interest." Please return these sentences in the format of a JSON file.*

Field of Land

> *I am running an experiment where I examine embeddings of the word "field" with two different contexts. Please generate 400 unique sentences using the word "field" in context with the following definition: "an area of open land, especially one planted with crops or pasture, typically bounded by hedges or fences." Please return these sentences in the format of a JSON file.*

Additional Prompts ChatGPT-4o did not produce the full 400 sentences in one go. To address this, we used the following additional prompts until we had generated the required number of sentences, and then manually combined the generated outputs. The prompt for "field of study" sentences is slightly different, as we originally observed that ChatGPT-4o would reuse the same field of study across numerous sentences.

For *Field of Study*:

> *Please generate 100 more sentences. Do not repeat similar sentences or use "field" to refer to the same field of study multiple times.*

For *Field of Land*:

> *Please generate 100 more sentences.*

Tables Of Generated Sentences We include the following tables of generated sentences.

Field Of Land Sentences:

Index	Sentence
1	The scarecrow stood tall in the middle of the field.
2	The deer were spotted grazing in the field at dawn.
3	The field was an ideal spot for stargazing.
4	He loved to watch the sunset over the field.
5	The field stretched out as far as the eye could see.
6	Sunflowers swayed in the field under the clear blue sky.
7	The field stretched out to the edge of the forest.
8	The field was alive with the sound of chirping crickets.
9	They played hide and seek in the field, darting among the tall grasses.
10	He built a small shed at the edge of the field for storage.
11	The hot air balloon landed gently in the field.
12	She enjoyed picnicking in the field of wildflowers near her home.
	Continued on next page

Continued from previous page

Index	Sentence
13	She found an old, weathered barn at the edge of the field.
14	The field was fenced off to keep out wild animals.
15	They walked hand in hand through the field of wildflowers, lost in conversation.
16	He loved the quiet solitude of the open field.
17	The field was a perfect spot for birdwatching.
18	We had a picnic in the wide, open field.
19	The open field was covered in morning dew.
20	We watched the meteor shower from the field.
21	The open field was perfect for stargazing.
22	The field of strawberries was a patchwork of red and green.
23	The field was filled with the scent of blooming flowers.
24	Hikers followed the trail through the field of wild grasses, enjoying the solitude.
25	They played ultimate frisbee in the field.
26	The field of herbs was fragrant, each plant releasing its unique scent.
27	She found a hidden path that led to the field.
28	The field was a sea of green during the spring.
29	She found a hidden path that led to the field.
30	Wildflowers grew abundantly in the field.
31	A lone tree stood in the middle of the field, providing shade.
32	The field was a riot of color in the fall.
33	They harvested wheat from the vast field.
34	Deer grazed in the field at dusk, their silhouettes blending with the shadows.
35	The field was a vibrant green after the rain.
36	The field was a riot of color during the summer.
37	The field was a sea of gold during the harvest.
38	She enjoyed painting the landscape of the field.
39	He loved the feeling of the grass under his feet in the field.
40	We spotted deer grazing in the distant field.
41	The field was surrounded by rolling hills.
42	We walked through the field at sunrise.
43	The field was blanketed in snow during the winter.
44	The field was a playground for the neighborhood children.
45	The field was a sea of purple lavender in full bloom.
46	The field was blanketed in snow during the winter.
47	Cows grazed peacefully in the field enclosed by wooden fences.
48	The field, bordered by ancient oak trees, was a serene spot for a picnic.
49	She enjoyed walking through the field, picking flowers.
50	The field was blanketed with snow in winter.
51	He loved the peace and quiet of the open field.
52	The field was a patchwork of different crops.
53	The field was a sea of gold during the wheat harvest.
54	A scarecrow stood watch over the field.
55	He spent his afternoons walking through the field, lost in thought.
56	The field was divided into neat rows for planting.
57	The field was a perfect spot for a family picnic.
58	Birds chirped happily in the field, searching for insects among the plants.
59	The field was dotted with patches of wild grass.
60	She painted a landscape of the field in her art class.
61	The field was dotted with hay bales after a long day of harvesting.

Continued from previous page

Index	Sentence
62	He built a small fire pit in the middle of the field.
63	He loved the smell of fresh-cut grass in the field.
64	She found a quiet spot in the field to read her book.
65	The field was a burst of color in the autumn.
66	The field of rye swayed in the breeze, creating waves of green.
67	The field was alive with the sound of crickets.
68	The field was a popular spot for local festivals.
69	He loved the smell of fresh-cut grass in the field.
70	The field was a favorite spot for local photographers.
71	He loved to run through the field with his friends.
72	The field was alive with the sound of crickets.
73	We could see the farmhouse from across the field.
74	He loved the quiet solitude of the open field.
75	A scarecrow stood at the center of the field, arms outstretched.
76	We spotted a fox darting through the field.
77	The children flew paper airplanes in the field.
78	They set up a makeshift baseball diamond in the field.
79	A herd of sheep grazed peacefully in the field.
80	They played a game of tag in the spacious field.
81	He loved to explore the field with his dog.
82	A gentle breeze rustled the leaves of the crops in the field.
83	The field was covered in a blanket of fresh snow.
84	The horses galloped freely across the open field.
85	The dogs ran freely in the wide field.
86	The field of blueberries was a favorite spot for summer picking.
87	The field was a peaceful place to reflect and relax.
88	The scarecrow stood guard in the field, its tattered clothes fluttering in the breeze.
89	The field was a place of peace and serenity.
90	A gentle fog settled over the field in the morning.
91	The field was home to several species of birds.
92	The field was ideal for an outdoor concert.
93	She enjoyed walking through the field, listening to the birds sing.
94	The field was alive with the sound of crickets chirping at night.
95	The field was alive with the sound of crickets.
96	The field was a perfect spot for a family picnic.
97	The field of corn rustled in the wind, creating a soothing sound.
98	The field was a quiet refuge from the busy city.
99	He built a small bench at the edge of the field.
100	They played frisbee in the open field.
101	He loved the smell of fresh-cut grass in the field.
102	She enjoyed picnicking in the field with her friends.
103	The farmer worked tirelessly in the field to ensure a good harvest.
104	A small stream ran along the edge of the field, providing water for the livestock.
105	She enjoyed walking through the field, picking flowers.
106	The community garden was set up in the field.
107	A tractor moved slowly across the field, plowing the earth for new seeds.
108	They had an Easter egg hunt in the field.
109	We could see the farmhouse from across the field.

Continued from previous page

Index	Sentence
110	A gentle breeze blew across the field.
111	The field stretched out to the horizon, seemingly endless.
112	The field buzzed with the sound of bees collecting nectar.
113	The field was a riot of color in the fall.
114	The field was home to a variety of wildlife.
115	Birds nested in the hedges surrounding the field, singing melodious tunes.
116	The field was dotted with hay bales, ready for storage.
117	The field was a sea of gold during the wheat harvest.
118	The field was lush and green after the rain.
119	She loved to dance barefoot in the field.
120	The kids enjoyed a treasure hunt in the field.
121	The field of cherry blossoms was a sight to behold, petals drifting in the wind.
122	The farmer walked across the field, inspecting the growing wheat.
123	After the rain, the field was dotted with puddles reflecting the clouds.
124	Butterflies flitted about in the field, adding to its charm.
125	She could see the field from her kitchen window.
126	We found a quiet spot in the field to relax.
127	They set up a campfire in the field.
128	The farmer plowed the field in preparation for planting.
129	She enjoyed walking through the field, picking flowers.
130	The field's soil was rich and fertile, ideal for planting.
131	The field was a vibrant green after the rain.
132	The field was a peaceful place to escape to.
133	The field of sunflowers attracted bees with its abundance of pollen.
134	The field was blanketed in snow during the winter.
135	A small brook ran alongside the field, providing irrigation.
136	He watched the sunrise over the field from his porch.
137	She found a quiet corner of the field to meditate.
138	She found a hidden path that led to the field.
139	She picked wild strawberries in the field, their sweetness bursting in her mouth.
140	The large field was perfect for flying kites.
141	The field of cotton was ready for picking, the fluffy bolls bursting open.
142	The field of rapeseed glowed bright yellow against the blue sky.
143	He loved to run through the field with his friends.
144	The field was a canvas of colors in the spring.
145	The field was surrounded by a wooden fence.
146	Farmers plowed the field, preparing it for the next planting season.
147	He loved to watch the sunset over the field.
148	She could hear the distant sound of a tractor working in the field.
149	Children flew kites in the field, the colorful tails dancing in the wind.
150	The field was a place of beauty and tranquility.
151	They had a barbecue in the field last weekend.
152	The field of lettuce was irrigated regularly, ensuring crisp leaves.
153	She found a hidden trail that led to the field.
154	She enjoyed walking through the field, listening to the birds sing.
155	A narrow path cut through the field, leading to the old barn.
156	She found a perfect spot in the field for her garden.
157	The field was a sea of green grass in the spring.
158	Farm workers toiled from dawn to dusk, tending to the vast field.

Continued from previous page

Index	Sentence
159	The field of oats rustled softly as the wind passed through.
160	She loved to dance barefoot in the field.
161	A gentle mist rose from the field in the early morning.
162	The field of soybeans stretched for miles, a sea of green leaves.
163	The field was a place of peace and serenity.
164	The farmer surveyed the field, planning his next move.
165	The field was a sea of gold during the wheat harvest.
166	The field was a patchwork of different crops, each thriving in the rich soil.
167	She spent her afternoons wandering through the field.
168	The wheat field swayed gently in the wind.
169	Sunflowers bloomed vibrantly in the field, their faces turning towards the sun.
170	The field was a perfect place for a family gathering.
171	The field was alive with the sound of crickets.
172	The field was lush with green crops swaying in the breeze.
173	In the distance, a barn overlooked the sprawling field.
174	The field was a sea of green during the growing season.
175	The field glistened with morning dew.
176	They picked strawberries in the field.
177	The field was a playground for the neighborhood children.
178	A herd of cows roamed freely in the field.
179	A flock of birds flew over the field.
180	The field was blanketed in wildflowers during the spring.
181	The field was full of life, even in the winter.
182	The field was a favorite spot for watching the stars at night.
183	Children played a game of soccer in the field behind the school.
184	The field was a perfect spot for birdwatching.
185	The field was a peaceful place to escape to.
186	The kids enjoyed running freely in the open field.
187	He set up a telescope in the field to watch the stars.
188	The children lay down in the field to watch the clouds.
189	The field was dotted with blooming flowers.
190	He found a perfect spot in the field for his garden.
191	The cows roamed freely in the open field.
192	The field of corn was ready for harvesting.
193	The field of daisies swayed gently in the wind, a sea of white petals.
194	The field provided a perfect backdrop for photos.
195	The field was a sea of gold during the harvest.
196	They held a yoga class in the field at dawn.
197	The field lay fallow, resting before the next planting season.
198	The sun set behind the distant field.
199	He could see the field from his bedroom window.
200	The field was a vibrant green after the rain.
201	She ran through the field of tall grass, her laughter ringing out.
202	They set up a tent in the field for the event.
203	The field was a favorite spot for local photographers.
204	She enjoyed collecting wildflowers from the field.
205	They flew kites in the large, empty field.
206	The field was a vibrant green after the rain.
207	The festival was held in the open field every summer.

Continued from previous page

Index	Sentence
208	The field was a haven for wildflowers.
209	The field of radishes was ready for picking, their bright red roots peeking out.
210	The field was lush with green crops swaying in the breeze.
211	They saw a fox darting across the field.
212	She found a quiet corner of the field to meditate.
213	Rows of corn stretched across the field, reaching up towards the sky.
214	The field was a playground for the neighborhood children.
215	She took a stroll through the field, enjoying the fresh air.
216	He loved the smell of fresh-cut hay in the field.
217	The field was a patchwork of colors during the flower festival.
218	She spent her afternoons wandering through the field.
219	The field was covered in a blanket of wildflowers.
220	The picnic was set up in the field by the lake.
221	The field was a sea of green during the growing season.
222	A beautiful field of sunflowers stretched as far as the eye could see.
223	The scarecrow stood watch over the field, deterring hungry birds.
224	The horses galloped across the field, kicking up dust behind them.
225	The horses grazed peacefully in the field.
226	He loved the peace and quiet of the open field.
227	The field of tulips was a riot of color, reds, yellows, and pinks blending together.
228	The field was buzzing with activity during the harvest season.
229	He loved the quiet solitude of the open field.
230	She painted a beautiful landscape of the field.
231	He set up a telescope in the field to watch the stars.
232	They wandered through the field of pumpkins, searching for the perfect one.
233	In the winter, the field was covered in a thick layer of snow.
234	Cows grazed peacefully in the field enclosed by wooden fences.
235	The farmers planted potatoes in the field closest to the farmhouse.
236	They set up a tent in the field, ready for a weekend of camping.
237	The field was a haven for wildflowers.
238	At sunset, the field glowed with a golden hue, creating a picturesque scene.
239	The sheep roamed freely in the field, nibbling on fresh grass.
240	She enjoyed painting the landscape of the field.
241	He loved to explore the field with his dog.
242	The field was a patchwork of different crops.
243	They saw a rainbow stretching over the field.
244	He found solace in the quiet field, away from the hustle and bustle.
245	The field was a place of peace and serenity.
246	The field was an expanse of green grass.
247	The field was a haven for wildlife, including rabbits and deer.
248	He built a small bench at the edge of the field.
249	A gentle breeze rustled the leaves in the field.
250	She collected wildflowers from the field to make a bouquet.
251	The field, surrounded by rolling hills, was a picture of serenity.
252	She found an old, weathered barn at the edge of the field.
253	The festival was held in the large, open field.
254	She spent her afternoons wandering through the field.
255	The field was a playground for the neighborhood kids.
256	The field was a vibrant green after the rain.

Continued from previous page

Index	Sentence
257	The field of cabbages was neatly arranged in rows, their heads forming a patchwork.
258	She found a quiet spot in the field to read her book.
259	Farmers tended to the field of pumpkins, ensuring each one grew plump and round.
260	The field was a quiet refuge from the busy city.
261	They set up camp in the field, under a canopy of stars.
262	The field was a favorite spot for local artists.
263	The field was plowed into neat, straight rows.
264	The kids played catch in the large field.
265	The field was a favorite spot for local photographers.
266	The farmer rotated his crops to keep the field fertile.
267	We had a family reunion in the field.
268	He loved the smell of fresh-cut hay in the field.
269	The field of onions was harvested in the fall, bulbs dug up and stored for winter.
270	The field was blanketed in fog early in the morning.
271	The field provided ample space for the annual county fair.
272	She enjoyed collecting wildflowers from the field.
273	She loved to dance barefoot in the field.
274	The field was a riot of color in the summer.
275	The field was a perfect spot for birdwatching.
276	She ran across the field, her laughter echoing in the open space.
277	Butterflies fluttered over the wildflowers that dotted the field.
278	The field stretched out to the horizon.
279	They practiced their golf swings in the open field.
280	The field was perfect for a game of cricket.
281	In the summer, the field was a sea of golden barley ready for harvest.
282	The field was home to a family of rabbits.
283	The field was alive with the hum of insects.
284	The field was a vibrant green after the rain.
285	The field was dotted with patches of wild grass.
286	We enjoyed a picnic lunch in the sunny field.
287	We lay on the blanket in the middle of the field.
288	She found a quiet spot in the field to read her book.
289	Children played soccer in the open field near the village.
290	The field was covered in a blanket of snow during the winter months.
291	The field was a vibrant green after the spring rain.
292	He loved to explore the field with his dog.
293	Wildflowers dotted the field, adding splashes of color to the landscape.
294	They walked through the field of lavender, inhaling its sweet fragrance.
295	We had a bonfire in the middle of the field.
296	He found a quiet spot in the field to read his book.
297	The field was a sea of green during the growing season.
298	The field of barley was ready for harvest, the grains turning golden.
299	The field was surrounded by a white picket fence.
300	He built a small shed at the edge of the field.
301	The field of sugar cane stretched to the horizon, its stalks swaying gently.
302	The field was a burst of color in the autumn.
303	She enjoyed collecting wildflowers from the field.

Continued from previous page

Index	Sentence
304	He loved to watch the sunset over the field.
305	A beautiful field of sunflowers stretched as far as the eye could see.
306	She found an old, rusty plow at the edge of the field.
307	We watched the sunset from the edge of the field.
308	The dogs loved running around in the open field.
309	The field of lavender was a haven for bees, buzzing busily among the flowers.
310	The field was a riot of color in the fall.
311	Farmers worked diligently in the corn field.
312	The field was dotted with patches of wild grass.
313	Sheep roamed freely in the field, their woolly coats glistening in the sun.
314	The children played soccer in the field.
315	The field was a favorite spot for local artists.
316	He built a small bench at the edge of the field.
317	The field was a tapestry of colors in the spring, with various flowers in bloom.
318	We could see rabbits hopping in the field.
319	The field was a sea of gold during the harvest.
320	She sat under the oak tree in the field, enjoying the shade.
321	Cattle grazed peacefully in the field, surrounded by rolling hills.
322	The field looked magical under the light of the full moon.
323	The field was dotted with bales of hay.
324	The field was a riot of color during the summer.
325	He set up a picnic in the middle of the field.
326	The old oak tree stood alone in the field.
327	A scarecrow stood tall in the middle of the field, warding off birds.
328	The field was a favorite spot for local photographers.
329	She spent hours wandering through the field, collecting herbs.
330	She enjoyed picnicking in the field with her family.
331	The field was home to a variety of wildlife.
332	She lay down in the field, gazing up at the clear blue sky.
333	She found a hidden trail that led to the field.
334	The field was full of life, even in the winter.
335	The field was surrounded by a dense forest.
336	In the fall, the field turned a golden hue as the crops matured.
337	A light breeze swept through the open field.
338	He found a hidden trail that led to the field.
339	The path led us through a vast field.
340	He built a small shed at the edge of the field.
341	He found a perfect spot in the field for his garden.
342	The field was a haven for wildflowers.
343	The field was a riot of color during the summer.
344	The scent of freshly cut grass filled the air as the field was mowed.
345	They walked through the field of wheat, the stalks brushing against their legs.
346	Children ran around playing in the field all day.
347	The field was a quiet refuge from the busy city.
348	The field was a peaceful place to escape to.
349	He could see the field from his bedroom window.
350	The field was a favorite spot for local artists.
351	The field was full of life, even in the winter.
352	A fence made of wooden posts and wire encircled the field.

Continued from previous page

Index	Sentence
353	The field was a burst of color in the autumn.
354	He loved to run through the field with his friends.
355	A tractor moved slowly across the field, tilling the soil.
356	She lay in the field, watching the clouds drift by.
357	The field was a sea of green during the spring.
358	He loved the peace and quiet of the open field.
359	The field was a patchwork of different crops.
360	The field was a favorite spot for flying drones.
361	Farmers harvested hay from the field, stacking it neatly in bales.
362	She found a quiet corner of the field to meditate.
363	The field was a sea of green during the spring.
364	Children played soccer in the field behind the school, their laughter echoing.
365	The tractor moved slowly across the plowed field.
366	The field was dotted with patches of clover.
367	He built a small shed at the edge of the field.
368	The field was a place of beauty and tranquility.
369	He set up a telescope in the field to watch the stars.
370	The field was used for growing sunflowers.
371	She enjoyed walking through the field, listening to the birds sing.
372	The field of wheat stretched across the horizon, golden under the afternoon sun.
373	They planted a variety of vegetables in the field.
374	She loved the scent of fresh earth in the field after it rained.
375	The field was a peaceful place to reflect and relax.
376	They picked wildflowers from the edge of the field.
377	A lone tree stood in the middle of the field.
378	He could see the field from his bedroom window.
379	The field of hemp grew tall and strong, its fibers used for various products.
380	He loved the smell of fresh-cut hay in the field.
381	The field was buzzing with bees collecting nectar.
382	A rainbow arched over the field after the rain.
383	They planted rows of vegetables in the fertile field.
384	The field was a peaceful place to reflect and relax.
385	The field of vineyards produced grapes for fine wines, rows of vines neatly trellised.
386	She found an old, weathered barn at the edge of the field.
387	They picnicked in the field of clover, enjoying sandwiches and lemonade.
388	She enjoyed painting the landscape of the field.
389	We took a walk through the field at sunset.
390	They built a bonfire in the field, its flames lighting up the night sky.
391	The farmer's dog ran joyfully through the field.
392	The field was the perfect spot for a family gathering.
393	She enjoyed picnicking in the field with her family.
394	The field was covered in a thick layer of frost.
395	The field of potatoes was ready for digging, the earth yielding its treasures.
396	He could see deer grazing in the field from his window.
397	The field was a place of beauty and tranquility.
398	The field was a perfect spot for a family picnic.
399	Rain nourished the field, ensuring a bountiful crop for the season.

Index	Sentence
400	The field was a haven for birdwatchers.

Table 2: Field Of Land Sentences

Field Of Study Sentences:

Index	Sentence
1	The field of bioethics addresses the ethical issues in biology and medicine.
2	He is an innovator in the field of software development.
3	The conference attracted top professionals specialized in an interesting field of study.
4	The field of cultural studies examines how culture shapes identity.
5	The field of immunology studies the immune system.
6	The field of anthropology studies human cultures and societies.
7	His expertise in the field of structural engineering is invaluable.
8	My favorite baseball movie is field of dreams.
9	The field of socio-cultural anthropology examines human societies and their customs.
10	The field of cultural anthropology studies human societies.
11	The field of operations research uses mathematical methods to make decisions.
12	The field of evolutionary psychology explores the evolutionary origins of human behavior.
13	He is an authority in the field of health policy and management.
14	He is a leading expert in the field of forensic anthropology.
15	Her studies in the field of dance theory are intriguing.
16	He has made strides in the field of molecular genetics.
17	His work in the field of plasma physics is highly regarded.
18	The field of computational sociology uses computational methods to study social phenomena.
19	His studies in the field of marine biology are fascinating.
20	The field of telecommunications is rapidly advancing.
21	The field of supply chain management is vital for global commerce.
22	He decided to pursue a career in the field of computer science.
23	The field of biotechnology holds great promise for the future.
24	She has a background in the field of political science.
25	He is a leading researcher in the field of evolutionary genetics.
26	The field of digital forensics investigates cybercrimes.
27	The field of transpersonal psychology explores spiritual and transcendent aspects of the human experience.
28	He is a pioneer in the field of machine learning.
29	Her research in the field of music cognition explores how the brain processes music.
30	The field of sociology looks at how societies function.
31	Her research in the field of computational chemistry is groundbreaking.
32	Her expertise in the field of infectious diseases informs public health policies.
33	Her expertise in the field of environmental sociology addresses human interactions with the environment.
34	The field of optics studies light and its interactions.

Continued from previous page

Index	Sentence
35	The field of biogeography studies the distribution of species across geographical areas.
36	He received an award for his contributions to the field of engineering.
37	Her passion for the field of public health is evident.
38	The field of marketing explores consumer behavior and advertising strategies.
39	She is passionate about her work in the field of social work.
40	The field of actuarial science assesses financial risks.
41	The field of hydrology studies the distribution and movement of water on Earth.
42	She has received accolades for her work in the field of artificial intelligence.
43	The field of health informatics improves patient care through data.
44	The field of neuroinformatics combines neuroscience and data analysis.
45	She is highly respected in the field of architectural history.
46	He is a pioneer in the field of digital humanities.
47	The field of sports medicine focuses on athletes' health and performance.
48	The field of chemical engineering involves the creation of new materials.
49	He is a leading voice in the field of peace and conflict studies.
50	He is a prominent figure in the field of environmental sociology.
51	The field of sports medicine helps athletes recover from injuries.
52	The field of industrial design merges function with aesthetics.
53	The field of geriatric medicine focuses on elderly care.
54	The field of behavioral economics blends psychology and economics.
55	Her research in the field of climatology addresses global warming.
56	His research in the field of evolutionary biology is groundbreaking.
57	Her research in the field of computer graphics enhances visual simulation techniques.
58	The field of health informatics uses technology to improve healthcare delivery.
59	He has a deep interest in the field of computational neuroscience.
60	He is a renowned figure in the field of machine learning.
61	The field of medical anthropology explores the intersection of culture and health.
62	The field of acoustics studies sound and its properties.
63	Her research in the field of gerontology focuses on aging.
64	The field of molecular gastronomy explores the science behind cooking.
65	She is advancing knowledge in the field of developmental psychology.
66	The field of physical therapy helps people recover mobility.
67	The field of social epidemiology examines health disparities.
68	The field of artificial intelligence presents many ethical questions.
69	She is a trailblazer in the field of behavioral neuroscience.
70	Her expertise in the field of neuroimaging enhances brain research.
71	She is an innovator in the field of fashion design.
72	His work in the field of artificial intelligence has been widely recognized.
73	He has made significant strides in the field of computational neuroscience.
74	She is making waves in the field of renewable energy.
75	The field of computational neuroscience models neural systems and behavior.
76	His studies in the field of immunology are groundbreaking.
77	He is a leading scholar in the field of information science.
78	He is a leading figure in the field of aerospace engineering.
79	The field of digital sociology explores the impact of digital technologies on society.

Continued on next page

Index	Sentence
80	Her expertise in the field of gerontology addresses aging.
81	The field of linguistics helps us understand language structure.
82	The field of library science organizes and manages information resources.
83	Her expertise in the field of data science is highly sought after.
84	The field of literary criticism involves analyzing and interpreting texts.
85	He is a pioneer in the field of disaster risk reduction.
86	She is an influential figure in the field of gender studies.
87	The field of cognitive anthropology studies cultural variations in cognition.
88	The field of agronomy deals with crop production and soil management.
89	He is a leading figure in the field of quantum information science.
90	He has published extensively in the field of theoretical physics.
91	The field of health informatics combines healthcare and IT.
92	Her research in the field of psychopharmacology examines the effects of drugs on behavior.
93	He has authored several books in the field of history.
94	The field of international law governs legal relations between states.
95	The field of ethology examines animal behavior in natural environments.
96	The field of social psychology studies how individuals influence each other.
97	The field of political economy studies the relationship between politics and economics.
98	The field of anthropology examines human societies and cultures.
99	Her expertise in the field of marine archaeology uncovers submerged history.
100	Her work in the field of human-computer interaction designs user-friendly interfaces.
101	He is well-known in the field of quantum physics.
102	He has dedicated his career to the field of atmospheric sciences.
103	She has a distinguished career in the field of comparative literature.
104	The field of cultural studies examines cultural phenomena.
105	Her work in the field of artificial intelligence is innovative.
106	He is a notable expert in the field of space exploration.
107	Her research in the field of cognitive anthropology explores cultural cognition.
108	Her work in the field of cognitive psychology studies mental processes.
109	He is a well-known expert in the field of civil engineering.
110	The field of behavioral economics explores how psychology impacts economic decisions.
111	The field of consumer psychology studies consumer behavior and decision-making.
112	The field of artificial intelligence is growing rapidly.
113	The field of aerospace science investigates flight and space.
114	She has published numerous papers in the field of environmental science.
115	She has a keen interest in the field of film studies.
116	His innovations in the field of electrical engineering are impressive.
117	Her research in the field of mobile computing enhances smartphone technology.
118	The field of computational economics applies computational methods to economic analysis.
119	The field of marine chemistry studies the chemical composition of oceans.
120	His work in the field of marine biology is groundbreaking.
121	Her innovations in the field of textile science are notable.
122	The field of consumer psychology explores why people buy things.

Continued from previous page

Index	Sentence
123	The field of evolutionary psychology explores human behavior.
124	The field of computational biology uses data to understand biology.
125	He has extensive experience in the field of quantum computing.
126	The field of neuroscience delves into the workings of the brain.
127	The field of veterinary science focuses on animal health.
128	She has a strong foundation in the field of theoretical physics.
129	The field of music therapy uses music to improve mental health.
130	She has a profound impact on the field of forensic science.
131	His work in the field of linguistics has redefined language theories.
132	Her interest in the field of space exploration began in childhood.
133	The field of industrial design creates functional and aesthetic products.
134	His studies in the field of artificial intelligence are influential.
135	The field of educational psychology enhances teaching methods.
136	He is a notable figure in the field of mechanical engineering.
137	The field of geophysics examines the physical properties of the Earth.
138	Her work in the field of urban planning promotes sustainable urban development.
139	The field of medical imaging develops techniques to visualize internal organs.
140	She has been working in the field of bioengineering for over a decade.
141	He has a background in the field of developmental psychology.
142	The field of musicology delves into the study of music.
143	He is a renowned scholar in the field of classical studies.
144	The field of computational archaeology uses computer models to study archaeological data.
145	He is an authority in the field of cybersecurity.
146	Her contributions to the field of immunology have been invaluable.
147	The field of mathematical biology applies mathematical models to biological processes.
148	Her research in the field of neuroscience is highly respected.
149	The field of sports psychology helps athletes improve performance.
150	The field of environmental engineering seeks sustainable solutions.
151	The field of social neuroscience investigates the neural basis of social behavior.
152	The field of social geography studies the spatial distribution of social phenomena.
153	The field of landscape architecture focuses on designing outdoor spaces.
154	The field of psycholinguistics investigates the relationship between language and the mind.
155	He is a trailblazer in the field of genetic counseling.
156	The field of materials science investigates the properties of materials.
157	The field of computational linguistics develops algorithms for natural language processing.
158	He has a background in the field of political sociology.
159	The field of semiotics analyzes signs and symbols in communication.
160	The field of planetary science explores the formation and evolution of planets.
161	Her research in the field of robotics engineering advances automation technology.
162	He is a specialist in the field of aerospace engineering.
163	Her research in the field of cultural psychology investigates cultural influences on cognition.

Continued on next page

Continued from previous page

Index	Sentence
164	She has published numerous papers in the field of quantum mechanics.
165	He is an expert in the field of agribusiness management.
166	The field of robotics is seeing remarkable advancements.
167	The field of entomology studies insects and their behaviors.
168	The field of literary criticism analyzes literary works.
169	Her expertise in the field of transportation engineering is crucial for infrastructure projects.
170	The field of pharmacology investigates how drugs affect the body.
171	She received an award for her work in the field of environmental science.
172	She is working on a project in the field of urban planning.
173	Her research in the field of endocrinology has been transformative.
174	She is conducting groundbreaking work in the field of bioinformatics.
175	The field of veterinary medicine cares for animal health.
176	Her work in the field of evolutionary psychology examines psychological traits.
177	She has made a name for herself in the field of textile engineering.
178	The field of forensic science applies scientific methods to criminal investigations.
179	The field of quantum optics studies the behavior of light and matter at the quantum level.
180	He is renowned in the field of human-computer interaction.
181	The field of biotechnology holds great promise for the future.
182	The field of paleoclimatology reconstructs past climate conditions.
183	His contributions to the field of economics have been groundbreaking.
184	He has a deep interest in the field of robotics.
185	The field of musicology analyzes music history and theory.
186	Her expertise in the field of forensic anthropology aids in criminal investigations.
187	The field of computational genetics analyzes genetic data using computational methods.
188	Her expertise in the field of legal studies is unmatched.
189	He is a specialist in the field of cardiology.
190	She has made significant strides in the field of biotechnology.
191	Her contributions to the field of environmental law are significant.
192	He is a key player in the field of financial technology.
193	Her research in the field of computational neuroscience is influential.
194	She is interested in the field of cognitive science.
195	He has a background in the field of telecommunications.
196	He is a respected authority in the field of clinical research.
197	Her discoveries in the field of biochemistry have been revolutionary.
198	Her research in the field of artificial life simulates biological processes in computer models.
199	She has a strong background in the field of political science.
200	The field of bibliometrics analyzes academic publication patterns.
201	Her contributions to the field of educational technology are noteworthy.
202	The field of meteorology studies weather patterns and forecasting.
203	Her work in the field of financial engineering optimizes investment strategies.
204	The field of bioethics navigates moral issues in medicine.
205	The field of environmental economics studies the economic impact of environmental policies.
206	She has a strong foundation in the field of human resources.

Continued from previous page

Index	Sentence
207	He has a background in the field of peace studies and conflict resolution.
208	The field of organizational behavior studies how individuals and groups behave within organizations.
209	He has made significant contributions to the field of renewable energy.
210	The field of forestry studies the management of forests and natural resources.
211	The field of agricultural science seeks to improve food production.
212	The field of photonics involves the study of light generation and manipulation.
213	He is a recognized expert in the field of computational physics.
214	He is an innovator in the field of genetic research.
215	The field of computational biology uses computational methods to analyze biological data.
216	Her research in the field of human-computer interaction improves user experience.
217	The field of molecular biology examines the building blocks of life.
218	His research in the field of telecommunications has advanced the industry.
219	He is researching climate change within the field of environmental studies.
220	The field of historical linguistics studies language change over time.
221	The field of aerospace medicine focuses on the health of pilots and astronauts.
222	The field of educational sociology examines educational institutions and processes.
223	She has dedicated her career to the field of education.
224	Her expertise in the field of public health is widely recognized.
225	She is advancing the field of clinical psychology.
226	The field of visual arts encompasses various creative disciplines.
227	She is a renowned expert in the field of pediatric medicine.
228	He has a strong background in the field of systems engineering.
229	The field of astrophysics seeks to understand the universe.
230	Her work in the field of bioacoustics explores animal communication through sound.
231	He is a renowned expert in the field of computational linguistics.
232	He has a profound impact on the field of digital marketing.
233	The field of marine science explores oceanic systems.
234	The field of materials science involves studying the properties of materials.
235	The field of bioinformatics combines biology and computer science.
236	The field of environmental chemistry studies chemical processes in the environment.
237	The field of cognitive development explores how thinking processes evolve over time.
238	The field of toxicology studies the effects of chemicals on living animals.
239	Her research in the field of climate science is groundbreaking.
240	Her contributions to the field of computational fluid dynamics are substantial.
241	The field of fluid dynamics studies the behavior of liquids and gases.
242	The field of petrochemical engineering deals with petroleum products.
243	The field of ergonomics designs equipment for efficiency.
244	She is a key figure in the field of digital humanities.
245	He has a background in the field of educational leadership.
246	He is a pioneer in the field of nanotechnology.
247	The field of genetics explores the inheritance of traits.
248	He has a deep interest in the field of computational linguistics.

Continued on next page

Continued from previous page

Index	Sentence
249	The field of political sociology studies political institutions and behavior.
250	The field of paleontology uncovers the history of life on Earth.
251	The field of astrophysics reveals the wonders of the cosmos.
252	The field of cognitive science examines how we think and learn.
253	He has a prolific career in the field of synthetic biology.
254	The field of quantum computing is still in its infancy.
255	Her career in the field of art history has been illustrious.
256	He is making significant contributions to the field of microbiology.
257	He has a deep understanding of the field of financial mathematics.
258	The field of criminology examines the causes of crime.
259	The field of computational linguistics combines language and computing.
260	He is a leader in the field of pharmacology.
261	The field of actuarial science helps manage financial risks.
262	The field of environmental economics addresses the impact of economic activity on natural resources.
263	Her work in the field of cognitive neuroscience investigates brain function.
264	Her research in the field of behavioral ecology examines animal behavior.
265	Her research in the field of nutrition has led to healthier eating guidelines.
266	The field of developmental linguistics studies language acquisition in children.
267	The field of gerontology explores aging and its effects on individuals and societies.
268	The field of dialectology studies regional differences in language.
269	She has dedicated her life to the field of humanitarian aid.
270	The field of information technology is constantly changing.
271	He is an expert in the field of acoustical engineering.
272	The field of developmental psychology studies human growth and development.
273	She is advancing the field of artificial intelligence.
274	The field of climate science studies weather and climate change.
275	He is a thought leader in the field of sustainable development.
276	The field of evolutionary ecology examines the adaptation of organisms to their environments.
277	He has made notable contributions to the field of computer engineering.
278	She is a distinguished researcher in the field of plant biology.
279	Her research in the field of conservation biology protects biodiversity.
280	The field of computational chemistry models chemical structures and reactions.
281	His work in the field of artificial neural networks is groundbreaking.
282	Her work in the field of atmospheric science predicts weather patterns.
283	The field of synthetic chemistry creates new compounds.
284	The field of archaeology uncovers the secrets of ancient civilizations.
285	The field of chemistry explores the properties of matter.
286	Advances in the field of medicine have improved patient outcomes significantly.
287	He has a deep understanding of the field of artificial intelligence.
288	Her contributions to the field of visual perception are significant.
289	He has made significant contributions to the field of behavioral economics.
290	Her expertise in the field of environmental sociology addresses human-environment interactions.
291	He is a respected voice in the field of climatology.
292	The field of visual arts encompasses painting, sculpture, and more.
293	He has made significant advances in the field of cognitive robotics.

Continued on next page

Continued from previous page

Index	Sentence
294	The field of cyber security is critical in today's digital world.
295	The field of geology studies the Earth's physical structure.
296	The field of educational psychology applies psychology to educational settings.
297	The field of behavioral genetics investigates the genetic basis of behavior.
298	He is a pioneer in the field of computational photography.
299	He has a background in the field of social psychology.
300	She has a strong interest in the field of sociology.
301	Her work in the field of psychology has been groundbreaking.
302	He has a deep understanding of the field of environmental microbiology.
303	The field of cognitive neuroscience studies the biological basis of cognition.
304	She is a prominent researcher in the field of computer vision.
305	He is an expert in the field of social network analysis.
306	The field of computational linguistics develops algorithms for natural language processing.
307	The field of ergonomics designs equipment to improve human use.
308	He is an expert in the field of urban sociology.
309	She chose to specialize in the field of bioinformatics.
310	The field of educational psychology applies psychological principles to education.
311	The field of artificial intelligence is evolving rapidly.
312	The field of developmental biology examines the growth of organisms.
313	The field of occupational therapy helps people perform daily activities.
314	The field of neuropsychology studies the brain-behavior relationship.
315	He is a leader in the field of sustainable agriculture.
316	Her expertise in the field of digital anthropology explores online cultures.
317	He is a leader in the field of renewable energy.
318	The field of economics encompasses a wide range of topics.
319	He has a notable career in the field of emergency management.
320	The field of population genetics investigates genetic variation within populations.
321	The field of cultural heritage management preserves historical artifacts.
322	The field of computational genomics analyzes genetic data using computational methods.
323	The field of cultural sociology examines cultural patterns and practices.
324	He is conducting research in the field of renewable energy.
325	The field of biomedical informatics combines healthcare and data science.
326	The field of astrophysics explores the mysteries of the universe.
327	The field of cryptography focuses on securing communication.
328	The field of computational physics uses numerical methods to study physical phenomena.
329	She has a degree in the field of marine ecology.
330	Her work in the field of museum studies enhances cultural preservation.
331	The field of environmental toxicology studies the effects of pollutants.
332	The field of media studies examines how media affects society.
333	He is a prominent figure in the field of data analytics.
334	He has a background in the field of industrial psychology.
335	Her research in the field of child psychology is pioneering.
336	His contributions to the field of artificial intelligence are notable.
337	The field of biomedical engineering innovates healthcare technologies.

Continued on next page

Continued from previous page

Index	Sentence
338	He is a leading expert in the field of developmental economics.
339	He is a recognized authority in the field of bioinformatics.
340	The field of neuroeconomics combines neuroscience, psychology, and economics.
341	He is a pioneer in the field of artificial life research.
342	She is an authority in the field of biomedical engineering.
343	The field of archaeology uncovers the mysteries of ancient civilizations.
344	The field of computational social science uses data to study social phenomena.
345	She has published extensively in the field of medieval literature.
346	Her work in the field of digital humanities bridges technology and humanities research.
347	She is an authority in the field of network security.
348	He has a deep understanding of the field of nanomaterials.
349	He is an authority in the field of digital anthropology.
350	The field of game design creates interactive entertainment experiences.
351	Her research in the field of evolutionary linguistics explores language evolution.
352	He is a leading researcher in the field of human rights law.
353	The field of forensic science is crucial for solving crimes.
354	He is a leading expert in the field of urban ecology.
355	The field of marine biology studies ocean ecosystems.Her innovative ideas have reshaped the field of urban design.
356	The field of biomedical sciences advances medical knowledge.
357	His career in the field of nanotechnology is flourishing.
358	She is a leading expert in the field of genetics.
359	The field of data science is transforming industries worldwide.
360	The field of genetic engineering is a hot topic in scientific circles.
361	He is well-versed in the field of cultural anthropology.
362	The field of ethnomusicology studies music within cultural contexts.
363	The field of psychometrics measures psychological traits and abilities.
364	Her work in the field of game theory has practical applications in economics.
365	She is a thought leader in the field of educational technology.
366	The field of psychology studies the human mind and behavior.
367	The field of linguistics offers many fascinating areas of study.
368	The field of public policy shapes governance and society.
369	Her research in the field of linguistics has garnered international acclaim.
370	The field of international relations examines global politics.
371	Her contributions to the field of artificial intelligence are substantial.
372	He is a key player in the field of international relations.
373	The field of ecological economics integrates ecology and economics for sustainable development.
374	The field of sociology examines social behavior and institutions.
375	He is considered a pioneer in the field of nanotechnology.
376	He is an authority in the field of risk management.
377	He is a recognized authority in the field of rehabilitation engineering.
378	The field of cognitive science integrates psychology, neuroscience, and linguistics.
379	His expertise in the field of supply chain management is invaluable.
380	The field of computer vision develops algorithms for interpreting visual data.
381	She is a thought leader in the field of environmental law.
382	The field of cybersecurity is essential for protecting information systems.

Continued on next page

Continued from previous page

Index	Sentence
383	He is a respected scholar in the field of urban planning.
384	The field of biophysics combines biology and physics principles.
385	The field of climate modeling predicts future climate changes.
386	Her work in the field of neuroethics addresses the moral implications of neuroscience.
387	Her insights in the field of strategic management are highly valued.
388	She is exploring new techniques in the field of digital art.
389	The field of educational psychology helps improve teaching methods.
390	Her work in the field of social work helps vulnerable populations.
391	The field of artificial intelligence is continuously evolving.
392	He is highly respected in the field of electrical engineering.
393	He has a deep understanding of the field of molecular biology.
394	Her expertise in the field of computational chemistry aids drug discovery.
395	The field of urban sociology explores the dynamics of cities.
396	Her studies in the field of strategic management help businesses thrive.
397	He has made significant contributions to the field of game development.
398	Her work in the field of computational neuroscience models neural processes.
399	The field of medicine requires years of rigorous training.
400	The field of educational technology enhances teaching and learning through technology.

Table 3: Field Of Study Sentences